Renewable and Sustainable Energy Reviews 31 (2014) 221–257

Contents lists available at ScienceDirect

Renewable and Sustainable Energy Reviews

journal homepage: www.elsevier.com/locate/rser

Conversion of carbon dioxide into methanol – a potential liquid fuel: Fundamental challenges and opportunities (a review)

Ibram Ganesh *

Centre for Photoelectrochemical (PEC) Cells, International Advanced Research Centre for Powder Metallurgy and New Materials (ARCI), Hyderabad 500 005, AP, India

A R T I C L E I N F O

Article history:
Received 2 April 2013
Received in revised form
25 October 2013
Accepted 18 November 2013
Available online 14 December 2013

Keywords:
Carbon dioxide
Methanol
Renewable and sustainable energy
Artificial photosynthesis
Stoichiometric reactions
Molecular catalysts

A B S T R A C T

As on today, the conversion of carbon dioxide (CO_2) into value added chemicals including methanol using exclusively solar energy (i.e., artificial photosynthesis) has been considered as one of the top most research priorities all over the world as this process can indeed deal with (i) the mitigation of CO_2 associated global warming problem, (ii) creation of highly sustainable and renewable energy resources, and (iii) development of one of the best processes to store the energy in a most convenient form of liquid fuels with sufficiently high energy density in comparison to all the existing methods of energy storage. As the CO_2 sequestration process is expensive, there has been a quest for finding other alternative options. The CO_2 can be converted into several value added chemicals including methanol following stoichiometric reactions, thermochemical, electrochemical, photoelectrochemical, photocatalytic, etc., routes. Methanol synthesized from CO_2 can be employed directly in place of fossil fuels without disturbing the present existing energy distribution infrastructure. Further, if H_2 required for CO_2 reduction is produced from water using exclusively solar energy, and methanol is produced with minimum overpotentials with the help of suitable catalytic systems, this process can be employed to address the above-mentioned three major problems. The process for converting CO_2 into methanol can be developed by careful analysis and understanding of the information available on this process reported so far in the literature. Since, none of the existing review articles deals exclusively with this important process of converting CO_2 into methanol, in this review article, all the information including fundamental challenges and opportunities that are associated with the conversion of CO_2 into methanol following various routes has been summarized, discussed and meticulously presented by citing all the up to date relevant references.

Contents

* Tel.: +91 40 244 41075; fax: +91 40 244 42699.
E-mail addresses: ibram_ganesh@yahoo.com, dribramganesh@gmail.com, ibramganesh@arci.res.in

1364-0321/$ - see front matter
http://dx.doi.org/10.1016/j.rser.2013.11.045

1. Introduction

Recently, conversion of carbon dioxide into value added chemicals using solar energy (popularly known as artificial photosynthesis) has received a great deal of attention from the scientific community as it can indeed deal with the global warming [1–15], energy crisis (i.e., the depletion of fossil fuels) [16–29] and energy storage [30] problems. Recently, the Intergovernmental Panel on Climate Change (IPCC) has concluded that the fossil fuel burning and deforestation are responsible for increasing CO_2 concentrations in the atmosphere [31]. The atmospheric anthropogenic CO_2 concentrations have risen by 30% from pre-industrial (prior to 1750) levels of 280 ppm to 400 ppm today. The present CO_2 levels in atmosphere is higher than at any time during the last 6,50,000 years for which the reliable data was extracted from ice cores [3,4]. In fact, the CO_2 associated greenhouse effect was first noted by Joseph Fourier in 1824 and was further substantiated quantitatively later on by Svante Arrhenius in 1896 [32]. The greenhouse gases warm the planet's atmosphere and surface by absorption and reemission of the infrared radiation of sunlight. The civilization and industrialization have not only brought technology, modern life, and convenience to the human society but also pollution and emissions from factories, vehicles, and chemical plants [33]. Several national governments have signed and ratified the Kyoto Protocol of the United Nations Framework Convention on Climate Change aiming at reducing CO_2 gas emissions [2,31]. Recently, the International Energy Agency (IEA)-World Energy Outlook (WEO) revealed that, based on policies being practiced at the moment, by 2030 CO_2 emissions will attain 63% from today's level, which is almost 90% higher than those of 1990 [3]. Hence, to avoid further increases over the next few decades, improved actions than those of present should be taken, which include the development and employment of technology options to cut CO_2 emissions. One such option is to capture the CO_2 gas generated at major outlets such as thermal power plants and cement industry, where each tonne of coal is burned to generate about 4 t of CO_2, and then prevent it from entering into atmosphere by suitably storing it in safe places and/or by converting it into value added chemicals and fuels [3]. At present, the readily available technology to tackle CO_2 associated global warming problem is the CCS process (i.e., the carbon dioxide capturing and storing in safe places such as, depleted coal seams, under deep sea levels, etc.) [3,31]. The CCR process (i.e., the carbon dioxide capturing and reusing) has been considered to be economical and a valuable choice in comparison to the CCS process. Besides economical benefits, the socio-political benefits also come in terms of a positive image for companies adopting policies of reusing the generated CO_2 from fossil fuels [3,31].

The use of CO_2 as a building block for the synthesis of chemicals and chemical intermediates, and as an environmentally benign fluid in several applications can in fact contribute to a sustainable chemical industry, and as a consequence reduces CO_2 emissions into the atmosphere. At the moment all over the world, an increasing research and development (R&D) efforts are being made to develop effective methods for reusing of the captured CO_2 [34–43]. Many industrial methods have been already developed to have an encouraging influence on atmospheric CO_2 so that it need not have to be buried as a part of CCS process. Bulk chemicals at present being produced from the captured CO_2 are urea, salicylic acid, and polycarbonate-based plastics. CO_2 is also a solvent, for example, supercritical CO_2 (the state exists at 31 °C and 72.8 atm.) tender several advantages in terms of stereochemical control, product purification, and environmental issues for synthesizing certain fine chemicals and pharmaceutical compounds. Other opportunities for using CO_2 include enhanced oil and gas recovery, enhanced agricultural production, and ponds of genetically modified algae so that biodiesel can be produced from CO_2 captured at power-plants [43,44]. All these methods can reduce CO_2 emissions by at least 3.7 gigatons/year (Gt/y) (approximately 10% of total present annual CO_2 emissions), which in fact, can reduce the use of fossil fuels. Further reductions in CO_2 emissions are possible if these technologies are expanded far widely. Since, total anthropogenic CO_2 emission is ~25 Gt/y, the capturing and disposal of CO_2 appears to be a major readily available solution at the moment to mitigate CO_2 related global warming problem on urgent basis.

On the other hand, today, the majority of the world's primary energy requirement is met from fossil fuels [16–26,30,32,45–47]. Power plants use fossil fuels (coal, oil or natural gas) to produce electricity. As per today's consumption rate, the available coal reserves will last for another 130 years, natural gas for 60 years, and oil for 42 years [48]. As shown in Fig. 1, Hubbert's curve shows that in next 40 years the recoverable oil becomes significantly low and suggests finding an alternative energy economy in the 20-year timeframe from now [48]. While the Hubbert's curve is hotly debated, what is clear is that oil has a host of useful industrial applications, and if it is irreversibly burned, it will jeopardize the future. The vertical scale in Fig. 1 is in an arbitrary relative units,

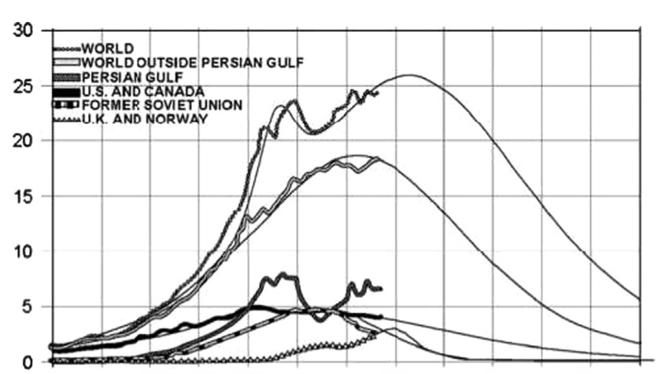


Fig. 1. The classic Hubbert curve [48].

but to get an idea of scale, world production averaged at about 80 million barrels per day in 2008 [48]. Furthermore, it is also important to realize the reliable alternative energy resources, before the oil resources are completely exhausted. Oil is the starting material for lubricants, dyes, plastics, and synthetic rubber, whereas, the natural gas supplies hydrogen for synthesizing ammonia, glass, and plastics. Similarly, coal produces creosote oil, benzene, toluene, ammonium nitrate, soap, aspirin, and several organic solvents. Thus, we cannot afford to use such an important and limited oil, natural gas and coal resources only to meet just the energy needs instead of several other important products of the future. Furthermore, these resources are not only for just few decades and but for the continued industrial applications of next several centuries [16–26,30,32,45–47]. In addition to these, the current fossil fuel consumption rate and their particular geographic distribution, and the political control over them pose problems for the nations which are fully depended on fossil fuels. The rapidly growing population and industrialization also further demanding the increased energy requirement.

Out of today's total energy consumption, about 43% is provided by oil and the derived liquid fuels which include gasoline, diesel, jet fuels, gasoil, etc. [49]. Only about 17% energy requirement is met by the electricity. It is hard to depend only on electricity as the actual energy density of electricity storing batteries is too low for many of the energy-intensive applications as their capacity for storing energy per kilogram of weight or for the unit volume is only about 1% in comparison to gasoline's energy density (Fig. 2). Fig. 2 also shows energy densities for various fuels including fossil and renewable sources (such as, ethanol and DMF), H_2 (liquid, gas, compressed at 700 bar, and stored in advanced nano-materials) and electrical energy (Li ion batteries, conventional and advanced) [30]. In this figure, NG stands for natural gas; DMF for dimethyl furan, and LPG for liquefied petroleum gas. Even if there is a break-through in the research of energy storing in batteries, the batteries energy storage do not meet many of the existing applications as these batteries are associated with certain limitations with respect to their cost, life-time, recharging time, etc. [24,30]. It has also been estimated that even if all the vehicles run with electricity in the future, the demand for electricity would increase by only $<1\%$ extra [25]. Besides this, at the moment, batteries cannot be used to run certain heavy vehicles such as, planes, buses, trucks, etc., as they need an on-board energy feeding. Furthermore, liquid fuels possess about 100 times higher energy density (~ 50 MJ kg^{-1}) in comparison to many of the available energy storage methods (Fig. 2). Thus it is important to develop the carbon-neutral, sustainable and easy to scale-up fuel storage methods as alternatives to the fossil fuels [50].

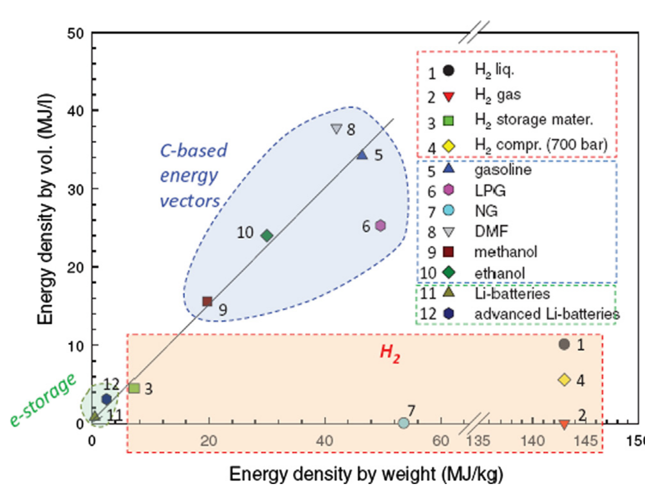


Fig. 2. Energy density per weight vs. per volume for a series of liquid and gaseous fuels [30].

The important resources of renewable energy are biomass, solar, wind, tides and hydro-based systems. Except, biomass all others produce electricity. The production of liquid fuels from biomass has been identified to be quite laborious, and probably much more research is still needed to find out a more economic and easier way to use biomass [51–53]. Furthermore, both nuclear and biomass (non-fossil energy alternatives) cannot supply the today's energy demand that is met from fossil fuels. In addition to these, other than liquid fuels, even if any other fuel is identified or developed from renewable energy resources like sunlight, that will disturb the presently existing energy supply (distribution) infrastructure leading to substantial consequences to the global economy. In the recent past, it was thought that H_2 could replace the fossil fuels, but it could not done so [30,32,45–47]. At this moment, the main source of the most of commercial H_2 is still fossil fuels, and for generating a unit of heat from H_2, more CO_2 is produced than directly burning those fossil fuels. At present, there is no method to produce H_2 from non-fossil fuel sources such as, water using highly cost-effective and renewable or nuclear energy sources. Furthermore, as on today, the self-sufficiency in energy is each and every country's objective. In fact, most of the following strategies for achieving this goal are either environmentally unacceptable or are not feasible except those depend on fossil fuel based resources such as, natural gas [30,32,45–47]. As the conventional nuclear power plants need uranium, which is limited and has always associated with the problems of radiation leakage due to natural calamities, etc., the solar energy is considered to be the only abundant, non-polluting (hence no damage to ecology), inexhaustible, carbon-free, omnipresent, and inexpensive non-fossil fuel based renewable energy resource. It is estimated that in a fortnight, the surface of the earth receives the energy that is equal to the total energy that is present in the entire world's fossil fuel resources (10^{16} kW). The mean solar irradiance at normal incidence outside the atmosphere is 1360 W/m^2 and the total annual incidence of solar energy in India alone is about 10^7 kW and for the southern region, the daily average is about 0.4 kW/m^2 [45]. In every hour, the earth receives solar energy that is equivalent to the entire world population's energy requirement in a year [30,32,45–47].

In year 2004, the world's energy requirement was 18 TW and it is expected to reach about 28 TW in the year 2030. The Department of Energy (DoE), USA, predicted that if the solar irradiance of 1% of the Earth's surface is converted into storable energy with 10% efficiency, it would provide a resource base of 105 TW that is equal to the several times of the estimated world energy requirement in the year 2050 [30]. Whereas, the amount of energy that could be extracted in the same year 2050 from wind, tides, biomass, and geothermal would be 2–4 TW, 2–3 TW, 5–7 TW, and 3–6 TW, respectively, [23]. In addition to this, the energy is required continuously day and night. Even though, solar energy is enough; it is not available in the nights and on the cloudy days. Hence, to supply solar energy continuously to the society, a proper method is required to store it in a proper way [49]. However, the most of the solar energy storage methods developed so far possess very low energy densities. The energy density by mass of compressed air (300 atm.), batteries, flywheels, supercapacitors, H_2O pumped 100 m uphill are estimated to be ~ 0.5 MJ kg^{-1}, ~ 0.1–0.5 MJ kg^{-1}, ~ 0.5 MJ kg^{-1}, ~ 0.01 MJ kg^{-1}, and ~ 0.001 MJ kg^{-1}, respectively. Although several technologies including photovoltaic (PV) cells, Peltier (Seebeck) modules, Fresnel lenses, concentrated solar radiation, solar thermal energy, dye-sensitized solar cells (DSSCs), etc., have already been developed for converting solar light into electricity, there is a discontinuity between solar irradiation and power consumption during the year, and in terms of geographical distribution. The same is true even for wind and tide based energy resources. Therefore, it is required to realize a suitable method to

store and transport the solar energy in a suitable manner [54–56]. As on today, solar energy can be stored in the form of hydrogen by splitting water into hydrogen and oxygen using electricity that is produced from solar energy ($2H_2O$+energy (Δ, electricity or $h\nu$)$\rightarrow 2H_2+O_2$; Eq. (1)) [57,58]. An advantage is that H_2 could be produced under pressure in certain modern electrolyzers, while other existing methods such as, bio-route using cyanobacteria or green algae [59,60], high temperature thermochemical route that uses concentrated solar energy [61–63], and photoelectrochemical H_2O splitting or photoelectrolysis [64–67], etc., produce H_2 at atmospheric pressure, which needs to be compressed eventually before using it in any of its applications. Recently, the advantages and disadvantages associated with various hydrogen production routes have been reviewed in many articles [30,37,54,68–76]. Among various methods developed so far for producing hydrogen from water, the PV have been identified to be the best one [30,56]. Furthermore, the energy density of H_2 gas is not suitable for most of the applications considering today's hydrogen storage technology [69–77]. In fact, almost all practical applications require high energy density per weight as well as per volume. In the case of light weight H_2 gas, energy density per volume is the main criterion. It can also be clearly seen from Fig. 2 that the energy densities of H_2 and electrical storage are far low in compared to those of liquid fuels based on fossil or renewable (biomass) sources [30]. Furthermore, H_2 gas usage also requires large expenditure for creating a new energy distribution infrastructure as it cannot be directly employed in the existing energy infrastructure such as, automobiles, thus not allowing a smooth transition from fossil fuel based dependency to renewable or non-fossil fuel or solar based energy dependency. Thus, it demands the production of liquid fuels with high energy density (even if they are carbon-based) using electrical energy, because these liquid fuels can be directly employed in place of fossil fuels used today, and can even be preserved for the future applications usage too [74,78].

The challenges for converting CO_2 into value added chemicals including methanol are great, but the potential rewards are also enormous. The conversion of CO_2 into methanol using energy that is not produced from fossil fuels has been suggested to be one of the best ways of storing energy and solving both global warming and energy crisis problems to a great extent. The additional advantages in producing methanol from CO_2 include (i) high energy density by volume and by weight; (ii) no need of high pressures to store at room temperature like H_2 need, (iii) relatively low toxic and safe to handle fuel, and shows limited risks in its distribution (non-technical); (iv) no need to modify the internal combustion engines of the vehicles to use methanol; and (v) no impact on the environment during production and usage as methanol being a primary feedstock for many of the organic compounds, and a vital intermediate for several bulk chemicals used in day-to-day life products such as silicone, paint, and plastics. Furthermore, methanol is a green fuel and has almost half of the energy density in comparison to the mostly used fuel, gasoline (methanol: 15.6 MJ/L; gasoline: 34.2 MJ/L) [79]. Furthermore, methanol can also be employed directly in the fuel cells.

At present, most of the commercial methanol is produced from synthetic gas (also called as syngas, which is a mixture of CO and H_2) on a quite large scale industrial plants in several millions tons per year capacity [79]. Besides this, the processes like, selective oxidation of methane, catalytic gas phase oxidation of methane, liquid phase oxidation of methane, mono-halogenation of methane, microbial and photochemical conversion of methane, etc., are also being employed to produce methanol. Nevertheless, production of methanol from CO_2 using solar energy to drive the reaction is highly attractive as it saves the natural fossil fuel resources. Nature does this job by converting CO_2 into bioenergy *via* natural photosynthesis using exclusively solar energy. In this process, somewhat less than 1% of the solar energy is converted into bioenergy in the form of plant materials, which when accumulated and transformed over geologic ages yielded fossil fuels. Thus, artificial photosynthesis has a tremendous potential and it is a scientific challenge, and upon successful development of it, the market is expected to be gigantic. Owing to its extremely stable chemical nature, converting CO_2 back to a useful chemical in an endothermic reaction, on the same scale and with the same rate it is currently being produced is out of today's scientific and technological ability [74,78]. However, a close study of the existing information on this subject hints that the successful development of artificial photosynthesis is no longer an unrealistic dream. Furthermore, this process could be developed quite efficiently in comparison to the natural photosynthesis. There are already certain endothermic reactions, which are being performed by thermochemical routes to produce syngas, H_2, and methanol over certain metal oxide catalysts using concentrated solar radiation energy [51–72].

Considerable research efforts have already been made to convert CO_2 into several industrially important chemicals and chemical intermediates following a great variety of methods using different forms of energy. These efforts can, in fact, be seen from a large body of literature summarized in several review articles as listed in Table 1 [30,41,44,56,80–101]. Nevertheless, none of these review articles exclusively deals with the literature on converting CO_2 into methanol. To fill this gap, the complete literature reported so far on conversion of CO_2 into methanol following stoichiometric, thermochemical, electrochemical, photoelectrochemical, and photocatalytic reactions performed over both inorganic as well as organic molecular (homogeneous and heterogeneous) catalytic systems is summarized, discussed and presented in this review article along with the several fundamental aspects of CO_2 reduction reactions and the opportunities associated with these reactions with a main perspective of designing a simple, efficient and reliable method for continuous reduction of CO_2 into methanol using solar or any other renewable energy resource.

2. Potential advantages of converting CO_2 into methanol

As direct H_2 storage, transportation and utilization have been associated with several issues, it was suggested to store H_2 in the form of certain liquids such as ammonia as it selectively releases back H_2 gas over certain catalysts surfaces [30,78,102]. Ammonia can also be synthesized following conventional Haber–Bosch process using H_2 that is formed in water hydrolysis using electricity produced from sunlight (using PV modules, etc.). However, direct synthesis of ammonia from hydrogen and nitrogen gases using solar energy is yet to be mastered. Of course, this process has been very well developed by the nature [30,78,102]. Nevertheless, ammonia is toxic and smells badly, and it is also a potent greenhouse gas and causes severe constraints if it is leaked into the atmosphere. Furthermore, there are certain risks related to BLEVE (Boiling Liquid Expanding Vapor Explosion) and UVCE (Unconfined Vapor Cloud Explosion). The current liquid fuels such as gasoline, and diesel, fulfill all these requirements for suitable energy storage, except emission of greenhouse gases. If the captured CO_2 is effectively reused to produce liquid fuels such as methanol using renewable solar energy, it is not even required to search for any other new energy vectors, and to develop any other energy storing methods and materials [30,78,102]. Furthermore, producing solar fuels using the captured CO_2 does not produce any additional CO_2 into the atmosphere. The methanol economy and uses of methanol conversion from CO_2 has been largely discussed by Nobel Laureate Olah et al. [79,103–105], while an economy based on

Table 1
A list of review articles published on CO_2 utilization and other aspects.

First author	Article title	Published year	Reference
J.-P. Collin	Electrochemical reduction of carbon dioxide mediated by molecular catalysts	1989	[91]
I. Taniguchi	Electrochemical and photoelectrochemical reduction of carbon dioxide	1989	[78]
K.W. Frese	Electrochemical and electrocatalytic reactions of carbon dioxide	1993	[79]
M. Jitaru	Electrochemical reduction of carbon dioxide on flat metallic cathodes	1997	[90]
H. Arakawa	Catalysis research of relevance to carbon management: progress, challenges, and opportunities	2001	[42]
Y. Hori	CO_2 reduction catalyzed by metal electrodes	2003	[80]
D.C. Webster	Cyclic carbonate functional polymers and their applications	2003	[88]
D. Chaturvedi	Versatile use of carbon dioxide in the synthesis of carbamates	2006	[94]
I. Omae	Aspects of carbon dioxide utilization	2006	[97]
C. Song	Global challenges and strategies for control, conversion and utilization of CO_2 for sustainable development involving energy, catalysis, adsorption and chemical processing	2006	[82]
M. Gattrell	A review of the aqueous electrochemical reduction of CO_2 to hydrocarbons at copper	2006	[83]
T. Sakakura	Transformation of carbon dioxide	2007	[39]
T. Seki	Catalytic oxidations in dense carbon dioxide	2009	[85]
G.A. Olah	Chemical recycling of carbon dioxide to methanol and dimethyl ether: from greenhouse gas to renewable, environmentally carbon neutral fuels and synthetic hydrocarbons	2009	[81]
Z. Jiang	Turning carbon dioxide into fuel	2010	[84]
W. Li	Electrocatalytic reduction of CO_2 to small organic molecule fuels on metal catalysts	2010	[86]
D.J. Darensbourg	Chemistry of carbon dioxide relevant to its utilization: a personal perspective	2010	[89]
B. A. Rosen	Low temperature electrocatalytic reduction of CO_2 utilizing room temperature ionic liquids	2010	[92]
S. C. Roy	Toward solar fuels: photocatalytic conversion of carbon dioxide to hydrocarbons	2010	[54]
M. North	Synthesis of cyclic carbonates from epoxides and CO_2	2010	[98]
G. Centi	CO_2-based energy vectors for the storage of solar energy	2011	[28]
M.T.H. Le	Electrochemical reduction of CO_2 to methanol	2011	[93]
I. Ganesh	Conversion of carbon dioxide to methanol using solar energy – a brief review	2011	[95]
W. Wang	Recent advances in catalytic hydrogenation of carbon dioxide	2011	[96]
Y. Oh	Organic molecules as mediators and catalysts for photocatalytic and electrocatalytic CO_2 reduction	2013	[87]
I. Ganesh	Conversion of carbon dioxide into several potential chemical commodities following different pathways – a review	2013	[101]

formic acid (FA) has been proposed by Ferenc [106] and earlier by Leitner [107]. However, the formation of renewable H_2 is the key step in the conversion of CO_2 into methanol and there are already certain established technologies for producing H_2 from water (a carbon-neutral resource) using electricity. Based on several factors as discussed in several published review articles, mainly in [30], the PV/electrolyzer approach shows unmatched potential for the CO_2 catalytic hydrogenation route. However, the biochemical, thermochemical and photoelectrochemical splitting of water into hydrogen would show better results if these processes are directly integrated with the CO_2 reduction reaction in comparison to the PV/electrolyzer based process, where H_2 needs to be produced separately and then used for reducing CO_2 in a separate process [30].

3. Conversion of CO_2 into methanol following stoichiometric reactions

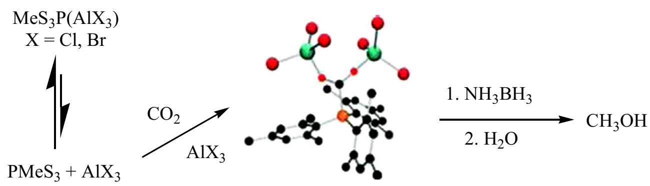
Table 2 lists the stoichiometric reaction conditions in which CO_2 was reduced into methanol [108,110,112,128,131]. It is a known fact that the stoichiometric reactions do not need any external thermodynamic energy inputs to proceed as they are not non-spontaneous reactions, and use only chemicals potentials to drive the reaction. Ammonia borane (AB), which provides hydride ions, was successfully employed as a reducing agent to convert CO_2 into methanol in the presence of Al-based frustrated Lewis pairs (FLP) as catalysts [108,109]. The tris(2,4,6-trimethylphenyl)phosphine ($PMes_3$) (Mes=2,4,6-$C_6H_2Me_3$) reversibly captures CO_2 with the help of AlX_3 (X=Cl or Br) to perform stoichiometric conversion of CO_2 into methanol. The FLP characteristics could be created by combining a Lewis acid with a base [110]. When an acid to base ratio was maintained as 2:1, the best results were noted. This stoichiometric CO_2 conversion into methanol was found to be fast when an excess AB was employed under ambient conditions while quenching with water (Scheme 1) [109]. An average yield of 37–51% was noted in this process. Alternatively, the tetramethylpiperidine/$B(C_6F_5)_3$ was also employed as FLP and noted a methanol yield of 24% in this stoichiometric reaction after 6 days at 160 °C [111]. Furthermore, the zirconium–borane complexes were also employed as catalysts for homogeneous reduction of CO_2 with hydrosilanes to produce methane [112]. However, these latter catalysts are sensitive to air and moisture, and also suffer from relatively lower catalytic activity.

In another stoichiometric reaction, the CO_2 was reduced into methanol using silanes as a source of hydrides and N-heterocyclic carbines (NHCs) as catalysts under very mild reaction conditions [113]. A considerably high methanol yield with $>90\%$ selectivity is noted in this latter reaction. This process shows promising for an efficient chemical activation and fixation of CO_2. In contrast to transition metal complexes, NHCs exhibit superior efficiency under mild and less stringent reaction conditions [104,114–120]. In fact, usage of NHCs as organocatalysts and ligands in organic synthesis is a well-known practice [104,114–120]. Due to the presence of a lone pair of electrons on carbene, NHCs behave as strong nucleophiles. Imidazolium carboxylates have been produced from CO_2 using NHCs as nucleophiles [121–123]. The release of CO_2 from the imidazolium carboxylates and the completion of a catalytic cycle with NHCs are considered to be an important metal-free pathway for CO_2 reduction into value added chemicals

Table 2
Conversion of CO_2 into methanol in stoichiometric reactions.

Catalyst	Source of protons and electrons (or hydrides)	Reaction temp. (°C)	Reaction time (h)	Methanol yield (%)	References
Al-based frustrated Lewis pairs + PMes3	Ammonia borane	RT	15 min	37–51	[109]
Tetramethylpiperidine/B(C_6F_5)$_3$	Ammonia borane	160	6 days	24	[111]
N-heterocyclic carbine (NHC)	Silane	RT	24	90	[113]
Formate dehydrogenase, formaldehyde dehydrogenase, and alcohol dehydrogenase	NADH	RT	3	91.2	[129]
Phosphine–borane organocatalyst	Hydroboranes	70	4	95	[108]

PMes3, tris(2,4,6-trimethylphenyl)phosphine; NADH, nicotinamide adenine dinucleotide (NAD) + hydrogen (H).



Scheme 1. CO_2 reduction into methanol in a stoichiometric reaction with the help of tris(2,4,6-trimethylphenyl)phosphine (PMes$_3$) (Mes=2,4,6-$C_6H_2Me_3$) and AlX$_3$ (X=Cl or Br) [109].

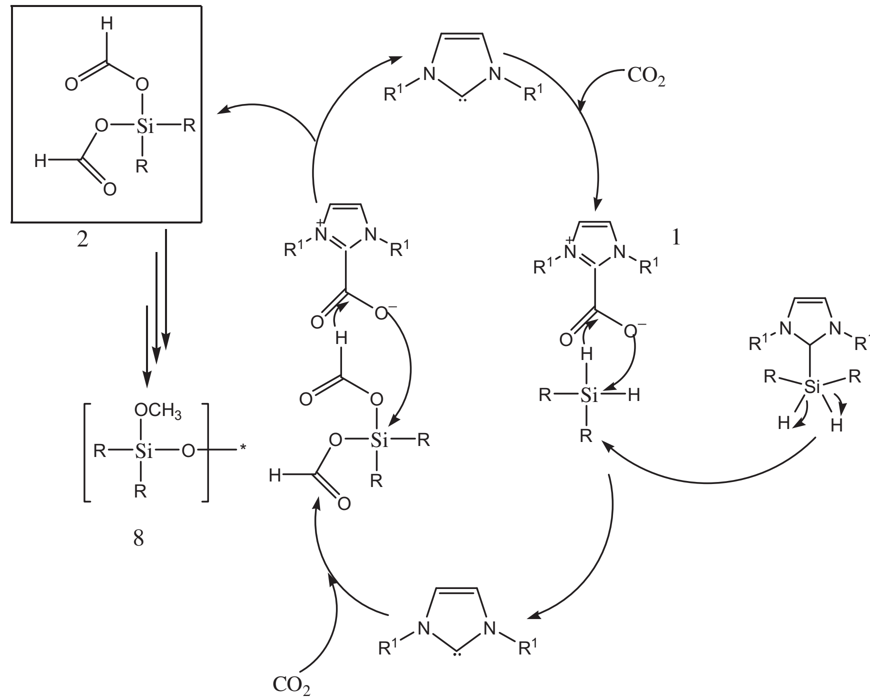
$$CO_2 + 3\,R_3SiH \xrightarrow{NHC} R_3SiOCH_3 + R_3SiOSiR_3 \xrightarrow{H_2O} R_3SiOH + CH_3OH$$

Scheme 2. Overall stoichiometric reaction of CO_2 reduction with silanes over NHC catalyst [109].

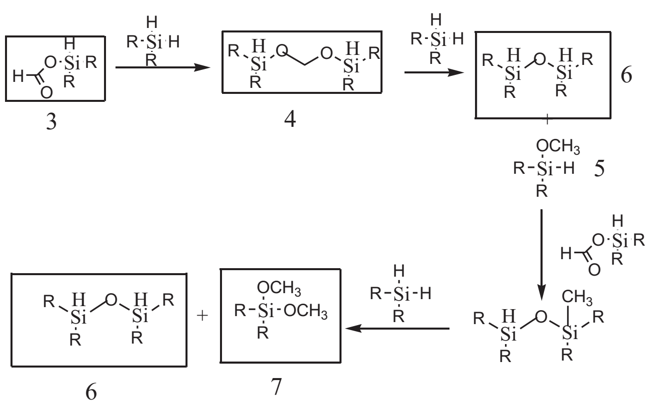
[113]. The spectroscopic analysis of sequence of reactions occurred in the formation of methanol from the reactions of CO_2 with silanes under the reaction conditions employed suggest that the reaction mechanism would precede as shown in Schemes 2–4 [109,113]. In this reaction, initially, the nucleophilic carbene activates CO_2 to form an imidazolium carboxylate, which subsequently reacts with silanes. The Si–H bond of silane has been found to be activated by a free carbine [109]. The carboxyl moiety of imidazolium carboxylate will then attack the electropositive silane center and promote hydride transfer to form formoxysilanes (2) and (3). Formoxysilane (3) then reacts with other free hydrosilanes in the presence of an NHC catalyst to produce intermediates (4)–(6) and the final methoxide products $Ph_2Si–(OMe)_2$ (7) and $(Ph_2(MeO)SiO–)_n$ (8). This catalytic cycle continues as long as the supply of hydrosilane as a hydride donor is available. Unlike transition-metal catalysts, which normally require almost a week time to provide the final reduction products, the NHCs are fast and highly efficient catalysts to convert CO_2 into methanol [109]. The rate of reaction in this process was found to be limited only by the amount of silane introduced to the reaction mixture.

The simultaneous protic and hydridic hydrogen transfer mechanism has also been utilized for effective reduction of CO_2 into methanol using ammonia–borane as a reducing agent [124]. In this latter reaction no high-energy single-electron-reduced intermediate product is formed as the highest occupied molecular orbital (HOMO) of CO_2 is pre-occupied with protons, while, the lowest unoccupied molecular orbital (LUMO) is concurrently reduced by a hydride ion. During two hydrogen transfer mechanism, it is believed that the formation of a six-membered-ring transition state takes place. It is also believed that in this process, three two-hydrogen transfer steps take place sequentially. The CO dehydrogenase (for example, in carboxydothermus hydrogenoformans bacteria) is a well-known biological system that utilizes simultaneous acid–base coordination to reduce CO_2 in the nature [124]. In this enzyme catalyzed reaction, nickel serves as a Lewis base, while iron serves as a Lewis acid, which stabilizes and promotes a two-electron transfer to CO_2 [125,126]. The key to the efficiency of this process is the simultaneous utilization of amphoteric nature (i.e., both acid and base functionalities) of CO_2 that avoids formation of high-energy intermediates and performs economical kinetics [125,126]. As per this nature's reaction, a crucial step in efficient reduction of CO_2 could be the exploitation of the amphoteric reactivity of CO_2 *via* simultaneous acid–base reactions. Ammonia–borane (AB) is also a simultaneous two-hydrogen-transfer reagent to convert CO_2 to formic acid [124]. Although this process utilizes a sacrificial reagent, the two-hydrogen-transfer mechanism exemplifies how high product selectivity might be achieved by analogous mechanisms that avoid formation of single-electron- or single hydrogen-transfer reduction steps [127,128]. Furthermore, although AB is isoelectronic to ethane, the B–N bond of former molecule actually consists of a nitrogen lone pair donating into an empty boron *p*-orbital, resulting in a relatively weak dipolar (or dative) bond. The electronegativity difference between nitrogen and boron is responsible for acidic hydrogens bound to nitrogen and hydridic hydrogens bound to boron. Similar to CO_2, any other molecule that possesses both a highest occupied molecular orbital (HOMO) able to accept $H^{\delta+}$ (protic) and a lowest unoccupied molecular orbital (LUMO) capable of accepting $H^{\delta-}$ (hydridic) can be reduced in this process [127,128]. The first step in the reduction of CO_2 is believed to be the formation of formic acid by the transfer of two hydrogens from ammonia–borane to CO_2. In tetrahydrofuran (THF) solvent, this reaction involves a free-energy barrier of about 24.2 kcal/mol for the formation of ammonia–borane–CO_2 adducts, thus making the reaction feasible under mild reaction conditions. The further two hydrogen transfer to formic acid produces methanediol [$CH_2(OH)_2$], and a third two-hydrogen transfer leads to the formation of methanol (Scheme 5 and Fig. 3) [124]. In Fig. 3, the lower barrier for decomposition of AB by HCOOH means the reduction of CO_2 will not rapidly continue to $CH_2(OH)_2$ or methanol. Exothermic oligomerization of AB (NH_2BH_2) entails that steps producing NH_2BH_2 are irreversible. However, the second step is not so fast because the relatively superficial acid-catalyzed decomposition of ammonia–borane takes place into NH_2BH_2 and H_2 [124]. Furthermore, as per Scheme 5, the substitution of AB for a reagent not sensitive to the decomposition reaction would favor the formation of more reduced products such as $CH_2(OH)_2$ or CH_3OH.

The CO_2 was also sequentially reduced into methanol using different dehydrogenase enzyme catalysts and nicotinamide adenine dinucleotide (NADH) as a terminal electron and proton donor [129]. This process involved an initial reduction of CO_2 to formate catalyzed by formate dehydrogenase (F_{ate}DH), followed by reduction of formate to formaldehyde by formaldehyde dehydrogenase (F_{ald}DH), and finally formaldehyde is reduced to methanol by alcohol dehydrogenase (ADH). This process utilizes NADH as a terminal electron donor for each dehydrogenase-catalyzed reduction as shown in Scheme 6 [129]. The use of the dehydrogenases to catalyze the reverse reactions in the presence of an excess of NADH is a well-studied system [130]. In this latter reaction, utilizing silica sol–gel matrix was found to be very useful. It was found that when enzymes were



Scheme 3. The plausible underlying mechanism in CO_2 reduction with silanes over NHC catalyst [109].



Scheme 4. Proposed catalytic cyclic and reaction pathway in CO_2 reduction with silanes over NHC catalyst. R1 = mesityl, R = Ph [109].

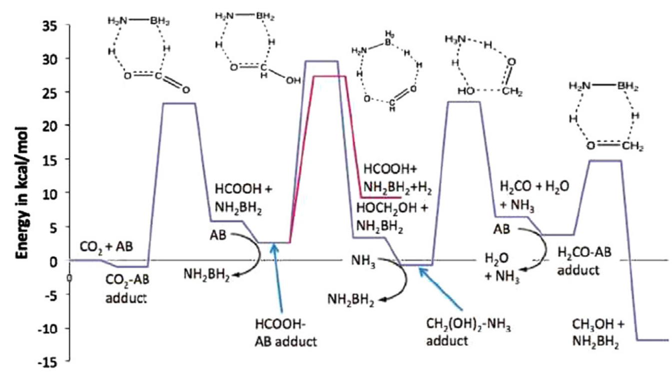
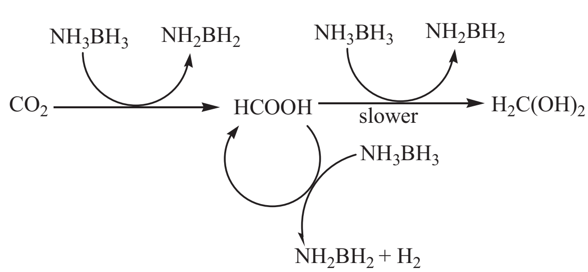
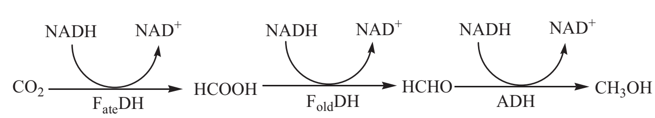


Fig. 3. Potential energy surface ($\Delta G^{298\ K}$) for the reduction of CO_2 to methanol by ammonia–borane (AB), including catalytic decomposition of AB by HCOOH [124].



Scheme 5. Proposed mechanism of CO_2 reduction by simultaneous two-hydrogen transfer and subsequent AB decomposition by HCOOH-catalyzed dehydrogenation [124].



Scheme 6. Reduction of CO_2 to methanol with the help of nicotinamide adenine dinucleotide (NADPH) in the presence of various enzyme catalysts [129].

encapsulated in the porous silica sol–gel matrix, the methanol formation was found to be increased substantially as compared to the one observed in the solution medium. Fig. 4 shows the results of methanol formation in solution as well as in the sol–gel systems [129]. As NADH assists as a limiting reagent in the overall reaction, it provides a relative measure of the efficiency of the reaction and the yield of the methanol production. It can be seen that 3 mol of NADH are consumed per mole of methanol formation (Scheme 6) [129]. Table 3 compares the relative yields of methanol formed per mole of NADH added [129]. As can be seen from this table, the overall yield of the reaction in solution medium is quite low, whereas it is substantially high in the sol–gel matrix.

The CO_2 was also reduced into methanol stoichiometrically following a biochemical approach in which formate dehydrogenase, formaldehyde dehydrogenase, and alcohol dehydrogenase were employed as catalysts [131]. These dehydrogenase catalysts were encapsulated in an alginate–silica hybrid gel that has been prepared through in situ growth of the silica precursor within the alginate solution. In this alginate solution, the Ca^{2+} cross-linking occurs during synthesis of the hybrid gel. The methanol yields noted are 98.8%, 71.3% and 98.1%, respectively, when the processes involved (i) no dehydrogenases, (ii) dehydrogenases immobilized

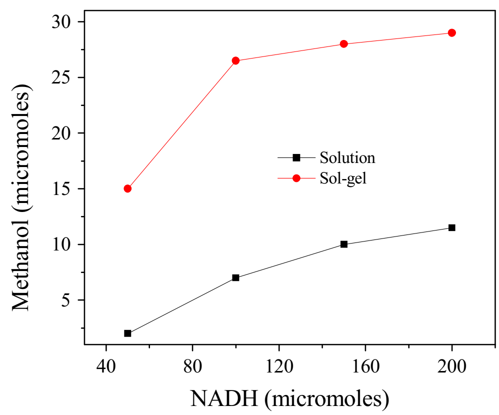


Fig. 4. Plot of methanol formation as a function of terminal electron donor (NADH) present in solution medium and silica sol–gel matrix [129].

Table 3
Relative comparison of CH_3OH formation in solution medium and silica sol–gel medium [129].

NAD (μmol)	Solution			Sol–gel		
	MeOH (μmol)	MeOH/NADH	% Yield[a]	MeOH (μmol)	MeOH/NADH	% Yield[a]
50	1.3 ± 0.7	0.02	7.8	15.2 ± 0.4	0.30	91.2
100	7.0 ± 0.9	0.07	21.0	26.6 ± 0.6	0.26	79.8
150	10.2 ± 0.6	0.07	20.4	28.5 ± 0.7	0.19	57.0
200	11.2 ± 0.9	0.05	16.8	29.2 ± 0.6	0.15	43.8

[a] % yield = [moles of MeOH/{0.33 (moles of NADH)}8] × 100.

in pure alginate, and (iii) dehydrogenases immobilized in alginate–silica matrix [131]. This latter alginate–silica catalyst showed a methanol yield of 76.2% even after stored for 60 days.

A highly active phosphine–borane organo-catalyst has also been employed for the reduction of CO_2 into methanol using hydroboranes as a source of hydrides in a stoichiometric reaction [108]. In this reaction, a catecholborane derivative 1-Bcat-2-PPh_2-C_6H_4 was employed as a catalyst that acts as an ambiphilic metal-free system for the reduction of CO_2 in the presence of hydroboranes (HBR_2 = HBcat(catecholborane), HBpin (pinacolborane), 9-BBN (9-borabicyclo[3.3.1] nonane), $BH_3.SMe_2$ and BH_3-THF) to generate CH_3OBR_2 or $(CH_3OBO)_3$ [108]. These latter compounds undergo hydrolysis readily to yield methanol. The noted product yields were as high as 99% with exclusive formation of CH_3OBR_2 or $(CH_3OBO)_3$ while the associated turnover number (TON) and turnover frequencies (TOF) reaching > 2950 and 853 h^{-1}, respectively. Furthermore, this catalyst exhibited a living behavior, i.e., once the first reaction cycle is completed, it resumes its activity again for additional reaction cycles immediately after loading the reagents into the reactor having catalyst [108].

4. Fundamental challenges in the reduction of CO_2 into methanol

Since, CO_2 is a linear molecule with two double bonds between the carbon and oxygen atoms (O=C=O), it is very stable and needs extra efforts to make it reactive. Eq. (2) shows the energy requirements needed for converting CO_2 into methanol upon reaction with water

$$CO_2(g) + 2H_2O_{(l)} \rightarrow CH_3OH_{(l)} + 3/2\ O_{2(g)};\ H^\circ = -727\ \text{kJ mol}^{-1}\ \&\ G^\circ = -703\ \text{kJ mol}^{-1} \quad (2)$$

Owing to its high stability ($\Delta G^\circ = -400$ kJ mol^{-1}), a substantial energy input, optimized reaction conditions, and catalysts with high stability and activity are required for converting CO_2 into value added chemicals [86,132–134]. Converting one mole of CO_2 to methanol requires an energy input of about 228 kJ, and six electrons to reduce C^{4+} of CO_2 to C^{2-} of methanol. According to Gibbs–Helmholtz relationship ($\Delta G^\circ = \Delta H^\circ - T\Delta S^\circ$), chemical reactions (conversions) are driven by mainly differences in the Gibbs free energy between the reactants and products of a chemical reaction (under certain conditions). Prior to any attempt to use CO_2 as a 'chemical feedstock' it is required to consider the relative stability of the ultimate reaction products in comparison to the reactants. Both terms (ΔH° and $T\Delta S^\circ$) of the Gibbs free energy are not favorable for converting CO_2 into other molecules [133]. As the carbon–oxygen bonds are strong in CO_2, high energy inputs are required for breaking these bonds. Similarly, the entropy ($T\Delta S^\circ$) term is also not thermodynamic driving force for any reaction involving CO_2. In fact, enthalpy ΔH° term can be conveniently considered for assessing the thermodynamic stability and feasibility of any CO_2 conversion. However, it was suggested that a positive change in free energy should not be taken as a sufficient reason for not pursuing potentially useful reactions of CO_2 reductions into value added products. Even though ΔG° gives discouraging values about the yield of products at equilibrium through the relationship ($\Delta G^\circ = -RT \ln K$), kinetics indeed favor certain reactions. Thus, in order to convert CO_2 into value added chemicals a good catalytic system is required [133,134]. Given the kinetics is favorable, CO_2 reduction to CO (believed to be a key step in all conversion reactions) is possible at metal surfaces, or some other catalytic materials, e.g. nanoscale metal particles encapsulated in nano- and meso-porous hosts [37,134]. There was a perception that the CO_2 conversion would be so endothermic that its conversion would not be feasible [84,135]. But it should be noted that a large number of industrial-scale chemical manufacturing processes are currently operated worldwide on the basis of strongly endothermic chemical reactions. One such classic example is the steam reforming of hydrocarbons to produce syngas and H_2 (Eq. (3)). This highly endothermic reaction is in fact used worldwide for producing "commercially available hydrogen" or "merchant hydrogen" required for several industrial applications. The corresponding CO_2 reforming of CH_4 (called as "dry reforming") is an example of important reaction of CO_2 with a hydrocarbon. This reaction can be considered as a central importance for considering the conversion of waste stream CO_2 to valued added chemical fuels (Eq. (4))

$$CH_4 + H_2O \rightarrow CO + 3H_2;\ \Delta H^\circ = +206.3\ \text{kJ mol}^{-1} \quad (3)$$

$$CH_4 + CO_2 \rightarrow 2CO + 2H_2;\ \Delta H^\circ = +247.3\ \text{kJ mol}^{-1} \quad (4)$$

The dry reforming ($CO_2 + CH_4 \rightarrow 2CO + 2H_2$) requires about 20% extra energy input in comparison to steam reforming ($H_2O + CH_4 \rightarrow CO + 3H_2$), but this is certainly not a prohibitive extra energy cost for this chemical reaction. Importantly, these two reactions give rise to syngas with different H_2/CO molar ratios. Both are useful for the formation of syngas, and for ultimate liquid fuel, i.e., gasoline, production. The conversion of energy from gaseous state into liquid fuel is an important gain in the reaction of high temperature hydrogenation of CO_2 to methanol as far as energy density or energy storage is concerned [85,136–139]. Nevertheless, there is no commercial process for converting CO_2 into liquid fuels and chemicals, which consume a large amount of CO_2. This process can be made feasible by thorough understanding of fundamental chemistry of CO_2 activation and by developing efficient catalytic systems for breaking C–O bond and making C–H and C–C bonds using electricity [136].

In neutral aqueous solution the overall thermodynamic requirements for reduction of water to hydrogen and of carbon dioxide to CO and formate are similar. Two-electron reduction

potentials at pH 7 and 25 °C are shown in Eqs. (5)–(7) [140]. Moreover, in seeking catalysts for these reactions similar issues arise. Both reductions are very difficult *via* one-electron processes, since the one-electron reduction products H atom and $\cdot CO_2^-$ (formate radical) are extremely energetic species. By using pulse-radiolytic methods, Schwarz and Dodson have recently determined $E°$ for the $CO_2/\cdot CO_2^-$ couple to be −1.9 V vs. NHE in water [141], and the intrinsic barrier for this one-electron reduction is estimated to be ca. 0.6 V. The $\cdot CO_2^-/{:}CO_2^{2-}$ potential has been estimated to be −1.2 V vs. NHE [142]. Values for $H^+/H\cdot/H^-$ have been discussed previously and the one-electron reduction potentials at pH 7 and 25 °C [140] vs. NHE for hydrogen and CO_2 are given in Eqs. (8) and (9), respectively

$$2H_2O(l)+2e^- \rightarrow H_{2(g)}+2OH^-_{(aq)},\ E°=-0.41\ \text{V vs. NHE} \quad (5)$$

$$CO_2(l)+H_2O_{(l)}+2e^- \rightarrow CO_{(g)}+2OH^-_{(aq)},\ E°=-0.53\ \text{V vs. NHE} \quad (6)$$

$$CO_2(l)+H_2O_{(l)}+2e^- \rightarrow HCO^-_{2(g)}+2OH^-_{(aq)},\ E°=-0.31\ \text{V vs. NHE} \quad (7)$$

$$H^+ \overset{-2.7V}{\longrightarrow} H^\bullet \overset{+0.03V}{\longrightarrow} H^- \quad (8)$$

$$CO_2 \overset{-1.9V}{\longrightarrow} CO_2^{-\bullet} \overset{-1.2V}{\longrightarrow} : CO_2^{2-} \quad (9)$$

Thus in either H_2O or CO_2 reduction, paths involving the (free) one-electron reduction products are expected to be vanishingly slow. Hence, the means of circumventing these paths or stabilizing the one-electron species are sought. In the H_2O/H_2 reaction, metal hydride complexes may provide catalytic routes. In the CO_2/CO or HCO_2^- reaction, catalysis by metal complexes may involve coordination of CO_2 [143] or insertion into a metal hydride bond to yield a formate species [144]. In the presence of HCO_3^-, the H_2O and CO_2 reductions appear to involve a common intermediate. Interestingly, the presence of water is required in a number of systems when CO_2 reduction occurs. Unfortunately, the presence of water also complicates the issue of the carbon substrate undergoing reduction. In aqueous media, the equilibriums (appropriate to ~0.5 M ionic strength, 25 °C [145]) shown in Eqs. (10)–(13) must be considered

$$CO_{2(g)} \leftrightarrows CO_{2(aq)}\ K=3\times10^{-2}\ \text{M atm.}^{-1} \quad (10)$$

$$CO_{2(g)}+H_2O \leftrightarrows H_2CO_3\ K=2.6\times10^{-3}\ \text{M} \quad (11)$$

$$H_2CO_3 \leftrightarrows H^+ + HCO_3^-\ K=2.5\times10^{-5}\ \text{M} \quad (12)$$

$$HCO_3^{2-} \leftrightarrows H^+ + CO_3^{2-}\ K=1.6\times10^{-10}\ \text{M} \quad (13)$$

Above pH 10 and below pH 4, "CO_2" solutions contain CO_3^{2-} and H_2CO_3/CO_2, respectively. Near pH 7, the three species HCO_3^-, CO_2 and H_2CO_3 are present and their distribution is pH dependent. Consequently pH variations carried out to assess the role of H^+ in CO_2 reduction system may be difficult to interpret when the dominant "CO_2" form(s) change. Furthermore, the equilibration of gaseous and aqueous CO_2 must be taken into account, and depending upon the experimental procedures (and time scales), the above equilibriums may lead to substantial changes in the CO_2 partial pressure above a solution and in the concentration(s) of dissolved species. Finally, the free-energy change for "CO_2" reduction is a function of the substrate and pH (Table 4). Fig. 5 summarizes the data presented in Table 4 in a graphic form. In Fig. 5, the following standard state conventions are used: H_2O, liquid; H_2 and CO, gas (i.e., 1 atm.); CO_2, HCO_2H, HCO_2^-, HCO_3^-, and CO_3^{2-}, aqueous (i.e., 1 M).

Table 4
Half-reactions of CO_2 in aqueous electrochemical cells.

pH	Half-reaction	$E°$ (V)	H^+/H_2; $E°$ (V)
0	$CO_{2(g)}+2H^++2e=CO_{(g)}+H_2O$	−0.12	0.00
7	$HCO_3^-+3H^++2e=CO(g)+2H_2O$	−0.48	−0.41
9	$HCO_3^-+3H^++2e=CO(g)+2H_2O$	−0.66	−0.53
11	$CO_3^{2-}+4H^++2e=CO(g)+2H_2O$	−0.87	−0.65

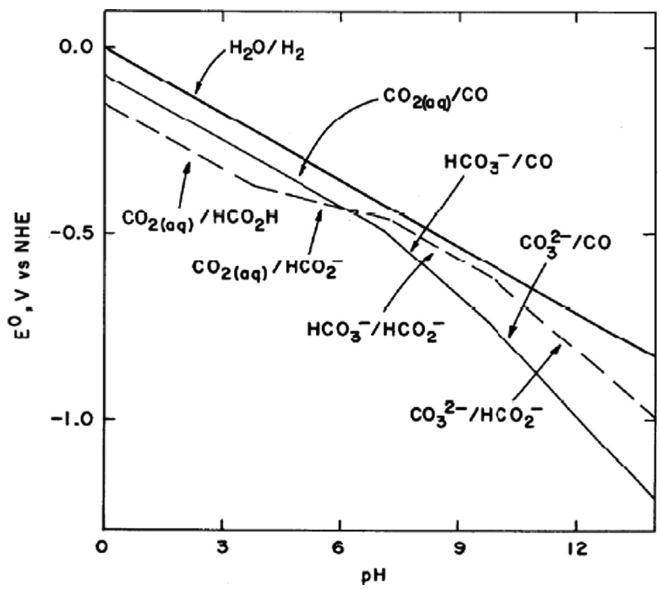


Fig. 5. $E°$ values (vs. NHE) for two electron reduction of H_2O and CO_2 as a function of pH and dominant forms of reactants and products [141].

5. Conversion of CO_2 into methanol following thermochemical routes

Table 5 lists the various catalytic systems employed for synthesis of methanol from CO_2 by following catalytic hydrogenation (i.e., thermochemical) routes [98,99,146–158]. Methanol can be prepared from CO_2 by catalytic hydrogenation ($CO_2+3H_2 \leftrightarrows CH_3OH+H_2O$) and thus obtained methanol could be transformed into dimethyl ether, DME ($2CH_3OH \leftrightarrows CH_3OCH_3+H_2O$), *via* dehydration. These two reactions can also be performed together in a single-step. In the catalytic hydrogenation of CO_2 to methanol, the first step is believed to be the reverse water–gas shift (RWGS) reaction ($CO_2+H_2 \leftrightarrows CO+H_2O$) [44]. In the conventional methanol synthesis process, CO formed is mixed with H_2 to react with and form methanol ($CO+2H_2 \leftrightarrows CH_3OH$) over copper–zinc-oxide-based catalysts under extreme reaction conditions (125–525 °C under 2–12 MPa pressure) [159–163]. Since, all these reactions are equilibrium reactions, they occur almost at the same temperature and on the same catalyst. In fact, the synthesis of methanol from syngas over copper–zinc-oxide-based catalysts is a well-established process, and about 40 Mtons of methanol per year is being produced every year at present by following this route. In this commercial process, about 3% CO_2 is supplied together with syngas to enhance the reaction rate. Since RWGS is a reversible reaction, the same catalyst can be employed to carry out both reactions of water–gas shift (WGS) and RWGS. The best catalyst noted for these reactions has been a multi-component $Cu/ZnO/ZrO_2/Al_2O_3/SiO_2$ composition.

When methanol was synthesized from CO_2/H_2 mixture ($CO_2+3H_2 \leftrightarrows CH_3OH+H_2O$) instead of from syngas ($CO+2H_2 \leftrightarrows CH_3OH$), about 3–10 times lower productivity was noted [44]. The water formed as a byproduct in the direct methanol synthesis from CO_2 was found to inhibit the reaction rate. It has been

Table 5
Catalysts employed in the catalytic hydrogenation of CO_2 into methanol.

Catalyst	Catalyst preparation method	Reaction temp. (°C)	CO_2 conversion (%)	Methanol selectivity (%)	Methanol activity (mol kg^{-1} cat. h)	Reference
$Cu/Zn/Ga/SiO_2$	Co-impregnation	270	5.6	99.5	10.9	[146]
Cu/Ga/ZnO	Co-impregnation	270	6.0	88.0	11.8	[147]
Cu/ZrO_2	Deposition–precipitation	240	6.3	48.8	11.2	[148]
$Cu/Ga/ZrO_2$	Deposition–precipitation	250	13.7	75.5	1.9	[149]
$Cu/B/ZrO_2$	Deposition–precipitation	250	15.8	67.2	1.8	[149]
$Cu/Zn/Ga/ZrO_2$	Co-precipitation	250	n/a	75.0	10.1	[150]
$Cu/Zn/ZrO_2$	Co-precipitation	250	19.4	29.3	n/a	[151]
$Cu/Zn/ZrO_2$	Urea-nitrate combustion	240	17.0	56.2	n/a	[152]
$Cu/Zn/ZrO_2$	Co-precipitation	220	21.0	68.0	5.6	[153]
$Cu/Zn/ZrO_2$	Glycine–nitrate combustion	220	12.0	71.1	n/a	[154]
$Cu/Zn/Al/ZrO_2$	Co-precipitation	240	18.7	47.2	n/a	[155]
$Ag/Zn/ZrO_2$	Co-precipitation	220	2.0	97.0	0.46	[153]
$Au/Zn/ZrO_2$	Co-precipitation	220	1.5	100	0.40	[153]
$Pd/Zn/ZrO_2$	Incipient wetness	250	6.3	99.6	1.1	[156]
Ga_2O_3-Pd/SiO_2	Incipient wetness	250	n/a	70.0	7.9	[157]
$LaCr_{0.5}Cu_{0.5}O_3$	Sol–gel	250	10.4	90.8	n/a	[158]

suggested that if water formed during reaction is continuously removed by catalytic distillation or by the use of inorganic H_2O permselective membranes, the yield is expected to increase [44]. The possible membranes for this process could be hydrophilic nano-pore zeolite (NaA) film deposited on a ceramic tubular support. This membrane is used at present for pervaporation of water–ethanol solutions. Not only low yields but also almost one-third of H_2 is consumed in the formation of water as a byproduct in direct methanol synthesis process from CO_2. Hence, synthesis of methanol from syngas is more profitable when compared with the direct synthesis of methanol from CO_2 following thermochemical routes [44]. Nevertheless, considerable research efforts are still being made with an aim to develop highly efficient catalysts for direct methanol synthesis from CO_2 for industrial applications. For this purpose, Cu has been selected mainly as an active catalyst. Effect of metal oxide support on 5 wt% Cu catalyst has been studied and several kinds of excellent Cu–ZnO based catalysts such as Cu–ZnO–Al_2O_3–Cr_2O_3, Cu–ZnO–TiO_2, Cu–ZnO–Ga_2O_3 and Cu–ZnO–ZrO_2–Al_2O_3–Ga_2O_3 have been developed [164–166]. Surprisingly, addition of small amount of CO to the H_2/CO_2 feed has also significantly increased the direct methanol formation from CO_2 and H_2 [164–166]. Among various catalyst systems studied so far, the copper–zinc oxides doped with ZrO_2, Ga_2O_3, and SiO_2 have been found to be best for this reaction [167]. It has been identified the metallic Cu surface of these catalysts is the main active center, and the activity of these catalysts was found to be directly proportional to the exposed surface area of metallic Cu [168–172]. Furthermore, the catalytic activity for this reaction was found to be independent of the CuO surface area [160], whereas it was found to be dependent on the amount of Cu^+ sites [173]. When compared with a pure oxidized Cu (100), a mixture of metallic Cu (100) plus oxidized Cu (100) exhibited an order of magnitude higher activity for this reaction [174]. The Cu (I) sites formed out of the oxidation of Cu have been found to stabilize carbonate, formate, and methoxide reaction intermediates during this reaction [175]. These observations have been further substantiated by near-infrared-visible absorption study of Cu^+–O–Zn in dissolved Cu(I) on ZnO matrix [176].

From the above discussion, it can be understood that the activity of direct formation of methanol by the catalytic hydrogenation of CO_2 is not only influenced by active catalytic sites but also by the support material. The Cu supported on CuO/ZnO with 30/70 weight ratio provided a methanol yield of 3.63×10^{-5} kg per square meter of the catalyst per hour at 250 °C under a pressure of 75 atm., whereas pure Cu provided a yield of less than 10^{-8} kg per square meter of the catalyst per hour [173]. Since, the wurtzite ZnO is an *n*-type semiconductor, besides oxygen vacancies, it also contains an electron pair, hence, believed to serve with active sites for methanol formation. According to a theory, an addition of ZnO to Cu/CuO catalysts creates cation and anion lattice vacancies, which are responsible for improved adsorption and transformation of CO_2 as well as the enhancement of Cu dispersion on the catalyst support. The formate intermediate was found to adsorb at the interface between Cu and ZnO or Cu–O–Zn [177]. By employing the mixtures of Cu/SiO_2+ZnO/SiO_2 as catalysts, it was found that ZnO creates Cu–Zn active sites for this reaction and the morphology of Cu was found to undergo any change during the reaction [178]. Further, ZnO is believed to stabilize many active sites by absorbing the impurities present in the syngas stream. A small amount of sulfur could be a poison for Cu catalyst if ZnO is absent as a support, thus ZnO inhibits the sulfur poisoning of Cu active sites during this reaction [179].

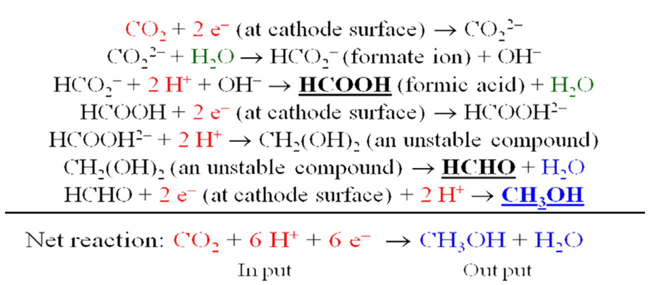
The reaction activity, product yield and catalyst life are not only found to be by the catalyst composition but also by the reaction conditions employed. As both catalytic hydrogenations of CO and CO_2 into methanol are exothermic reactions, methanol conversion was found to be increased upon increasing the reaction pressure and decreasing the reaction temperature according to the Le Chartelier's principle. Since the equilibrium constant decreases with an increase in temperature, a low temperature condition is preferred for methanol formation. However, increasing reaction temperature could also increase the reaction rates for both these hydrogenation reactions. Nevertheless, methanol formation has been found to be sensitive to optimal temperature ranges over different catalysts. Higher reaction temperatures could also rapidly reduce the activity and shorten the catalyst lifetime by promoting the sintering process and agglomeration of Cu on the catalyst surface. Catalysts also tend to undergo deactivation faster at high pressures again by the enhanced sintering process. A search for ideal catalyst system that is very active under low pressures and low temperatures with long lifetime is still active.

The most advanced method for the production of methanol from CO_2 is being followed by a leading Japanese chemical company, Mitsui Chemicals Inc., [180]. This company is producing H_2 from water using renewable solar energy and then reducing CO_2 into methanol using that hydrogen. Carbon Recycling International (CRI) Inc. also developed a process for converting CO_2 into methanol with the help of Nobel Laureate George A. Olah. This company is located in Iceland and it has a capacity to produce around 2 million liters of methanol per year. The H_2 for this reaction also produced by electrolysis using energy produced from renewable sources mainly geothermal, hydro, and wind.

6. Electrochemical reduction of CO_2 to methanol

Although the Sabatier and Fischer–Tropsch thermochemical routes are still practiced today, the electrochemical reduction of CO_2 into value added chemicals appears to be better than those of historical thermochemical processes in terms of mild reaction conditions are concerned. In contrast to methanol formation from syngas and CO_2 feed, which require extreme reaction conditions, the aqueous electrochemical CO_2 reduction into methanol is performed under ambient conditions [159–163]. Thus, this latter process could be a most convenient way of storing electrical energy in the form of liquid fuels without increasing additional CO_2 emissions. Since, either H_2 or water is the source of H^+ in this latter CO_2 reduction process, the environmentally friendly water is a bi-product. Even several hydrocarbons and O_2 could also be produced in this latter electrochemical process [159–163]. The other advantages of this latter process are the better chemical efficiency and higher physical yield of the final product in comparison to byproducts normally formed. By employing suitable electrode and catalytic systems, very high Faradaic efficiency could be achieved in electrochemical process. A reaction with high Faradaic efficiency means a lower energy requirement to complete the reaction. Development of a better method for the reduction of CO_2 into methane could also help in the in situ production of fuel on the way to traveling to Mars (i.e., Mars mission becomes simple). As electrochemical method offers several advantages [181] over thermochemical routes a great variety of organic compounds including benzylchlorides [182,183], allylic halides [184], vinyl bromides [185], vinyl triflates [186], carbonyl compounds [187], benzoyl bromide [188], 2-amino-5-chloropyridine [189], alkenes [190], alkynes [191], epoxides [192], etc. have been successfully synthesized by following electrochemical routes.

Scheme 7 shows the most probable reactions' sequence that could take place in electrochemical reduction of CO_2 into methanol [159–163]. The other compounds that are expected to form together with methanol are HCOOH, HCHO, and CH_4. Since CO_2 reduction into methanol and CH_4 requires 6 and 8 e^-(electrons), respectively, these two reduction reactions are considered to be kinetically more difficult, hence, they need very active and selective catalytic systems. The reduction of CO_2 with $6e^-$ and $6H^+$ over a catalyst surface into methanol does not need much of thermodynamic energy input similar to the dark reaction of the natural photosynthesis, but the formation of e^- and H^+ from water needs thermodynamic energy similar to the light reaction of the natural photosynthesis as the latter reaction is endothermic in nature (Scheme 8) [159–163]. In the natural photosynthesis, energy needed, for H_2O splitting into e^-, H^+ and molecular oxygen (O_2) in photosystems I and II, is drawn from sunlight by chlorophyll pigment of the plant leaves. This suggests that the production of e^- and H^+ from H_2O not only requires a suitable catalyst but also an energy input more than the theoretically required one. On the whole, in order to reduce CO_2 into methanol using exclusively solar energy in electrochemical cells (i.e., for realizing artificial photosynthesis process), three components are required: (i) a water oxidation/splitting catalyst, (ii) a solar energy harvesting system to produce electricity from sunlight in order to produce e^- and H^+ from water by electrolysis process, and (iii) a catalyst to reduce CO_2 into methanol by consuming e^- and H^+ formed in water splitting reaction [159–163]. The involved catalytic systems could be metals, metal oxides, inorganic complexes, inorganic or organic molecules, semiconductors, enzymes, and their combinations. Furthermore, these catalytic systems could also be either homogeneous or heterogeneous.



Scheme 7. A most probable reactions sequence to be occurred in the electrochemical reduction of CO_2 into methanol.

The CO_2 electrocatalytic reduction reactions are "reversible" in comparison to anode reactions that occur in fuel cells. Electrical energy is stored in the form of chemical energy in chemical bonds of fuels formed during electrochemical CO_2 reduction reaction. In thermodynamics, the Gibbs free energy of CO_2 reduction is always positive at medium and high pH range, and the theoretical potentials are negative. Thus, CO_2 reduction requires electrical energy input. In kinetics, the electrochemical reduction of CO_2 requires overpotential always >1.0 V (vs. standard hydrogen electrode, SHE or normal hydrogen electrode, NHE) to get reasonable amounts of fuels. In an aqueous electrolyte, CO_2 reduction is accompanied with H_2O reduction, hence, H_2 is a major byproduct, which always competes with CO_2 reduction reaction. Certain high H_2 overvoltage (overpotential) metals such as Hg suppresses H_2 evolution reaction (HER), but lead to the formation of only formate ions ($HCOO^-$) at very high overpotentials (means at high energy cost) [193,194]. This is the reason why CO_2 conversion requires either NH_3 and amine having high free energy content in stoichiometric reactions or certain external energy like thermal, electrical, and photo in other reactions. Involvement of appropriate catalytic system can promote reaction rates and directs the selective pathway, hence, to minimize the excess energy requirement to precede CO_2 reduction reaction [193,194].

In fact, the electrochemical reduction of CO_2 has been studied for more than a century [193,194]. In this process, theoretically, water is oxidized at the anode by releasing electrons, which travel through an external wire to reduce CO_2 at cathode to various products. The methanol formation is a combination of the reduction reaction at the cathode and oxidation reaction at the anode. Eqs. (14) and (15) depict reaction steps involved at anode and cathode during electrochemical reduction of CO_2 into methanol

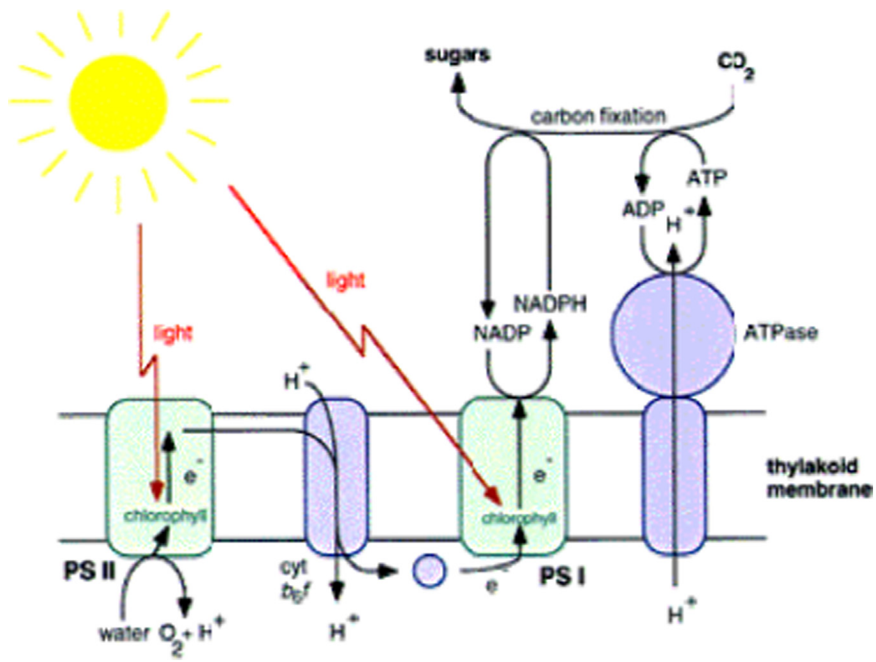
$$\text{Anode reaction: } 2H_2O \rightarrow O_2 + 4H^+ + 4e^-;\ E_o = 1.23 \text{ V vs. NHE} \quad (14)$$

$$\text{Cathode reaction: } CO_2 + 6H^+ + 6e^- \rightarrow CH_3OH + H_2O;\ E_o = 0.02 \text{ V vs. NHE} \quad (15)$$

Thermodynamically, it is possible to reduce CO_2 into methanol by following electrochemical methods. However, reduction potential of CO_2 is only about 20 mV positive of HER. Actually, it is necessary for any reaction to utilize complete supplied electrical energy to obtain the maximum product yield. However, in the reduction of CO_2 into methanol in electrochemical cells, the supplied electrical energy (i.e., the supplied potential) is shared by two reactions, i.e., (i) HER and (ii) the reduction of CO_2 into methanol. In order to achieve higher yields of methanol in this latter reaction, it is necessary to use a catalyst or electrode to suppress the HER so that all the H^+ and e^- formed in the water oxidation reaction will be consumed only by CO_2 reduction reaction. The reactivity of CO_2 reduction is very low; even though the equilibrium potentials of CO_2 reduction are not very negative compared to HER in aqueous electrolyte solutions under standard conditions

$$CO_2 + H_2O + 2e^- \rightarrow HCOO^- + OH^- \ (-0.43 \text{ V vs. NHE}) \quad (16)$$

$$CO_2 + H_2O + 2e^- \rightarrow CO + 2OH^- \ (-0.52 \text{ V vs. NHE}) \quad (17)$$



Scheme 8. A schematic showing the functions of photosystem-I (PS-I) and photosystem-II (PS-II) of natural photosynthesis.

$$CO_2+6H_2O+8e^- \rightarrow CH_4+8OH^- \; (-0.25 \text{ V vs. NHE}) \quad (18)$$

$$2CO_2+8H_2O+12e^- \rightarrow C_2H_4+12OH^- \; (-0.34 \text{ V vs. NHE}) \quad (19)$$

$$CO_2+6H^+ +6e^- \rightarrow CH_3OH+H_2O \; (-0.38 \text{ V vs. NHE}) \quad (20)$$

$$2CO_2+9H_2O+12e^- \rightarrow C_2H_5OH+12\ OH^- \; (-0.33 \text{ V vs. NHE}) \quad (21)$$

$$3CO_2+13H_2O+18e^- \rightarrow C_3H_7OH+18OH^- \; (-0.32 \text{ V vs. NHE}) \quad (22)$$

$$2H_2O+2e^- \rightarrow 2OH^- +H_2 \; (-0.41 \text{ V vs. NHE}) \quad (23)$$

The primary reactions that occur on the surface of electrode in aqueous solution at 25 °C vs. NHE are as follows [85,195]. CO_2 reduction does not occur easily and it requires higher potentials than the theoretical ones. This is mainly because of the single electron reduction of CO_2 to $CO_2^{\cdot -}$ (Eq. (24)) that occurs at −1.90 V vs. NHE. This step has also been considered to be a rate-determining step (RDS) in the CO_2 reduction processes. According to Nernst equation, the theoretical equilibrium potentials decrease with increasing pH [196]. For example, the theoretical or equilibrium reduction potential is only about +0.17 V vs. NHE for CO_2 reduction into methane at pH 0 (Eq. (25)). The CO_2 reduction reactions have been found to be greatly limited by reaction kinetics:

$$CO_2+e^- \rightarrow CO_2^{\cdot -} \; (-1.90 \text{ V vs. NHE}) \quad (24)$$

$$CO_2+8H^+ +8e^- \rightarrow CH_4+2H_2O \; (+0.17 \text{ V vs. NHE}) \quad (25)$$

Considering their low equilibrium potentials, thermodynamically, the products of methane (Eq. (25)) and ethylene (Eq. (19)) should occur at a less cathodic potential than HER (Eq. (23)), however, this does not happen due to kinetic limitations. Normally, HER takes place in aqueous electrolytes by cathodic polarization, competing with CO_2 reduction. Furthermore, HER is prevalent in acidic solutions, whereas CO_2 does not exist in a basic solution. This is the reason why CO_2 reduction experiments are normally conducted in close to neutral electrolyte solutions using 0.05–0.5 M $NaHCO_3$ supporting electrolyte [85,138,195,197–210]. The electrochemical reduction of CO_2 to methanol and methane involves high electrode overpotentials. This latter process is not economical because the amount of energy consumed during the synthesis of the reduction products is very high when compared with the one that is contained in the formed products [14,211,212].

6.1. Pure metals as cathode materials

In order to obtain CO_2 reduction products with high product yields, initially, metals and amalgams, which have high overpotentials towards HER, were employed as cathodes [213–216]. In 1904, Zn, amalgamated Zn and amalgamated Cu were employed as cathodes to reduce CO_2 in aqueous $NaHCO_3$ and K_2SO_4 solutions electrolytically to produce HCOOH [213]. The Cu electroplated with amalgamated Zn exhibited high efficiency for reducing pressurized CO_2 electrolytically [214]. Methanol was noted in minimal amounts over Pb electrodes in K_2SO_4 and $(NH_4)_2SO_4$ electrolytes. When CO_2 was reduced on Hg cathode, HCOOH was formed with 100% current efficiency [215]. In 1969, when steady state polarization techniques and cathodic galvanostatic charging techniques were employed to reduce CO_2 on Hg electrode in buffered neutral and acidic aqueous solutions and determined the resultant current efficiency, only HCOOH was identified in neutral solution; while in the acidic buffer, both HCOOH and H_2 were identified [216]. Although current efficiency was found to be high at initial stages, they fell rapidly with time for cathodes made of Hg. When rotating amalgamated cathode was employed to reduce CO_2 electrolytically, an improved current efficiency for formate formation without any loss in current efficiency was also observed [217]. In 1977, when CO_2 was reduced in electrochemical cell in a neutral electrolyte on an Hg electrode, only HCOOH was observed [218]. In this latter study, HCHO was also reduced to methanol at a current density of 10 mA cm^{-2}. During mid of 1980s, CO_2 was reduced over several metals and semiconducting materials such as GaAs and InP and observed the formation of methanol at lower current densities (<1 mA cm^{-2}) [219–221]. However, these latter reports are the first ones reporting the direct conversion of CO_2 into methanol in an electrochemical cell containing aqueous electrolytes and electrodes made of III–V semiconductor (GaAs and InP) or metals such as Ru and Mo for which the maximum current densities noted were <1 mA cm^{-2}.

In 1982, experiments were also conducted to evaluate the effect of electrolyte on the electrocatalytic reduction efficiency of CO_2 on Hg electrode, in which aqueous solutions of $NaHCO_3$, NaH_2PO_4–Na_2HPO_4, NaCl, $NaClO_4$, Na_2SO_4, $LiHCO_3$, and $KHCO_3$ and their combination were employed as electrolytes [222]. In 1985, a breakthrough in the electrochemical reduction of CO_2 to hydrocarbons (methane, ethylene, etc.) with high rates and efficiencies was seen when a Cu metal was employed as a cathode [138,201]. The direct reduction of CO_2 into hydrocarbons was noted with a current density of 5–10 mA cm^{-2} and current efficiency of $> 69\%$ at 0 °C in aqueous electrolyte on Cu cathode [85,138,139]. Later on various Cu-based catalysts (Cu single crystals, pure Cu electrode, and Cu alloys electrodes) have been extensively employed from both fundamental and applied perspectives to reduce CO_2 [197–204]. A gas mixture of hydrogen, methane, ethylene and CO called "hythane" formed over Cu electrode, which could be considered as an alternative fuel for existing vehicles [205,206]. An improved transportation of CO_2 was noted when gas diffusion electrode (GDE) and solid polymer electrolyte (SPE) were employed, which resulted into an improved CO_2 reduction reaction activity [207–210]. The major reduction products noted in these latter reactions have been formic acid, formaldehyde, isopropanol, methane, methanol, ethylene, and CO.

Pourbaix diagram for CO_2 shows the equilibrium reduction potentials as a function of pH in Fig. 6 [95]. The selectivity and efficiency of electrochemical reduction of CO_2 have been found to be a strong function of electrocatalysts and operating conditions [138]. These results further suggest that the end product of the electrochemical reduction of CO_2 is also highly influenced by the electrolyte used, the metal surface chosen, and the degree of cathode polarization. Considerable efforts were also made to suppress the HER and to improve CO_2 reduction reaction over Hg and Pb metal cathodes that have high overpotentials towards HER. Based on the major products formed in the electrochemical reduction of CO_2, the metal electrodes have been grouped into subdivisions (Fig. 7) [95]. A majority of the VB–VII group metals possess low overvoltages towards HER, hence, produce mostly H_2 gas with very small amounts of CO_2 reduction products. Groups IB, IIB and some of Group VII metals produce mainly CO and HCOOH. Cu and Ti electrodes produced more complex hydrocarbons. The information of Fig. 7 is much clearly summarized in Table 6. It can be seen from this table that all the metals do not possess the same potential. This information gives a general understanding about

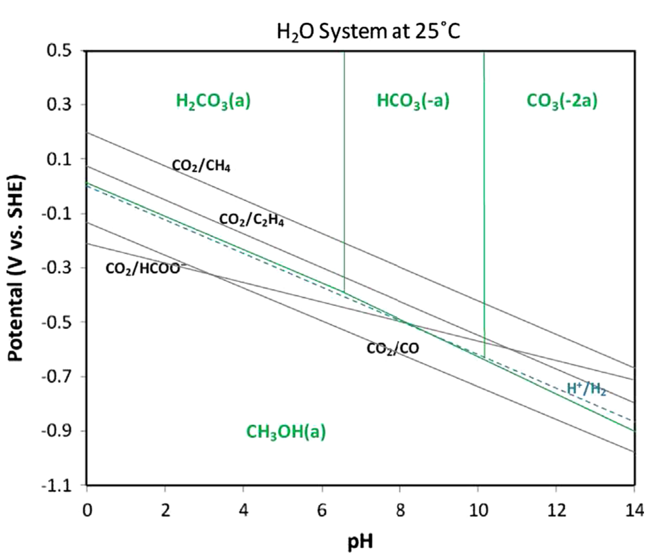


Fig. 6. Pourbaix diagram for carbon dioxide reduction reaction at 25 °C [95].

the required overpotential to reduce CO_2 into methanol or to any value added chemical.

In a recent review article, the literature reported up to 1997 on electrochemical reduction of CO_2 on flat metallic cathodes was reviewed and summarized [92]. Usually, the electrochemical reduction conditions are classified based on the products formed, but in this review article, the classification was made based on the nature of the cathode (*sp* or *d* group metal electrodes) and solvent employed for the supporting electrolyte (aqueous or nonaqueous solutions). According to this review, irrespective of the four possible combinations of electrodes and supporting electrolytes (*sp* group metals in aqueous and nonaqueous electrolytes, and *d* group metals in aqueous and nonaqueous electrolytes, respectively), the resultant products are almost same. Further, this review concludes that the formation of products depends mainly on the electrocatalytic activity of the cathodic metal. The *sp* group metal electrodes such as Pb, Hg, and In which possess high overpotentials for HER, showed considerable Faradaic efficiencies for HCOOH and oxalic acid. The In metal is a well-known cathode for selective reduction of CO_2 to formic acid at ambient pressure as well as at 60 atm. pressure in aqueous $KHCO_3$ solution to form HCOOH at current densities useful for technological applications (560 mA cm^{-2}) [92]. The Hg and graphite were found to be more selective towards oxalic acid and malic acid formation, whereas the group VIII metals were found to be selective for C_2–C_4 chemical intermediates that can be converted into valuable products in subsequent processes, Pd was found to be selective for the formation of formate ions and hydrocarbon molecules, and the Mo and Ru were found to be selective for methanol and methane formation [92,211]. Among the various metal electrodes employed for this purpose, the Cu has been found to be the most promising cathode for hydrocarbon manufacturing. As the current efficiency for methane and ethane depends on the continuous removal of the products from the electrode surface, the use of rotating disc electrodes has been recommended (vibrating electrodes may be the technical solution at the industrial scale). Further conclusions from this review are the precious metals such as Pt, Ti, Ru, which normally show high catalytic activity, do not reduce CO_2 in aqueous systems because they possess low overvoltage potentials for HER. These latter metals produce mainly H_2 at near 100% current efficiency. The Hg, Cd, Pb, Tl, In and Sn electrodes not only possess high overvoltages for HER, they also do not adsorb CO; hence, CO_2 could be reduced with high current efficiency over these electrodes but only to formate. The Pt, Ni, Fe and Ti electrodes with low hydrogen overvoltage and high CO adsorption strength reduced CO_2 to CO at 5–10 mA cm^{-2}, but the principle product has been only H_2 [223,224]. In aqueous systems, Au, Ag, and Zn exhibited high efficiency for the formation of CO on account of their relatively low H_2 overvoltages nearing 1 V (vs. NHE). For example, a Zn electrode produces mostly CO at an about 80% current efficiency at −1.54 V (vs. NHE) potential, which is 1 V higher than the one predicted by thermodynamics. The Au, Ag, Zn and Cu electrodes with a medium hydrogen overvoltage and a weak CO adsorption catalyzed the breaking of the C–O bond in CO_2 and also allowed desorption of CO. In summary, the Au, Ag and Zn produce CO with high current efficiencies, whereas the Cu produces hydrocarbons [82,201,225,226]. Alternatively, metals have also been grouped based on their electronic state, i.e., into *sp* or *d*, and based on the type of electrolyte (aqueous or nonaqueous) employed [92]. The latter classification has been more advantageous as it helps to identify products based on the physical nature of the metal, electronic environment, and electrolyte properties [227]. When CO_2 reduction reaction was performed over Ni catalyst, CO and H_2 were formed in 1:1 ratio at a current density of 10 mA cm^{-2} and a cell voltage of 3.05 V (vs. NHE) with an overall energy efficiency of 44.6% [228]. The electrocatalytic

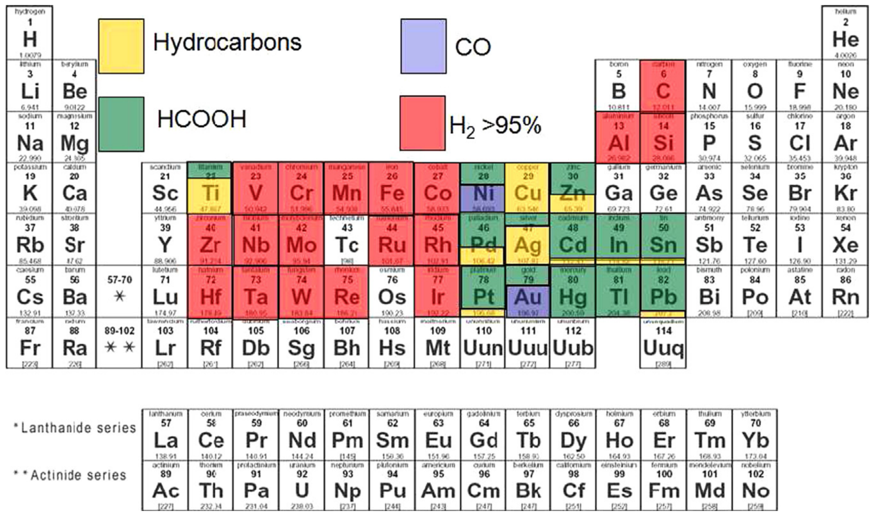


Fig. 7. Metal–metal (cathode) stored based on CO_2 reduction products in $KHCO_3$ based media [95].

reduction of CO_2 to HCOOH or CO at Pd, Pt and Hg electrodes is not commercially viable due to the high cost of these electrodes [15,229–231].

The CO_2 reduction into oxalic acid at −0.9 V (vs. NHE) and glyoxylic acid at −1.8 V in aqueous solution containing tetramethylammonium ions at pH 9 was noted over the surfaces of carbon and Hg cathodes when experiments were performed in a three compartment electrochemical cell, in which the compartments were separated by a cation exchange membrane [232]. The working electrode was a Shandon–Southern graphite disc electrode (5.0 cm diam.), the counter electrode was Pt gauze, and the reference electrode was Ag/AgCl. Electrolysis was carried out at −0.9 V (vs. NHE) for 3.25 h at 1.2 mA, the solution from the cathodic compartment was passed through an ion exchange column and then freeze dried to yield oxalic acid (1.3×10^{-4} mol or 78%).

The complete literature reported on aqueous reduction of CO_2 on Cu electrodes up to the year 2006 was also summarized in a recent review article, in which, it was concluded that the product distribution varies with the reaction conditions such as potential, buffer strength and local pH, local CO_2 concentration, stirring, the type and amount of other ions present in the solution, and CO_2 pressure employed [85]. The product distribution is also found to be highly sensitive to the surface crystal structure of Cu electrode. Nevertheless, the conversion of CO_2 into hydrocarbons in electrochemical cells has been considered to be an interesting and potentially useful reaction [200,201]. Furthermore, it was also concluded that Cu is a potential cathode metal for electrochemical CO_2 reduction into hydrocarbons.

The formation of syngas was noted at room temperature when CO_2 reduction reaction was performed in aqueous electrolyte by employing gas diffusion electrodes (GDEs) implanted with an aqueous $KHCO_3$ (pH buffer) layer between the Au/Ag based cathode catalyst layer and the Nafion membrane [233,234]. Fig. 8 shows an electrochemical cell that was employed to perform CO_2 reduction using GDEs and Nafion membrane [88]. Au catalyst exhibited a lower overpotential of 200 mV in comparison to Ag catalyst for this reaction. A decrease in CO current efficiency was noted with the increase of overall current density efficiency, which has been attributed to CO mass-transport limitation. The overall cell (with Pt–Ir as anode catalyst) energy efficiency was found to be about 47% at 20 mA cm^{-2} that has been decreased to about 32% at 100 mA cm^{-2} for both catalysts. Joule heating losses were identified to be responsible for these noted losses. On supported Au catalyst, the current densities as high as 135 mA cm^{-2} for CO formation for a short period were noted [233]. The noted ratio between CO and H_2 was 1:2 at a potential of about −0.2 V vs. SCE with a total current density of 80 mA cm^{-2}. This ratio is preferred for methanol synthesis following thermochemical route. A decrease in the catalyst selectivity for CO evolution with time was also noted [234].

When Mo [219–221] and several types of Ru electrodes [220,235–238] were employed, methanol formation in electrochemical reduction of CO_2 with Faradaic efficiencies up to 60% at current densities less than 2 mA cm^{-2} was observed. The highest current densities up to 33 mA cm^{-2} and Faradaic efficiencies greater than 100% were also observed towards methanol formation over the surface of oxidized Cu electrodes [239]. A six-electron reduction mechanism was considered to determine these efficiencies. An improved activity and selectivity for CO_2 reduction were also noted when Cu catalysts were subjected to some surface modifications [240–242]. The maximum amounts of methanol were noted on an intentionally preoxidized Cu electrode at a partial current density of 15 mA cm^{-2} [239]. However, these results were found to be not reproducible, even when employed the oxidized Cu as a cathode [241]. Nevertheless, a continuous steady formation of methanol on Cu electrode at a high current density is yet to be seen [138].

The Cu-based alloys such as Cu–Ni, Cu–Fe, formed by in situ deposition exhibited decreasing yields towards CH_4 and C_2H_4 in the electrochemical CO_2 reduction while increasing HER with the increase of Ni or Fe coverage on the surface of Cu [228]. The formation of CH_4 and C_2H_4 was noted when Cu–Cd was employed as a cathode in this reaction. With the increase of Cd coverage CH_4 and C_2H_4 yields decreased and CO yields increased [242]. When Cu based alloys such as Cu–Ni, Cu–Sn, Cu–Pb, Cu–Zn, and Cu–Cd were employed, CO and $HCOO^-$ were noticed as major products [202]. The surface alloying on Cu–Au electrodes severely suppressed the formation of hydrocarbons and alcohols, and increased the formation of CO.

6.1.1. *Effects of aqueous medium on CO_2 reduction reaction*

The understanding of the underlying reaction mechanisms in aqueous electrochemical CO_2 reduction reactions has been advanced by conducting numerous experiments in aqueous solution [88]. However, liquid phase CO_2 electrocatalytic reduction has been found to suffer from several serious problems such as (i) sluggish reaction kinetics (which leads to >1.0 V (vs. NHE) overpotential and greatly increases the energy cost for electrolysis process); (ii) low selectivity of CO_2 reduction (CO_2 reduction and

Table 6

$$\text{Current efficiency} = \frac{\text{current due to formation of product X}}{\text{total current measured}} \times 100\%$$

Cathode metal	Potential (V vs. SHE)	Current efficiency (%)				Electrolyte	Reference
		H_2 gas	CH_4	CO	HCOOH		
Cu (100)	−1.39	10.3	19.8	1.9	11.7	0.1 M $KHCO_3$	[138]
Cu (111)	−1.52	13.1	15.5	4.9	16.6	0.1 M $KHCO_3$	[138]
Cu	−1.44	20.5	33.3	1.3	9.4	0.1 M $KHCO_3$	[357]
In	−2.16	13.2	n.a.	4.2	83.2	0.1 M TEAP	[231]
Sn	−2.16	61.6	n.a.	4.2	37.6	0.1 M TEAP	[231]
Zn	−2.16	35.2	n.a.	16.8	53.4	0.1 M TEAP	[231]
Pb	−1.63	5.0	0.0	0.0	97.4	0.1 M $KHCO_3$	[357]
Au	−1.14	10.2	0.0	87.1	0.7	0.1 M $KHCO_3$	[357]
Ag	−1.37	12.4	0.0	81.5	0.8	0.1 M $KHCO_3$	[357]
Zn	−1.54	9.9	0.0	79.4	6.1	0.1 M $KHCO_3$	[357]
Ni	−1.48	88.9	1.8	0.0	1.2	0.1 M $KHCO_3$	[357]
Fe	−0.91	94.8	0.0	0.0	0.0	0.1 M $KHCO_3$	[357]
Pt	−1.07	95.7	0.0	0.0	0.0	0.1 M $KHCO_3$	[357]
Ti	−1.60	99.7	0.0	Trace	0.0	0.1 M $KHCO_3$	[357]
Pd	−1.20	26.2	2.9	28.3	2.8	0.1 M $KHCO_3$	[357]
Ga	−1.24	79.0	0.0	23.2	0.0	0.1 M $KHCO_3$	[226]
Cd	−1.40	39.0	0.1	14.4	39.0	0.1 M $KHCO_3$	[226]
Co	−1.40	102.0	0.3	0.0	0.0	0.1 M $KHCO_3$	[226]
Ru	−1.40	111.0	0.0	0.0	0.0	0.1 M $KHCO_3$	[138]
Ir	−1.40	99.0	0.1	0.0	0.0	0.1 M $KHCO_3$	[226]
W	−1.40	102.0	0.1	1.9	0.0	0.1 M $KHCO_3$	[226]
Mo	−1.40	103.0	0.0	0.0	0.0	0.1 M $KHCO_3$	[226]
Ta	−1.40	90.0	0.1	0.9	0.0	0.1 M $KHCO_3$	[226]
V	−1.40	86.0	0.1	1.1	0.0	0.1 M $KHCO_3$	[226]
Pb	−1.40	41.0	0.1	3.4	50.0	0.1 M $KHCO_3$	[226]

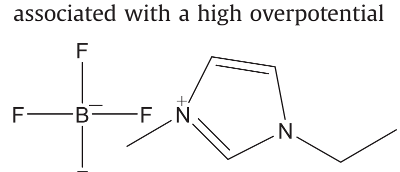
HER are competitive reactions); (iii) H_2 is inevitably a byproduct accompanying with CO_2 reduction in aqueous electrolyte; (iv) formation of various byproducts (they mainly remain in electrolyte solution, hence, the separation and recovery processes become expensive); (v) low solubility of CO_2 in aqueous electrolyte ($\approx$ 0.08 M) (high pressures are normally needed to increase CO_2 transport), deactivation of electrodes (the electrode catalysts lose their initial high activity and selectivity after a short period of operation); and (vi) low tolerance to impurities and contaminations (the surface contamination and non-pure electrolyte will often lead to low productivity and selectivity of hydrocarbon products; which are difficult to overcome), etc. [88].

6.1.2. Gas diffusion electrode (GDE) and solid polymer electrolyte (SPE)

Gas diffusion electrodes (GDEs)/solid polymer electrolytes (SPEs) including cation exchange membrane (CEM) and anion exchange membrane (AEM) have solved certain problems associated with the liquid phase CO_2 electrocatalytic reduction reactions and improved the mass transfer of CO_2 [88,204,207,209,243,244]. GDE is a porous composite electrode normally used in fuel cells. GDE is usually composed of Teflon bonded catalyst particles and carbon black. SPE membrane with GDE is expected to provide improved gas phase electrolysis of CO_2. Considerable improvements were noted when GDE/SPE-based electrodes were employed in place of several metal electrodes in the optimized conditions for electrocatalytic reduction of CO_2. Among the various metal electrodes investigated for CO_2 reduction reaction using GDEs, the Cu electrodes were found to be more efficient. Several metal oxides such as ZnO, ZrO_2, TiO_2, Al_2O_3 and Nb_2O_3 have been employed as supports for Cu metal catalysts. The pure oxide supports exhibited very little activity for CO_2 reduction, and HER was the main reaction indicating that Cu is an essential element for reducing CO_2. Cu up to 5 wt% exhibited very little activity for the CO_2 reduction, but when it was 50 wt% produced about 44% HCOOH and 4.4% CO. Thus, based on these results it can be concluded that GDEs are advantageous for these electrochemical CO_2 reduction reactions. The gaseous products noted in these reactions were mainly CO, methane and ethylene, whereas the liquid product was only formic acid.

6.1.3. Effects of room temperature ionic liquids (RTILs) over electrochemical reduction of CO_2

Recently, the Department of Energy (DOE), USA, has concluded that the major obstacle that is preventing efficient conversion of CO_2 into energy-bearing products is the lack of efficient catalysts [94,233]. Hence, DOE has called for research that investigates systems to reduce the overpotential of CO_2 conversion while maintaining high current efficiencies. The large overpotentials associated with electrochemical CO_2 reduction reactions have been identified to be due to the formation of a high energy intermediate $CO_2^{\cdot -}$ with a standard redox potential of −1.3 V vs. NHE. A room temperature ionic liquid (RTIL) comprising 1-ethyl-3-methylimidazolium tetrafluoroborate ($EMIM\text{-}BF_4$) (Eq. (26)) has been found to reduce the overpotential associated with the formation of $CO_2^{\cdot -}$ intermediate [94]. In this case, first, $EMIM\text{-}BF_4$ RTIL appears to convert CO_2 into $CO_2^{\cdot -}$ intermediate, which is then catalyzed over a transition metal cathode to form useful products such as CO. Furthermore, in this process, CO was formed at −250 mV overpotential vs. NHE in comparison to −800 mV in the absence of $EMIM\text{-}BF_4$ RTIL. These results indicate that CO_2 conversion to CO can occur without the large energy loss associated with a high overpotential



(26)

Like strong acids, such as H_2SO_4, HNO_3, and HCl, RTILs also completely dissociate into ions and are not diluted by any bulk solvent. Further, because of their poor vapor pressures at room temperature unlike acids like HCl, RTILs are thermally and electrically quite stable. Further, these RTILs consist of a bulky organic cation (e.g. imidazole) and an organic/inorganic anion (e.g. tratrafluoroborate, hexafluorophosphate). Owing to their poor coordinating nature, they are highly polar solvents without coordinating strongly to solutes. Besides, due to their low volatile nature, these RTILs are also environmentally friendly unlike organic solvents

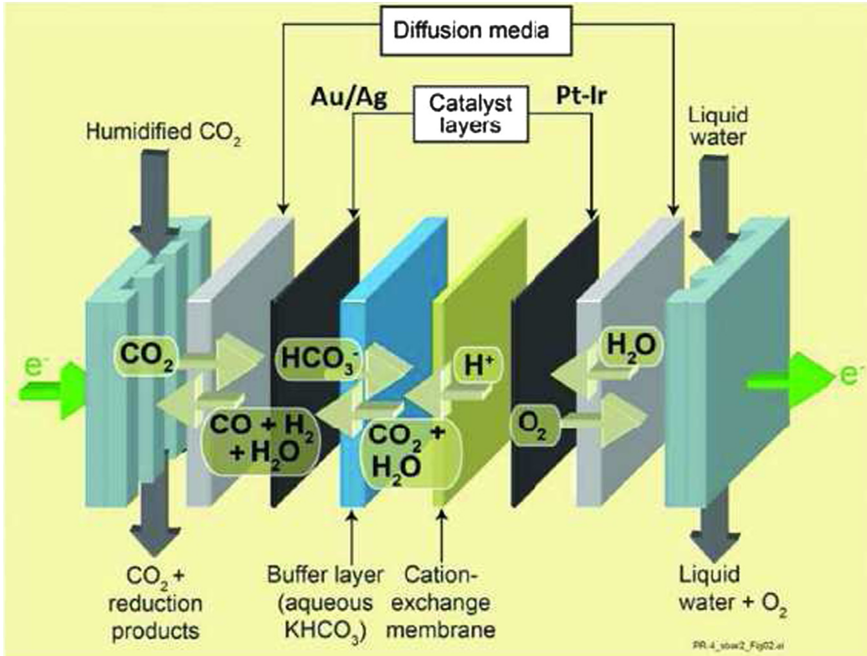


Fig. 8. Schematic representation of an electrolyte cell for producing synthesis gas ($CO+H_2$) by reduction of CO_2 and H_2O [88].

with significant vapor pressures, and RTILs also do not need any supporting electrolyte in electrochemical cells as they can bear 3–6 V charge [94].

High overpotentials are mainly responsible for not able to convert CO_2 into potential liquid fuels economically so that they can be employed in the present energy distributing infrastructure in place of fossil fuels. Furthermore, the overpotentials associated with CO_2 conversion in aqueous environments are partly due to its competition with HER. However, even when metals with high overpotentials towards HER are employed, there has been a considerable amount of overpotential for CO_2 conversion. This overpotential has been found to be due to the formation of reaction intermediates. The rate-limiting step in CO_2 reduction process has been determined to be the formation of a high energy $CO_2^{\cdot -}$ radical anion intermediate. This high-energy intermediate radical anion presents a large barrier towards the DOE's goal of CO_2 conversion at low overpotentials. The formation of $CO_2^{\cdot -}$ radical anion in aqueous solvents needs energy between -1.85 V and -1.90 V vs. NHE. Interestingly, owing to their ionic characteristics, RTILs stabilize the intermediate $CO_2^{\cdot -}$ in situ during CO_2 reduction reaction by columbic complexation. This stabilization considerably lowers the electrode potential required for CO_2 reduction [94]. The activation energy (overpotential) needed to form the $EMIM^+–CO_2^{\cdot -}$ intermediate has been found to be very low when compared with the one required to form $CO_2^{\cdot -}$ without stabilization by RTIL. Fig. 9 shows the overpotential reduction due to the involvement of RTIL [94]. In the presence of $EMIM^+–BF_4^-$, CO_2 reduction starts at as low as -250 mV vs. NHE as RTIL reduces about 80% of overpotential required for CO_2 reduction. Fig. 10 shows the calculated Faradaic efficiency of RTIL involved process with other processes reported in the literature for CO_2 reduction over a period of 10 years [94]. As CO_2 cannot survive in basic solution, neutral to slightly acidic media is employed for electrochemical reduction of CO_2. The HER is a strong function of pH and with increase of pH, the equilibrium potential towards this latter reaction decreases. Though CO_2 reduction produces hydroxide anions, its equilibrium potential is not much influenced by the pH in comparison to HER. Hence, under slightly acidic conditions, the HER is a thermodynamically preferred reaction in comparison

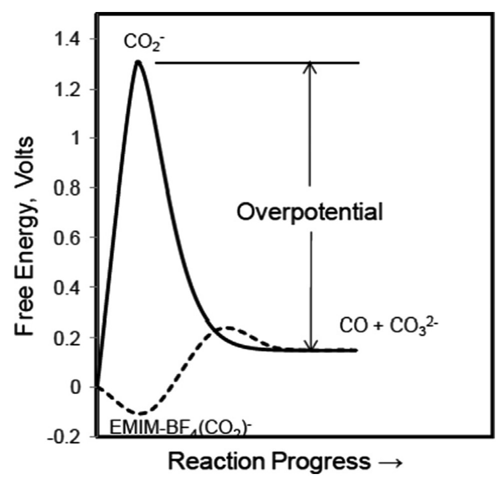


Fig. 9. Hypothesis for how and ionic liquid or amine could lower the overpotential for the CO_2 reduction [94].

to the reduction of CO_2. In aqueous medium, all the CO_2 reduction reactions lead to the formation of hydroxide ion. Due to hydroxide ions' formation, the pH near to the surface of the electrode is different from the equilibrium value as the rate of neutralization between the hydroxide anion and CO_2 is considerably slow in aqueous solution under ambient conditions [245]. Thus, the pH near the electrode surface is higher when compared with the rest of the solution pH. As high pH conditions do not favor CO_2 reduction, its reduction process is severely affected with reaction time. For this reason, electrolytes such as $KHCO_3$ or K_2HPO_4 are normally employed for CO_2 reduction reactions as they supply anions with buffering action, and can serve to diminish the pH changes occurred during reaction at the electrode surface. The reactions that normally take place due to surface neutralization of the hydroxide anion through these buffer solutions are shown in Eqs. (27) and (28) [94]. Certain salts such as KCl, $NaClO_4$, and K_2SO_4, which do not have the ability to release protons, are not preferred as supporting electrolytes for electrochemical CO_2 reduction reaction in aqueous medium. It can be inferred from

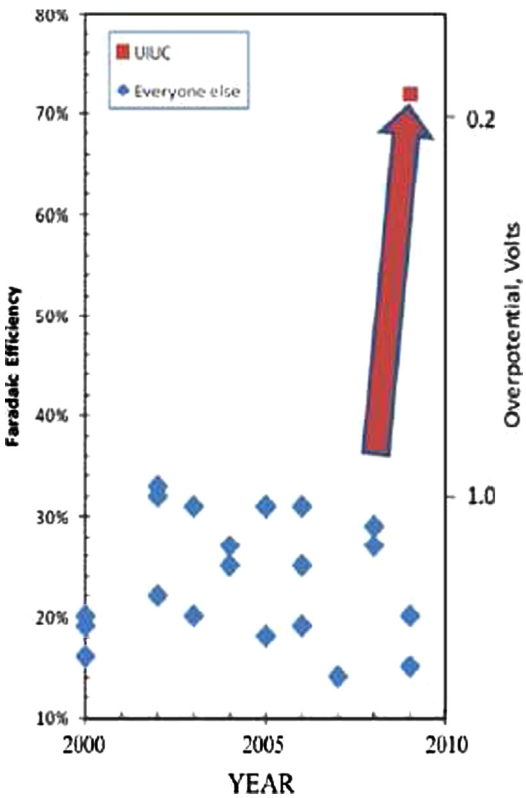


Fig. 10. Comparison of over-potential and Faradaic efficiency between this study and previous works [94].

these results that EMIM-BF_4 has several useful characteristics for reducing CO_2 at relatively less negative potentials and low temperatures in nonaqueous medium such as acetonitrile [94]

$$OH^- + HCO^{3-} \rightarrow H_2O + CO_3{}^{2-} \quad (27)$$

$$OH^- + HPO_4{}^{2-} \rightarrow H_2O + PO_4{}^{3-} \quad (28)$$

6.1.4. Effect of chemical modification on the efficiency of metal cathodes

In electrolytic CO_2 reduction reactions over Pd, Pt or Hg electrodes, the reduction of CO_2 is mainly restricted to only HCOOH or CO [92]. These metal electrodes exhibited Faradaic efficiencies of about 50% and at times nearly 100%. In a process patented in USA [211], Mo metal was employed as a cathode to reduce CO_2 to CH_3OH with high selectively and about 80–100% Faradaic efficiency. Reductions occurred at −0.7 V vs. saturated calomel electrode (SCE) at pH 4.2, only 160 mV negative of the standard reduction potential corrected for pH. These electrochemical experiments were conducted using CO_2 gas circulated in a closed system [219]. Tables 7 and 8 show the Faradaic efficiencies for the electrochemical CO_2 reduction reactions conducted under the saturated aqueous solution of 0.2 M Na_2SO_4 (pH 4.2) or 0.05 M H_2SO_4 (pH 1.5) with an HCl or a KOH/HF pre-treated Mo electrode, respectively [211]. The Faradaic efficiency for methanol formation is as high as 85%. The noted Faradaic efficiency for CO was <5% means >95% is methanol formation. The KOH/HF pre-treated electrodes provided <3% Faradaic efficiency for CO formation. In contrast to Ru electrodes [220], the efficiency and product distribution on Mo cathode did not change much with the solution temperature even when raised to 52 °C. The formation of CH_4 in these reactions was noted only in trace amounts. The lack of Faradaic

Table 7
Faradaic efficiencies for CH_4, CO, and CH_3OH formation on HCl pre-treated molybdenum electrode [211][a].

Electrolyte	Temp. (°C)	E (V vs. SCE)	J[b] (μA cm^{-2})	Q (coul.)	Efficiency[c]		
					CH_4	CO	CH_3OH
0.2 M Na_2SO_4	22	−0.70	26	11.8	2	21	42
0.2 M Na_2SO_4	22	−0.80	50	8.5	ND	3	55
0.05 M H_2SO_4	22	−0.57	100	50	3	1.5	23
0.05 M H_2SO_4	22	−0.68	550	86	0.15	0.11	3.7
0.05 M H_2SO_4	22	−0.68	310	18.7	ND	0.2	46
0.05 M H_2SO_4	52	−0.60	590	87.6	ND	0.5	21

[a] All controlled potential electrolysis in CO_2 saturated solutions.
[b] Average current density.
[c] % Faradaic efficiency.

Table 8
Faradaic efficiencies for CO and CH_3OH formation on KOH/HF pre-treated molybdenum electrode [211][a].

Trial	Time (h)	E (V vs. SCE)	J[b] (μA cm^{-2})	Q (coul.)	Efficiency[c]	
					CO	CH_3OH
1[d]	46.9	−0.52 to −1.1	100	16.9	0.3	77
2 A	23.3	−0.8	120	13.9	ND[g]	84
2B[e]	72.3	−0.8	57	21.5	0.4	36
3A	43.4	−0.8	61	27.5	ND[g]	45
3B[f]	69.8	−0.8	33	24.4	ND[g]	15

[a] All in CO_2 saturated 0.2 M Na_2SO_4 solution at 22 °C.
[b] Average current density.
[c] % Faradaic efficiency.
[d] Controlled current electrolysis.
[e] 2B is a continuation of 2A after sampling. Numbers for 2B do not include electrolysis before sampling.
[f] 3B represents the electrolysis of a fresh solution with the electrode used in 3A without pretreatment. Number for 3B do not include electrolysis before sampling.
[g] ND, not detected.

balance for these reactions has been attributed to HER as H_2 gas formed could not be detected by the flame ionization detector (FID) fixed in the gas chromatography (GC) employed for products analysis. The standard potential for reduction of CO_2 to methanol is −0.536 V vs. SCE at pH 1. Thus, the reduction of CO_2 to methanol is only 160 and 190 mV negative of the standard potential for pH's 4.2 and 1.5, respectively. Table 8 also shows the results for two extended electrolysis experiments conducted in 0.2 M Na_2SO_4 at pH 4.2 [211]. It can be seen that the electrode that had passed 14C over the period of 1 day produced methanol with a Faradaic efficiency of 84%. After another 2 days of continuous operation with another 22C passed, the methanol efficiency was dropped to 36% but its production did not come to a halt. The changes in the electrode surface during reactions have been suggested to be responsible for drop in the efficiency for this methanol formation reaction. This drop in efficiencies has been attributed to the deposition of impurities, such as Hg or As, on the electrode surface during reaction from the electrolyte [211].

6.1.5. Effect of molecular catalysts on the efficiency of metal cathodes

Everitt's salt (ES), $K_2Fe^{II}[Fe^{II}(CN)_6]$, in the presence of various metal complexes and a primary alcohol was employed as an electron

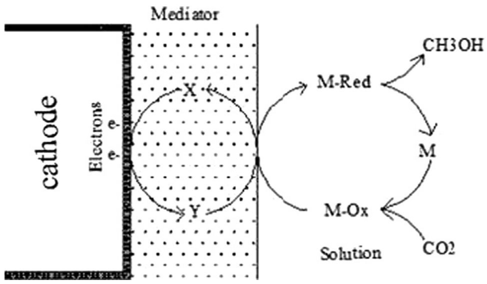


Fig. 11. Electron mediation process, where M, an homogeneous catalyst; X, oxidized mediator; Y, reduced mediator; M, Ox and M-Red, intermediates [246–248].

mediator to reduce CO_2 into methanol (Fig. 11) [246–248]. The reaction of CO_2 reduction into methanol in the presence of ES is shown in the following equation:

$$CO_2+6K_2Fe^{II}[Fe^{II}(CN)_6]+6H^+\leftrightharpoons CH_3OH+6KFe^{III}[Fe^{II}(CN)_6]+6K^++H_2O \quad (29)$$

The activation energies for methanol formation were estimated to be 5.8–10.6 kcal mol^{-1}, which are almost double in comparison to those determined for reduction of CO under identical experimental conditions employed. The IR spectra of the employed metal complex catalysts indicated that the reduction of CO_2 proceeds *via* a formate-type intermediate. The mechanism is more dominated by the insertion of CO_2 into M (central metal)–OR (primary alcohol) bond. The metal complexes employed were diaquabis(oxalato)chromate(III), K$[Cr(C_2O_4)_2(H_2O)_2]$, aquapentachlorochromate(II), $Na_3[Fe(CN)_5(H_2O)]$, aquapentachlorochromate(III), $[NH_4]_2[CrCl_5(H_2O)]$, and bis-(4,5-dihydroxybenzene-1,3-disulphonato)ferrate(III), $[Fe\{C_6H_2(OH)_2(SO_3)_2\}_2]^-$. The primary alcohol employed was either methanol or ethanol. Prussian blue (PB), $KFe^{III}[Fe^{II}(CN)_6]$, was first electrodeposited onto a platinum plate from a mixed solution of 0.01 M (mol dmm^3) $FeCl_3$ and 0.01 M $K_3Fe(CN)_6$ and was reduced to ES [249]. The average amount of the ES salt film deposited was estimated to be about 2.7×10^{-7} mol cm^{-2}. The formation of CH_3OH in these experiments was determined by both gas and steam chromatographic methods. The steam chromatograph employs steam as the carrier gas with a flame ionization detector and a Poropak R column, and the aqueous sample was analyzed without any pretreatment. Fig. 12 shows the steam chromatograms of the catalyst solutions containing the $[Fe\{C_6H_2(OH)_2(SO_3)_2\}_2]^-$ complex and ethanol [250]. Curve (a) is obtained before electrolysis, and (b) and (c) are after electrolysis for 3 and 6 h, respectively. In all curves, the peak at 7.6 min is due to ethanol that was added initially as a primary alcohol as a part of the catalytic system. In curves (b) and (c), two additional peaks appeared at 3.3 and 3.7 min. The first one is due to acetaldehyde produced by electrooxidation of ethanol in the anodic compartment that could be leaked to the test cell through the fine frit employed to separate two compartments, and the second peak is due to methanol, whose peak height after electrolysis for 6 h has been estimated to be equivalent to 2.3 μmol dm^{-3}. This result confirms that CO_2 can be reduced to methanol. Furthermore, this reaction can also be converted into a continuous process if the PB formed from ES during CO_2 reduction into methanol is continuously reduced back to ES by continuous supply of electricity [246,247,250–263]. Reaction shown in Eq. (29) was found to take place when the electrode potential was polarized in such way that the PB film undergoes reduction to ES [$<+0.15$ V vs. SCE]. As discussed in previous sections, the direct electrochemical reduction of CO_2 at a metal electrode surface requires a large overpotential (about -2.0 V vs. SCE), and hence reaction (Eq. (29)) results in a considerably lowering of the overpotential for the reduction of CO_2. Although yield of methanol in the CO_2 conversion was found to

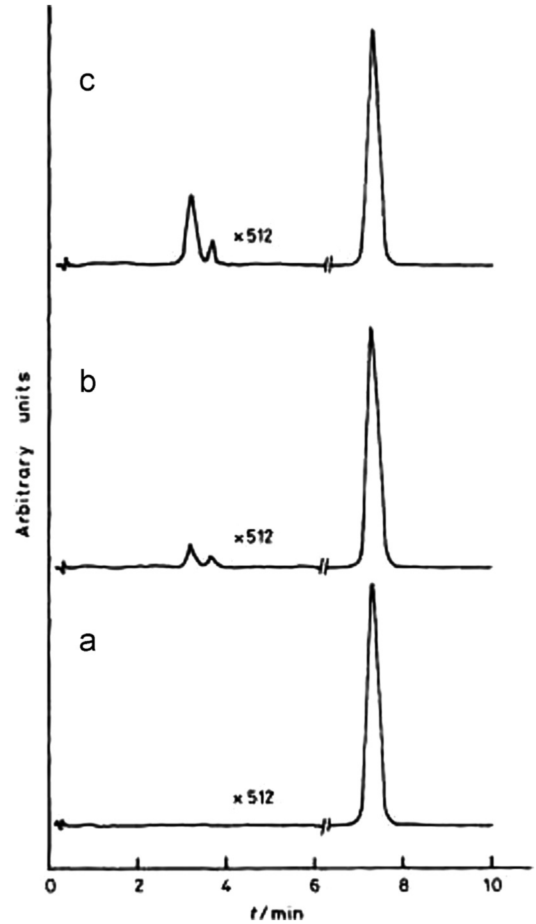
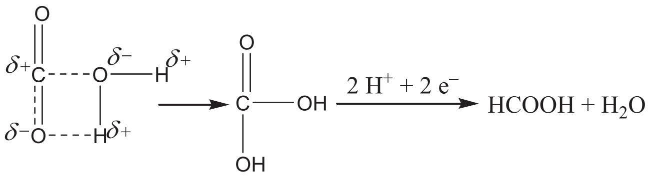


Fig. 12. Steam chromatograms of the catalyst solutions (0.1 mol dm^{-3} KCl, pH 3.5, 40 °C) containing 4 mmol dm^{-3} Fe^{III} – 8 mmol $dm^{-3}$$C_6H_2(OH)_2(SO_3)_2{}^{2-}$ and 20 mmol dm^{-3} ethanol before (a) and after electrolysis for 3 (b) and 6 h (c) at -1.0 V vs. SCE [250].

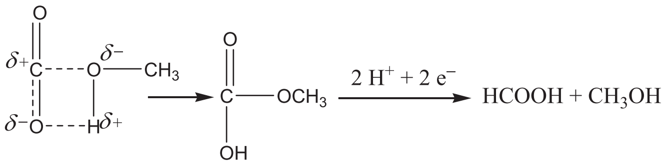
be very low for the catalyst solution containing ethanol, but it confirms the formation of methanol from CO_2. Nevertheless, when ethanol was replaced with methanol, much improved conversions were noted [246,247,250–263].

Fig. 13 shows that the formation of methanol has a linear relationship with reaction time [250]. At longer electrolysis times and higher temperatures, the lines become curved and this was due to the exhaustion of the reactant CO_2 and also due to the leakage of methanol formed from the reaction compartment. It was confirmed by FT-IR and cyclic voltammetry studies that the conversion of CO_2 into methanol takes place *via* a formate-type intermediate formation, and the metal complex operating as the catalyst suffered no degradation during electrolysis [246,247,250–263].

Scheme 9 shows a most probable underlying mechanism in this reaction [246–248]. A coordination bond is first formed between a central metal atom and a primary alcohol, and then CO_2 is inserted into this bond to form a formate-type intermediate. Finally, methanol and the initial complex are formed back by the reaction with ES. Furthermore, the current–potential studies also confirmed the formation of intermediates shown in Scheme 9 [261]. When experiments were conducted using either only pure aqueous 0.1 M KCl solution or the aqueous 0.1 M KCl solution containing methanol as an electrolyte, the formation of only HCOOH was noted. Eqs. (30) and (31) show the underlying mechanisms involved in these latter two different experimental conditions, respectively:

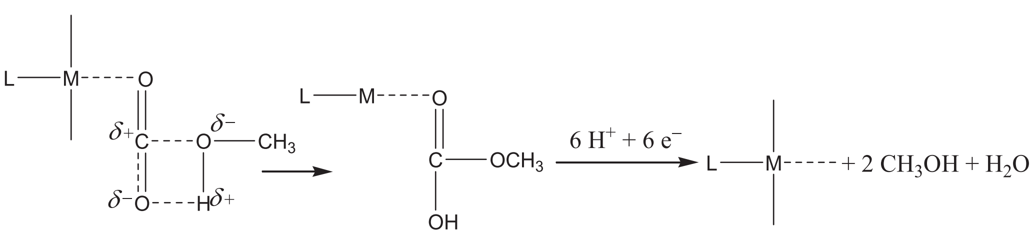


(30)



(31)

In the presence of only KCl electrolyte, CO_2 dissolves as carbonic acid, and gets reduced to HCOOH electrochemically, whereas in the case of KCl and methanol mixture, both mechanisms shown in Eqs. (30) and (31) were found to occur simultaneously, and the proportion of the occurrence was found to be a function of the concentration of added methanol. However, when a mixture of KCl, methanol and metal complex were employed as an electrolyte, methanol was identified as the sole reduction product. These results suggest that the simultaneous existence of a metal complex and methanol is indispensable for the reduction of CO_2 into methanol. Not only this, even the required electrons for CO_2 reduction must also be supplied from ES-modified electrode. In this latter case, the reduction of CO_2 occurs in concurrence with the oxidation of ES to PB. Furthermore, PB can be re-reduced electrochemically to ES, which operates as a mediator. Furthermore, in these latter reaction conditions, the metal complex must be involved as shown in the following equation:



(32)

From this study it can be concluded that CO_2 could be reduced to methanol using ES in the presence of a primary alcohol and a metal complex.

CO_2 has also been reduced to methanol using pyridine solution as a selective molecular organic catalyst in aqueous electrolyte solution over the surface of a hydrogenated Pd cathode [264]. In these latter experimental conditions, the formation of methanol was observed in aqueous electrolyte at electrode potentials, which fall within a few hundred millivolts of the standard redox potential. The aqueous 0.5 M KCl electrolyte with 10 mM *N*-methyl pyridinium ion was found to be an effective electrolyte [265]. In this study, Pd in the form of a rod and foil was employed as an electrode and a two compartment cell was employed to assure similar CO_2 pressures in both electrolyte compartments connected by an aqueous bridge containing the supporting electrolyte and terminated (on both sides) with a fine glass frit. A Pt foil was employed as the counter-electrode. Galvanostatic electrolytes were run employing current densities of about 30–50 μA/cm^2. The pH of the electrolyte solution was maintained at 5.0 by pumping CO_2. The cyclic voltammetry study revealed that pyridine exhibits its catalytic activity only at pH $\leq$ 5.4 as its p*K*a value is 5.25. At pH >7, pyridine did not reveal any cyclic voltammetric features, which indicates that the electroactive species are the protonated pyridinium cations. Furthermore, even in the absence of CO_2, pyridinium underwent reduction *via* an irreversible mechanism. Under aqueous conditions, reduction of pyridinium ions was found to be coupled *via* an electrocatalytic mechanism to the reduction of H^+ to H_2 as illustrated in Scheme 10 [266]. Pyridine has also been employed in several studies to reduce CO_2 to methanol at a variety of electrodes including Pd, in both aqueous and nonaqueous electrolytes [267]. In strongly acidic aqueous electrolyte conditions, pyridine was found to undergo reduction to piperidine at a Pd electrode [266]. According to the mechanism shown in Scheme 10, the dissolved CO_2 is reduced by species I to generate pyridine and reduced CO_2 product(s). Cyclic voltammetry study also indicated that CO_2 reduction takes place at ca. −0.55 V vs. SCE onset current. This corresponds to the thermodynamic potential for methanol formation at pH 5.4 (0.52 V vs. SCE) [80]. In this process, upon electrolysis for 19 h at ca. 40 μA/cm^2 under galvanostatic conditions, the electrode potential has not been observed to increase more than ca. 200 mV beyond the calculated methanol/CO_2 redox potential, which indicates the requirement of a very low (few hundred millivolts) overpotential. Furthermore, the H atom bonded to the nitrogen site in the reduced pyridinium species has been found to be a transferable reducing agent as no methanol formation was observed when *N*-methyl pyridinium ion was substituted in place of pyridinium ion during electrolysis for 50 h period. This study suggests that the Pd | pyridinium ion interface is the catalytic site for the relatively selective catalytic reduction of CO_2 into methanol with electrochemical yields in the range of 20–30% [264].

6.2. *Metal oxides and doped-metal oxides as cathode materials*

The CO_2 underwent electrochemical reduction into HCOOH and methanol with efficiencies of 40 and 7.7%, respectively, in acidic and neutral media over the surface of the RuO_2-coated boron-doped diamond electrode [237]. When the boron-doped diamond substrate was replaced with Ti metal substrate for RuO_2 catalytic film electrode under identical conditions, an improved Faradaic efficiency for methanol formation was also noted [236]. The presence of TiO_2 on Ti support together with RuO_2 has been found to be responsible for

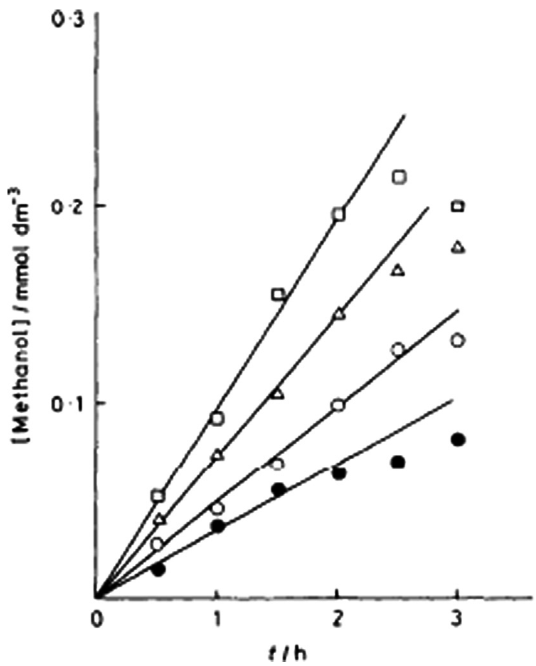
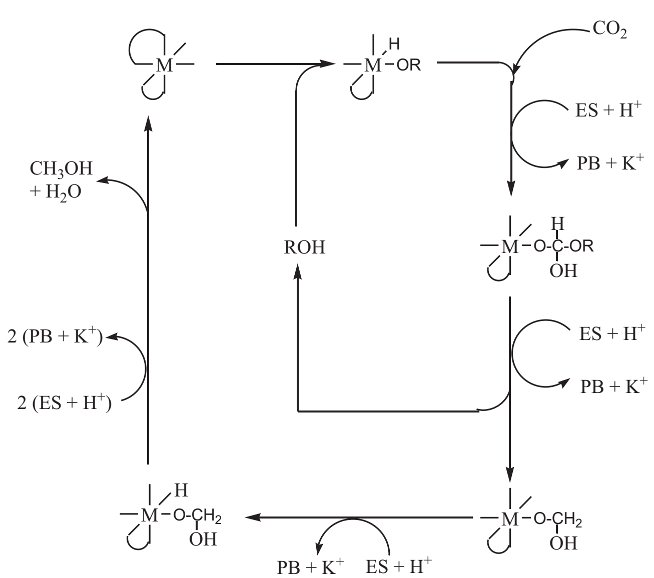
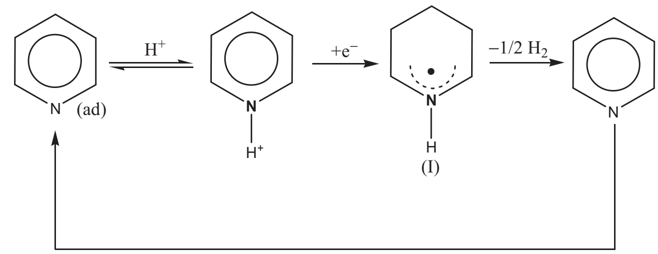


Fig. 13. Methanol formation as a function of time in a solution with 20 mmol dm^{-3} methanol and 5 mmol dm^{-3} pentacyanoferrate. Electrolysis potential, −0.9 V vs. SCE.; pH 3.5. Temperature: 20 (•), 30 (○), 40 (△), and 50 °C (□) [250].



Scheme 9. Proposed reaction mechanism [246–248].

the formation of enhanced methanol in this latter process [235,268]. Current–voltage curves at pH=4–7 showed a current-limiting behavior at small overpotentials for HER. The kinetic studies revealed that the surface recombination of adsorbed H_2 with CO_2 could be the rate-limiting step in these reactions. The CO_2 also underwent reduction to methanol and formic acid at relatively lower overpotentials over the surfaces of mixed oxides of RuO_2, TiO_2, Co_3O_4, MoO_2, Rh_2O_3, and SnO_2 [235]. In these studies, the CO_2 reduction was found to occur before the onset potential of HER. At low current densities (~50–100 μA/cm^2), when the electrodes were polarized near the H_2O reduction potential, a relatively higher current efficiency for methanol formation on mixtures of RuO_2+TiO_2 (35+65 m/o) and $RuO_2+Co_3O_4+SnO_2+TiO_2$ (20+10+8+62 m/o) is noted. For various oxides, the Tafel slopes found between 180 and 240 mV in 0.05 M H_2SO_4. The current



Scheme 10. Pyridine catalyzed electrochemical reduction of CO_2 over the surface of hydrogenated Pd electrode in aqueous 0.5 M KCl solution (below pH=5.5) [266].

efficiency for methanol dropped quickly with overpotential. The electrodes showed high stability against longtime polarization. When CO_2 was subjected to electrochemical reduction in 0.5 M $NaHCO_3$ solution in a two-compartment H-type electrochemical cell over the surface of Pt modified with RuO_2/TiO_2 NPs, the formation of methanol with a Faradaic efficiency from 40.2 to 60.5% was noted at −0.8 V vs. SCE [238]. The prolonged potentiostatic electrolysis of CO_2 resulted in the formation of methanol under low overpotentials. In comparison to both RuO_2 and RuO_2/TiO_2 nanoparticles (NPs) composite electrodes, the RuO_2/TiO_2 NTs composite modified Pt electrode provided higher electrocatalytic activity for the electrochemical reduction of CO_2 to methanol. The CO_2 also underwent electrochemical reduction to methanol and acetone over the surfaces of Ru, RuO_2 and RuO_x+IrO_x electrodes, and noted current efficiencies up to 15.3–38.2% the formation of methanol over these latter electrode materials [236]. The formation of methanol in electrochemical CO_2 reduction reaction over the surface of Cu oxides, specifically Cu(I), and Cu based ZnO (10–10) was also noted [95]. The methanol yields were found to be directly related to Cu(I) intensities over the oxidized Cu electrodes. Nevertheless, the formation of methanol was found to be stable over Cu and Cu oxides supported on ZnO electrodes for longer reaction time and these electrodes were also found to be reusable. The methanol yields and Faradaic efficiencies observed at cuprous oxide electrodes were found to be remarkably high when compared with those found on air-oxidized or anodized Cu electrodes suggesting Cu(I) species play a critical role in the selectivity to methanol formation [95].

Based on the above discussed electrochemical CO_2 reduction studies, the following conclusions can be drawn:

(i) Although CO_2 could be reduced into methanol and methane in electrochemical cells with considerably high product yields, the involved overpotentials are high. These high overpotentials lead to energy inefficient processes that offer little or no advantage since the quantity of fuel consumed during the products formation is higher than the fuel value of the formed products.
(ii) The electrodes that could reduced CO_2 electrochemically into methanol and CH_4 in an aqueous medium are certain metals (Ru [220], Mo [221] and Cu [200,201,221]), mixed transition metal oxides [200,201,221,235,268,269] and the illuminated *p*- and *n*-type GaP semiconducting electrodes [231].
(iii) In aqueous solutions, CO_2 reduction is always in competition with HER. This often led to low product and electrochemical yields. Several approaches such as the use of redox active enzymes [270,271], molecular redox mediators (methyl viologen polymer) [272], Prussian-blue modified electrodes [261], and polypyridyl transition metal complexes [273–276] have been employed to overcome the limitations posed by high overpotentials. Although some of these approaches could accelerate the rate of CO_2 reduction in comparison to HER, the problem of high overpotential still remains. Hence, although product yields were found to be high, their corresponding electrochemical

efficiency was found to be always extremely low. Typically, schemes which rely on the presence of mediators have built-in high overpotentials, as most known mediators have redox potentials which are substantially (typically ≥ 1 V vs. NHE) negative of the CO_2 reduction potential.

(iv) The reduction of CO_2 to hydrogenated organic products in aqueous solution is believed to proceed by the indirect chemical reduction of CO_2 with adsorbed H_2 atoms formed by the electrochemical reduction of protons [277,278]. Therefore, the efficient reduction of CO_2 calls for designing a system wherein specific poisoning of the electrode material toward HER is coupled with the catalytic reduction of the CO_2.

(v) Pyridinium ion molecular catalysts appear to solve these overpotential problems to some extent [267].

7. Photoelectrochemical reduction of CO_2 into methanol

In photoelectrochemical (PEC) cells, the semiconductor electrode immersed in the electrolyte is connected through an external circuit to a counter electrode. When this semiconductor electrode is illuminated by any light that is having energy higher than the band-gap of this semiconductor, its electrons excite from the valance band to conduction band, and reach cathode counter electrode through an external wire. Furthermore, the electron–hole pairs thus formed are spatially separated by the semiconductor junction barrier, and are injected into the electrolyte at the respective electrodes to produce electrochemical oxidation and reduction reactions [211,279–283]. As of now, not even single semiconducting material has been identified which can be employed as a photoelectrode to split water into hydrogen and oxygen gases or reduce CO_2 into methanol using exclusively solar energy in an aqueous based PEC cell with desired stability and efficiency [284–293]. In fact, photoreduction of CO_2 requires a thermodynamic energy input of about 1.5 eV. However, it needs greater energy input to make up losses due to band bending (necessary in order to separate charge at the semiconductor surface), resistance losses, and overvoltage potentials [211,279–283]. When a semiconductor is placed in an electrolyte, partial differences between the two phases result in charging of the interface. This charging results in a perturbation of the energy levels of the semiconductor called "band-bending". Band bending is responsible for separation of electron–hole pairs in PEC reactions. Recombination and corrosion processes decrease the utilization of the electron hole pairs generated on illumination. Furthermore, photoelectrolysis of water is a part of PEC CO_2 reduction in aqueous based PEC cells. However, photoelectrolysis of H_2O with high efficiency is difficult to achieve in PEC cells. This is due to the fact that the overvoltages associated with H_2 and oxygen formation at most moderate band-gap ($1.0 < E_g < 2.0$ eV) semiconductors are very high and if electron or hole transfer to the substrate does not occur rapidly, recombination of electron–hole pairs take place at surface defects or grain boundaries in polycrystalline semiconductors [211,279–283]. Although the electrolyte–semiconductor interface has excellent characteristics for separation of charge and for generation of high oxidation or reduction potentials when irradiated, it often has very poor catalytic properties for reactions with significant activation energies. H_2O is particularly an attractive source of H_2 for the reduction of CO_2 as well as for the direct generation of H_2. H_2O can only be used, however, if the semiconductor electrodes are stable in its presence. PEC production of energy-rich chemicals (for e.g., H_2, CH_3OH, CH_2O, CH_2O_2, and NH_3) is always associated with O_2 evolution [211,279–283]. A major impediment to the exploitation of PEC cells in solar energy conversion and storage is the susceptibility of small band-gap semiconductor materials to photoanodic and photocathodic degradation. The photo-instability is particularly severe for n-type semiconductors where the photogenerated holes, which reach the interface, can oxidize the semiconductor material itself. In fact, many of the semiconducting materials are predicted to exhibit thermodynamic instability toward anodic photodegradation. Whether a photoelectrode is stable or not depends on the competitive rates of the thermodynamically possible reactions such as the semiconductor decomposition reaction and the electrolyte reactions.

7.1. *Passivation of semiconducting materials against photocorrosion*

The *p*-GaP being a non-oxide ceramic it is not very stable against photocorrosion. A major problem in photoelectrochemistry is that the oxidation of H_2O at the photoanode of non-oxide n-type materials, which is thermodynamically and kinetically disfavored over the reaction of the valence band holes with the semiconductor lattice. In fact, all known non-oxide and many oxide *n*-type photoanodes are susceptible to photodegradation in aqueous electrolytes [211,279–283]. In certain instances, the surfaces of semiconductors are coated with non-corroding layers of metals and with the relatively stable semi-conductor films to arrest the corrosion problems. These continuous metal films which block solvent penetration can protect *n*-type GaP electrodes from photocorrosion. However, if the films are too thick for the photogenerated holes to penetrate without being scattered, they assume the Fermi energy of the metal. Then the system is equivalent to a metal electrolysis electrode in series with a metal–semi-conductor Schottky barrier. In such a system, the metal–semiconductor junction controls the photovolatge but not the electrolytic reactions. In general, a bias potential is required to drive the H_2O oxidation in a PEC conversion of CO_2 into methanol in aqueous electrolytes. In other cases, the metal can form an Ohmic contact that leads to the loss of the photoactivity of the semiconductor. In discontinuous metal coatings, the electrolyte contacts the semiconductor, a situation, which can lead to photocorrosion. For example, discontinuous gold films do not seem to protect n-type GaP from photocorrosion [211,279–283]. Corrosion-resistant wide band-gap oxide semiconductor (TiO_2 and titanates mostly) coatings over narrow band-gap n-type semiconductors such as GaAs, Si, CdS, GaP, and InP have been shown to impart protection from photodecomposition. However, a thick film blocks charge transmission, or a thin film still allows photocorrosion [211,279–283].

7.2. *The electroactive and the charge conductive polymers*

The chemical bonding of electroactive polymers to the semiconductor surface affects the interfacial charge-transfer kinetics such that the less thermodynamically favored redox reaction in the electrolyte predominates over the thermodynamically favored semiconductor decomposition reaction [282,283]. P-type semiconductors are relatively more stable against photocorrosion in comparison to n-type semiconductors. Furthermore, overvoltage for the evolution of H_2 from p-type electrode surfaces is quite large. It has been demonstrated, however, that the catalytic property of a *p*-type Si photocathode is enhanced for H_2 evolution when a viologen derivative is chemically bonded to the electrode surface and Pt particles are dispersed within the polymer matrix [282,283]. The *N*,*N*'-dimethyl, 4,4′-bipyridinium (methyl viologen, MV^{+2}) mediates the transfer of the photogenerated electron to H^+ by the Pt to form H_2. A thin Pt coating directly on *p*-type Si surface also improves the catalytic performance of the electrode. Charge conduction is generally much higher in electrically conductive polymers than in typical electroactive polymers [211,279–283]. The charge conductive polymers are also employed to protect electrodes against photodegradation in electricity-generating cells.

Charge conductive polymers transmit photogenerated holes in the semiconductor to oxidizable species in the electrolyte at much higher rate than the thermodynamically favored rate of decomposition of the electrode. In another study, *n*-type Si semiconductor photoelectrode was coated with charge conducting polypyrrole and found much improved stability against surface oxidation in electricity-generating cells [211,279–283]. The n-type GaAs has also been coated with polypyrrole to reduce photodecomposition in electricity-generating cells, although the polymer exhibited poor adhesion in aqueous electrolyte [211,279–283]. Although polypyrrole has suppressed the photodecomposition of n-type Si, it is not known whether these polymers can be used in conjunction with catalysts. Metal electrode surfaces were also modified with methyl viologen, MV^{+2}, a potential electron mediator to enhance rates of PEC reactions and to suppress photocorrosion and recombination [280]. An improved H_2 evolution was noted in the presence of MV^{+2}. The MV^{+2}/MV^{+1} system provides either an oxidized material, which is efficiently photoreduced, or a reduction product, which can efficiently transfer electrons to H_2O or H^+ ions at metal (Pt) catalysts to produce H_2 (Eq. (33)). On the surface of p-type semiconductor the reaction shown in Eq. (34) is expected. However, solutions of methyl viologen absorb visible light very intensively by the MV^{+1} species even if it is in low concentrations:

$$MV^{+2} \overset{h\nu,E}{\Longrightarrow} MV^{+1} \tag{33}$$

$$MV^{+1} + H_2O \xrightarrow{Pt} MV^{+2} + OH^- + \frac{1}{2}H_{2(g)} \tag{34}$$

7.3. Transition metal complexes as CO_2 reduction catalysts

Transition-metal complexes have been employed as photochemical and thermal catalysts because they can absorb a significant portion of the solar spectrum, have long-lived excited states, promote multi-electron transfer, and also activate small molecules through binding [279]. In transition-metal complexes, a central metal has octahedral, tetrahedral, square planar, square–pyramidal, or trigonal–pyramidal symmetry depending on the surrounding ligands. Reduced metal centers such as M^IL, in which the oxidation number of the central metal (M) is plus one, and the ligand (L) possess four-coordinating atoms with typically one or more vacant coordinate sites. These sites can be used to bind and activate CO_2 (or other small molecules). The CO_2 moiety is stabilized through two-electron transfer upon oxidative addition of CO_2 to M^IL to form a metallocarboxylate, $M^{III}L(CO_2{}^{2-})$. The $M^{III}L(CO_2{}^{2-})$ can then react with H^+ to form $M^{III}L$, CO and OH^-. The systems in which transition metal complexes are employed for photochemical reduction of CO_2 can be divided into the following six categories:

(i) $Ru(bpy)_3{}^{2+}$ (bpy – 2,2′-bipyridyl) as both the photosensitizer and the catalyst;
(ii) $Ru(bpy)_3{}^{2+}$ as the photosensitizer and another metal complex as the catalyst;
(iii) $ReX(CO)_3(bpy)$ (X=halide or phosphine-type ligand) or a similar complex as both the photosensitizer and the catalyst;
(iv) $Ru(bpy)_3{}^{2+}$ or $Ru(bpy)_3{}^{2+}$-type complex as the photosensitizer in microheterogeneous systems;
(v) *a* metallophorphirin as both the photosensitizer and the catalyst;
(vi) organic photosensitizers with transition-metal complexes as catalysts.

The Co (II) and Ni (II) complexes containing macrocyclic tetradentate nitrogen donor ligands have been employed for photocatalytic formation of H_2 linked to CO_2 reduction [294]. The $[LM^{II}]^{2+}$ (M=Co, Ni) complex employed has served as the redox shuttle as well as the catalyst in the presence of a $Ru^{II}(bpy)_3{}^{2+}$ photosensitizer and a sacrificial electron donor (an ascorbate). This reaction was found to be highly efficient and selective in contrast to certain PEC reactions [295]. Mechanisms believed to be involved in PEC systems containing transition-metal complexes are the following:

(i) light absorption by a photosensitizer to produce the excited state;
(ii) a quenching reaction between the excited state and an electron donor to produce a reduced complex;
(iii) electron transfer from the reduced complex to a catalyst;
(iv) activation of CO_2 by the reduced catalyst.

Nevertheless, the major products formed in the above discussed processes are mainly HCOOH and CO but not methanol [279,280].

7.4. Non-oxide p-type semiconductors as cathode materials

In 1978, for the first time a photoelectrode made of a single crystal *p*-gallium phosphide (*p*-GaP) was employed in a PEC cell for converting CO_2 into formic acid, formaldehyde and methanol [231]. Unlike the reduction of CO_2 on metal cathodes, which stops essentially after two electron transfer because of high overpotential associated with formic acid reduction, the photoelectrolysis on *p*-GaP proceeds further to yield formaldehyde and methanol. After 90 h of irradiation, the concentrations of formic acid, formaldehyde and methanol formed were estimated to be 5×10^{-2} M, 2.8×10^{-4} M, and 8.1×10^{-4} M, respectively. In this process, the efficiency of the system was calculated using the formula suggested by Arthur J. Nozik [284–293] and by Tomkiewicz and Woodall [296]. Optical conversion efficiency is nothing but the efficiency of conversion of radiant energy into the chemical energy. Optical conversion efficiency is equal to $100I_c\,[(\Delta H/Z)-V_B]/I_a)$; where I_c is the current density (mA cm^{-2}); I_a is the incident light intensity (mW cm^{-2}); ΔH is the heat of combustion (=2.962, 2.639, 5.915 and 7.259 eV, respectively, for hydrogen, formic acid, formaldehyde and methanol); Z is the number of electrons required in the reduction of one molecule of CO_2 to a molecule of product (=2, 2, 4 and 6 for production of hydrogen, formic acid, formaldehyde and methanol, respectively); V_B is the electrical bias (V). These results clearly indicate that in contrast to the reduction of CO_2 on certain metal cathodes, the photoelectrolysis on *p*-GaP does not stop after formic acid formation, but proceeds further, yielding formaldehyde and methanol.

Subsequent to the above study, there were several studies aimed at reducing CO_2 into highly reduced products using different types of semiconducting materials in PEC cells [297]. As part of this, CO_2 was also reduced to methanol over *n*- and *p*-GaAs, *n*-Si and *p*-InP semiconductors [219,298]. Reduction at *n*-GaAs was found to be selective with nearly 100% Faradaic efficiency. At pH 4.2, a potential of −1.2 V to −1.4 V vs. SCE was required to drive the reduction with high Faradaic efficiency against the theoretical value of −0.563 V vs. SCE at pH 4.2. The theoretical value could be calculated using heat of formation found in Selective Values of Chemical Thermodynamic Properties, United States National Bureau of Standards, Technical Note no. 290-2. However, these semiconductors are susceptible to corrosion [297,299]. The CO_2 was also reduced to HCOOH, HCHO, methanol and CH_4 over various other semiconducting materials that include WO_3, TiO_2, ZnO, CdS, GaP, and SiC [300]. HCHO and methanol were found to be the major products over SiC semiconductor catalyst after illumination for 7 h. The methanol yield was found to be increased as the conduction band becomes more negative with respect to

the redox potential of H_2CO_3/methanol, whereas methanol was not produced at all in the presence of WO_3 catalyst that has a conduction band more positive than this redox potential. The CO_2 was also found to be reduced electrocatalytically to HCOOH, HCHO, methanol and CH_4 at unilluminated TiO_2 electrode or at the illuminated *p*-GaP electrode when both semiconductor electrodes were polarized at a potential of −1.5 V vs. SCE for 2 h, which indicates that electrons in the conduction bands of these semiconductors reduce CO_2 in aqueous solution. It has been suggested that at semiconductor electrodes, the charge transfer rates between photogenerated carriers in semiconductors and the solution species depend on the correlation of energy levels between the semiconductor and the redox agents in the solution. If the redox potential of solution species is more positive with respect to the conduction band level, then these species undergo improved reduction. Fig. 14 illustrates the energy correlation at the semiconductor–solution junction [300]. The quantum yields for HCHO and methanol at TiO_2 catalyst were estimated to be $\sim 5.0 \times 10^{-4}$ and $\sim 1.9 \times 10^{-4}$, respectively, and with SiC, 5.0×10^{-4} and 4.5×10^{-3}, respectively.

The CO_2 also underwent reduction over a biological catalyst (a formate dehydrogenase enzyme) in a PEC cell over the surface of *p*-InP illuminated with a light source having wavelength range shorter than 900 nm (> 1.35 eV) [270]. This enzyme catalyst performs two electron reduction of CO_2 to formic acid with the help of a mediator that couples the photogenerated electrons in the semiconductor with the enzyme catalyst. Although this process appears to be more analogous to natural photosynthesis, the former process is more efficient at light collection and more specific in the production of reduced carbon species. When CO_2 was reduced over the surface of colloidal CdS particles in an aqueous solution of tetramethylammonium chloride that was illuminated with a visible light having the wavelength range of 320–580 nm up to 120 h, the formation of glyoxylic acid, HCOOH, HCHO and CH_3COOH was noted [301]. Furthermore, when CO_2 was reduced over *p*-InP, *p*-GaAs, and *p*-Si under a 40 atm. pressurized CO_2+methanol medium, the *p*-InP provided current densities up to 200 mA cm^{-2} with current efficiencies over 90% for CO formation [302]. The H_2 formation was found to be very meager in this latter process. When high current densities and CO_2 pressures were employed, the CO_2 reduction current was found to be primarily limited by the light intensity. Among the various reaction conditions varied, the CO_2 pressure was found to be very critical for obtaining higher product yields. When CO_2 reduction reaction was performed over *p*-GaP and *p*-GaAs semiconductors in a PEC autoclave fitted with a quartz window, a cation exchange diaphragm and a platinum counter-electrode under the illumination with a 150 W Xe lamp, the formation of HCOOH, HCHO and methanol was noted with a Faradaic efficiency of 80% on the surface of *p*-GaP at a cathodic bias of −1.00 V (vs. a standard silver electrode) in 0.5 M Na_2CO_3 solution under 8.5 atm. CO_2 pressure [303].

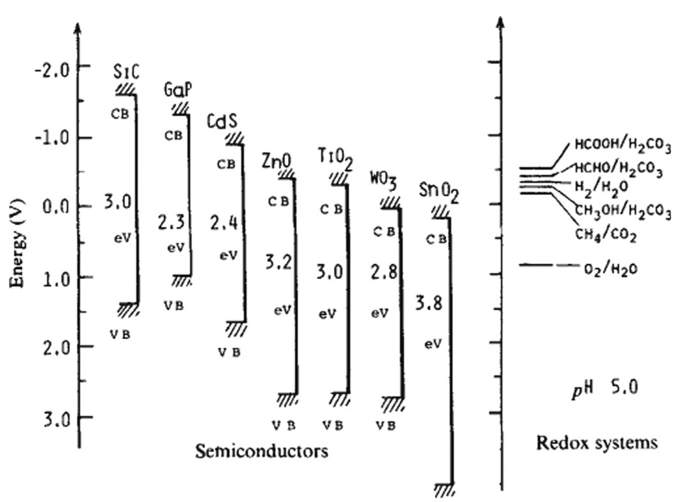


Fig. 14. A schematic illustration of the energy correlation between semiconductor catalysts and redox couples in water. CB and VB denote a conductive band and a valance band, respectively [300].

7.4.1. *Effect of molecular catalysts on the efficiency of semiconducting materials*

The CO_2 could also be reduced into methane, ethylene, and ethane in aqueous solution of Ru(II) tris(bipyridine) $[Ru(bpy)_3^{2+}]$ photosensitizer and triethanolamine [TEOA] electron donor under the illumination by visible light over the surface of Ru or Os colloid catalysts [304]. The bipyridinium charge relays employed in this process were *N*,*N*′-dimethyl-2,2′-bipyridinium $[MQ^{2+}]$, *N*,*N*′-trimethylene-2,2′-bipyridinium $[TQ^{2+}]$, *N*,*N*′-tetramethylene-2,2′-bipyridinium $[DQ^{2+}]$, or *N*,*N*′-bis-(3-sulfonatopropyl)-3,3′-dimethyl-4,4′-bipyridinium $[MPVS^0]$. In the absence of TEOA electron donor, H_2 also formed along with CO_2 reduction products, whereas in the presence of TEOA, no formation of H_2 was noted. CO_2 was also underwent reduction to methane when aqueous electrolyte had Ru colloids together with $Ru(bpz)_3^{+}$ [305]. In this latter process, an electron transition from $Ru(bpz)_3^{+}$ to the colloid-associated CO_2 was noted. Furthermore, when aqueous electrolyte was mixed with acetonitrile, triethylamine, Ru(2,2'-bipyridine)$_3^{2+}$ and cobalt(II) chloride, the formation of syngas was noted under the irradiation by visible light alone [306]. The formation of syngas in this process was found to be strongly influenced by the composition of the solution. Addition of free bipyridine drastically reduced CO formation but increased the formation of H_2. With different tertiary amines, NR_3, both the quantity ($CO+H_2$) and the ratio CO/H_2 increased markedly along the sequence R=methyl, ethyl, propyl. Higher selectivity towards CO formation than HER occurred when triethanolamine was used in place of triethylamine. $CoCl_2$ was found to be the most efficient electron mediator for both CO and H_2 formation, and has specifically promoted the formation of CO, whereas the salts of other cations investigated yielded only H_2. These processes represent an abiotic photosynthetic system allowing simultaneous formation of CO and H_2 with a regulated CO/H_2 ratio.

The CO_2 also underwent an electrochemical reduction selectively into methanol over the surface of a *p*-GaP with near 100% Faradaic efficiency at under-potentials greater than 300 mV below the standard potential of −0.52 V vs. SCE in a system pH of 5.2 containing pyridine as an organic molecular catalyst [264,307,308]. Fig. 15a shows the voltammetric response of an illuminated *p*-GaP electrode in the presence of 10 mM pyridine under argon or CO_2 at constant pH of 5.2 [264,307,308]. The *I*–*V* curves were recorded at illuminated *p*-GaP (Hg–Xe lamp 200 W) in 0.1 M acetate buffer containing 10 mM pyridine at pH 5.2 (black line) dark, (blue line) under Ar; (red line) under CO_2. The dashed line in this figure shows the standard potential for CO_2 reduction into methanol at pH 5.2. The radiant energy was solely used at potentials more positive than the line while electrical energy drove the reaction at potentials more negative than the line. Furthermore, as can be seen from this figure, there is an enhancement in current under CO_2, which has been attributed to the catalytic interaction between CO_2 and pyridinium ions. For *p*-GaP electrode, the measurements of the open circuit photovolatge revealed the flat-band potential to be 0.22 ± 0.01 V vs. SCE in the presence as well as in the absence of pyridine. Fig. 15b shows the photo-action spectrum for *p*-GaP at −0.4 V vs. SCE. With an indirect band-gap of 2.24 eV, the expected utilization of light should include wavelengths shorter than 550 nm. A measurable photocurrent was observed at wavelengths lower than 530 nm,

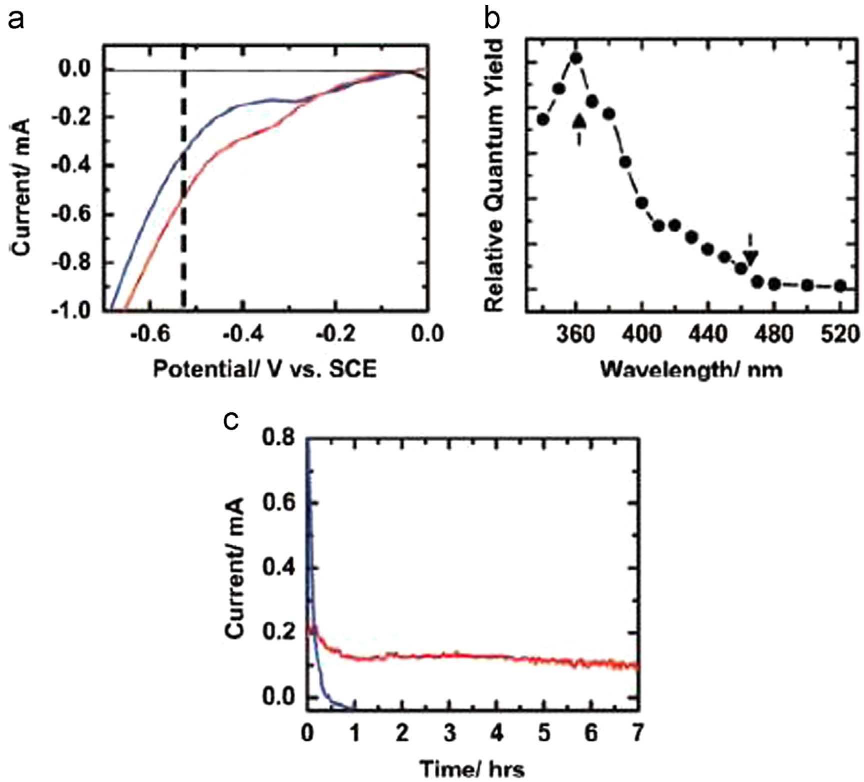


Fig. 15. (a) *I–V* curves, (b) photoaction spectrum and (c) time response for potentiostatic reduction of CO_2 at −0.4 V vs. SCE on illuminated *p*-GaP in 0.1 M acetate buffer containing 10 mM pyridine maintained at pH 5.2 [246,307,308]. (For interpretation of the references to color in this figure caption, the reader is referred to the web version of this paper.)

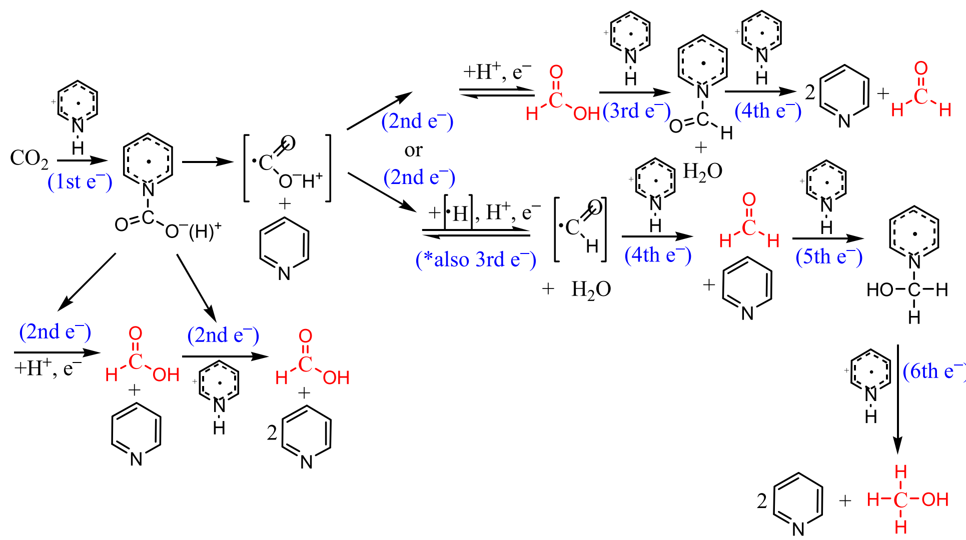
which is consistent with the indirect band-gap of the *p*-GaP. The sharp rise in photocurrent observed at 440 nm is indicative of the onset of the lowest energy direct band-gap (2.8 eV). In the absence of pyridine no formation of methanol was noted (Fig. 15c). However, in the presence of pyridinium, methanol formation was noted at −0.4 V vs. SCE with Faradaic efficiencies ranging from 88 to 100%. Both HCHO and HCOOH were not formed in this reaction [309]. At greater than 100 mV below the standard potential, the reaction was driven by radiant light. The initial photocurrent was observed to stabilize within an hour and then stayed steadily during experiments for the duration of 6–30 h. A 7 h run reaction can be seen from Fig. 15c. In similar studies, when high pressure arc light source was employed, the *p*-GaP electrode at a more negative potential (−0.5 V vs. SCE) led to a decreased Faradaic efficiency for the production of methanol with 22–25%. No change in the pyridine concentration was noted during entire time of the experiment.

The detailed underlying mechanism in the above reaction was reported in a recent article [308]. At metal electrodes, HCOOH and HCHO were observed to be the intermediate products along the pathway to the $6e^-$ reduced product of methanol, while pyridinium radical playing a major role in the reduction of both intermediate products. Pyridine molecule was found to be capable of reducing many different chemical species en route to methanol through six sequential electron transfers instead of metal-based multi-electron transfer (Scheme 11) [308]. Nevertheless, the two major drawbacks of this process are (i) *p*-GaP is not stable against photocorrosion for long reaction periods, and (ii) this process still requires certain amount of external bias voltage to run the CO_2 reduction reaction.

7.5. Oxide semiconductors as cathode materials

The photoreduction of CO_2 involves two main free radicals $H^{\cdot}$ and $^{\cdot}CO_2^-$, which are formed by taking electrons from photocathode (i.e., from semi-conductor), when the electrons of this semi-conductor are excited from the valence band to the conduction band by absorbing a photon having energy equal to or greater than that of the band-gap of the semiconductor. TiO_2 being a very stable material against photocorrosion and possesses band edges amenable to water oxidation/electrolysis reaction, it has been considered as an ideal material to use in PEC reduction or photocatalytic reduction of CO_2. Since the band-gap energy of TiO_2 is high (3.2 eV), which is equivalent to UV light, it cannot capture a larger portion of sunlight, hence, the efficiency of the system involving pure TiO_2 photoelectrode does not exceed 4% as the percentage of UV light in the entire solar spectrum is only about 4%. Several researchers have tried to improve the light absorbing capability of TiO_2 by doping it with several metals and non-metals [27,97,309–312]. In 1992, Cu powder was dispersed into an aqueous suspension of TiO_2 to enhance the photocatalytic activity of TiO_2 for reducing CO_2 into methanol [313]. The addition of Cu powder to TiO_2 not only creates reactive sites for CO_2 reduction with the excited electrons but also to reduce the recombination of photo-generated electron–hole pairs. When potassium bicarbonate (0.01 M $KHCO_3$) was introduced to the CO_2 saturated aqueous electrolyte suspended with TiO_2+Cu powder, almost the double yields of methanol were observed when compared with the bicarbonate-free solution [313]. Fig. 16 shows a model of the CO_2 photocatalytic reduction mechanism on Cu/TiO_2 [313]. When the light irradiation creates an electron–hole pairs (e^- and h^+) in TiO_2 and the $HO^{\cdot -}$ radicals and O_2 are formed by scavenging holes on TiO_2, then both CO_2 and H_2O molecules are interacted with the trapped electrons on the Cu clusters to form methanol [313]. The active solid surface for photocatalytic reduction of CO_2 on Cu-doped TiO_2 was also investigated [314].

The involvement of similar four distinct catalytic steps on the surface of Cu-doped TiO_2 during photocatalytic reduction of CO_2 in aqueous medium to those steps normally involved on the surface of a



Scheme 11. Overall proposed mechanism for the pyridinium-catalyzed reduction of CO_2 to the various products of formic acid (HCOOH), formaldehyde (HCHO) and methanol (CH_3OH) [308].

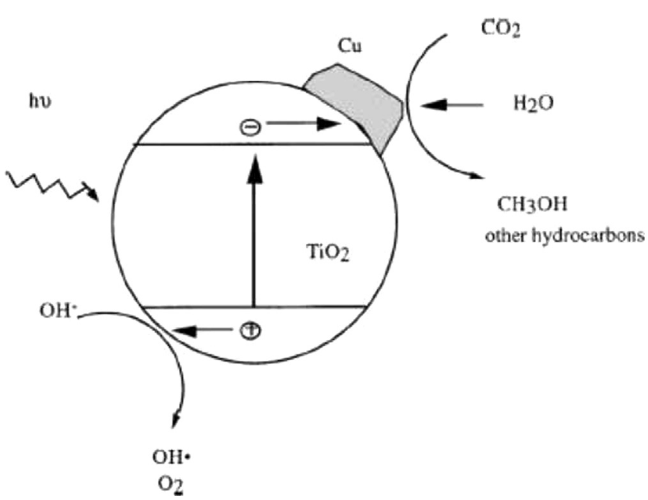


Fig. 16. Mechanism of CO_2 photocatalytic reduction on Cu/TiO_2 [314,315].

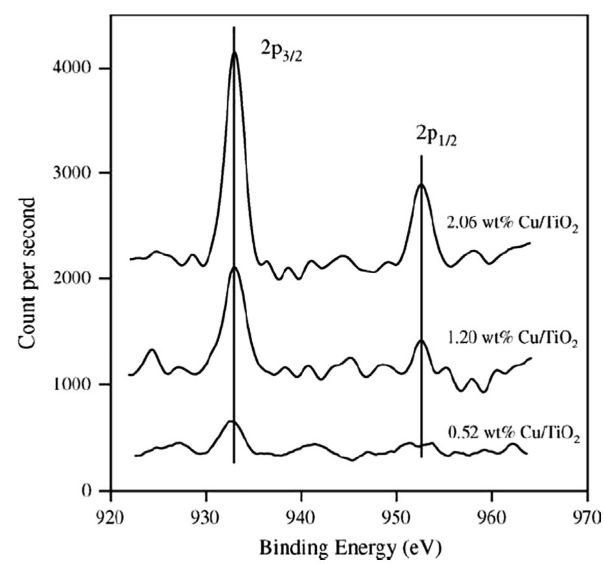


Fig. 17. XPS of Cu 2p on Cu/TiO_2 catalysts [317].

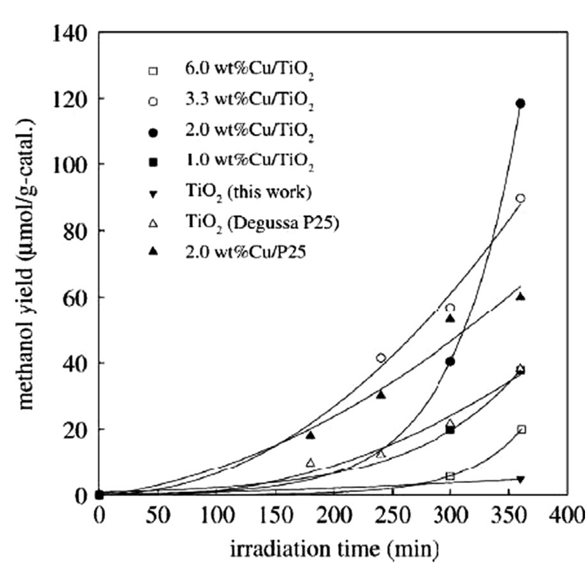


Fig. 18. Time dependence on the methanol yields of various catalysts [317].

heterogeneous solid catalyst during catalytic reaction was observed [314]. Those distinct catalytic steps include (i) photoelectron–hole pair generation, charge separation and trapping, (ii) oxidation and reduction reactions of the adsorbates, (iii) rearrangement and other surface reactions of formed intermediates, and (iv) the desorption of the products from the photocatalyst surface and the regeneration of the surface. The TiO_2 and TiO_2 supported Cu catalysts formed in a sol–gel route were also investigated for photocatalytic reduction of CO_2 [315]. A maximum yield of methanol at 0.45 m-mole/g catalyst/h over 1.2 wt% Cu/TiO_2 catalyst was noted by irradiating the CO_2 containing reaction mixture with a light having an intensity of about 16 W/cm^2 [316]. The XPS spectra of different amounts of Cu loaded TiO_2 powders revealed that Cu on TiO_2 exists in multiple oxidation states; however, Cu (I) were found to be the primary species (Fig. 17) [316]. The Cu_2O was found to serve as an electron trap to reduce the recombination rate of electron–hole pairs during excitation of the photocatalyst. The 2.0 wt% Cu/TiO_2 achieved highest dispersion among different amounts of Cu loaded TiO_2 catalysts. The methanol yield noted for this latter photocatalyst was about 118 μmol/g catalyst after 6 h of reaction under the irradiation by a UV light having the wavelength of 254 nm (Fig. 18) [316]. Nevertheless, these noted quantum efficiencies for CO_2 reduction even under UV light irradiation were very low [315,316]. The oxidized Cu species,

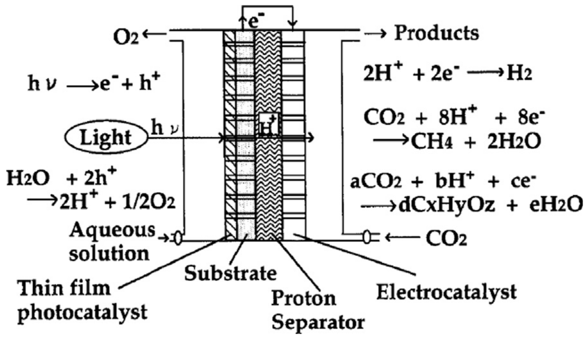


Fig. 19. Single unit photoelectrocatalysis system [322,323].

particularly the Cu/Cu(I) interfaces, were found to be the main active catalytic sites for electrochemical reduction of CO_2 into methanol [317,318]. Several other studies also confirmed that the Cu oxides, Cu cations, and the oxide interfaces are active catalytic sites for methanol formation in these photocatalytic reactions [162,319,320]. The ZnO stabilizes the oxidized Cu in hydrogenation reactions [316]. Furthermore, the electron–hole recombination was found to be the main reason for the noted lower photocatalytic efficiencies in this process. Product efficiency and selectivity was also found to be a strong function of catalyst composition involved. Even though Cu based TiO_2 has been identified to be a best composition for methanol formation in these photocatalytic reactions, in order to upgrade to an industrial scale process, the methanol yields need to be improved very significantly. Furthermore, to improve the efficiency of photocatalytic reaction under low intensity light, the specific surface area of the photocatalyst needs to be improved very significantly [316]. Since TiO_2 not only possesses required photocorrosion stability, band-gap energy, and band edges amenable to aqueous-PEC reduction of CO_2 into value added chemicals, but also a high photocatalytic activity for organic compounds' decomposition in an aqueous media, the photocatalytic CO_2 reduction reactions should not be conducted in a single-compartment photochemical cell using TiO_2 based photocatalysts, as the formed organic chemicals in these reactions will be decomposed back to again CO_2 and water on the surface of TiO_2 catalysts [27,97,309–312].

Not only powder catalysts, but also the thin films of Cu-doped TiO_2, and Cu containing zinc oxide surface coated Pt electrodes were employed for photocatalytic CO_2 reduction reaction in an aqueous based electrolyte [321,322]. Fig. 19 shows the schematic of a single unit photoelectrocatalysis system that was employed to reduce CO_2 [321,322]. This reactor consists of a perforated thin film of TiO_2 and an electrocatalyst, which were separated by a proton exchange membrane (Nafion, a DuPont brand). Since the photocatalyst and the electrocatalyst do not directly come into contact in this reactor, the recombination of titania-produced H^+ ions with dioxygen on the surface of electrocatalyst is totally avoided. Furthermore, as H^+ ions are effectively separated, they can be supplied to the electrocatalyst with minimum travel distance for efficient production of H_2 and/or for efficient hydrogenation of CO_2. It was also observed that the standard supported metal catalysts (Pt metal particles dispersed on TiO_2) were found to be much less efficient than this thin film catalyst [321,322]. Furthermore, in these experiments, a bias potential between photocatalyst and electrocatalyst was also applied to enhance the mobility of electrons generated in the photocatalyst. When a constant bias potential was applied between these two different catalyst systems, about 10.5% energy efficiency is noted. This energy efficiency is estimated by dividing the total heat energy attained by combustible products formed (as fuels) with the total photoelectrical energy supplied. The current efficiencies for methane, ethylene and H_2 were estimated to be about 17%, 11%

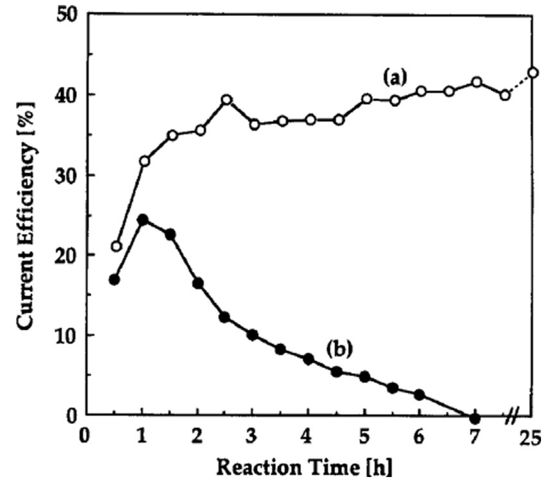


Fig. 20. Non-deactivating pulse bias operation for stable conversion of carbon dioxide to methane: (a) pulse bias and (b) constant bias [324].

and 42%, respectively indicating that the conversion of CO_2 was about 58% by hydrogenation. Other products detected in the solution were mainly HCOOH and ethanol. However, in this process, the deactivation of hydrogenation catalyst was found to be a major issue, which could be minimized by improving the selectivity of gaseous products like methane and ethane so that they escape easily from the solution and avoid the deactivation of the catalyst. This problem can also be solved by applying a bias potential in a pulsed mode. The pulse technique has been used in a regular electrochemical reduction of CO_2 with a pair of Cu electrodes, which normally prevent the deactivation of hydrocarbon formation catalyst [323]. Furthermore, when the pulsed mode technique was employed to supply bias potential, the noted results were remarkable and increased the activity for methane and ethylene formation. Fig. 20 shows an example case for CO_2 methanation by this technique on a photocatalyst of TiO_2/Ti, and electrocatalyst of ZnO/Cu. A similar feature was also noted even for ethylene formation in a 25 h run [323].

A prototype reactor (Fig. 21) was also employed to reduce CO_2 into CO and oxygen by direct solar irradiation [324]. In this first prototype PEC system, a solar focusing mirror and secondary concentrator were used to provide high solar intensity around a ceramic rod. This high-temperature and high solar irradiance environment heats up CO_2 so that it dissociates into CO and oxygen. Quenching of the back reaction was accomplished by the geometry and gas dynamics of the system. The best measured net conversion of CO_2 to CO was near 6%, whereas a plant design target is 12%. The peak observed conversion of solar energy to chemical energy was 5%. As per predictions, a mature system will yield 20% solar-to-chemical energy conversion with an additional 25% electrical energy generation. Fig. 22 shows the overall process energy balance goals [324]. It is reported that all these values are achievable simultaneously with the modest improvements in the mirror system and by changing the design in the exhaust channel/quenching system. The values in this figure are based on a hypothetical design with an optical power input of 100 kW. Of the 92 kW reaching the converter, 22 kW will be captured as chemical energy in the CO. The rate of energy capture of the final fuel product will depend somewhat upon the synthesis process chosen, but will be in the range of 18–20 kW. Most of the 70 kW of waste heat will be passed away at very high temperatures, enabling the harnessing of only 25 kW as electrical power when a standard steam turbine is employed. Converter system can be redesigned so that some of the waste heat can be recycled to preheat the CO_2 feed.

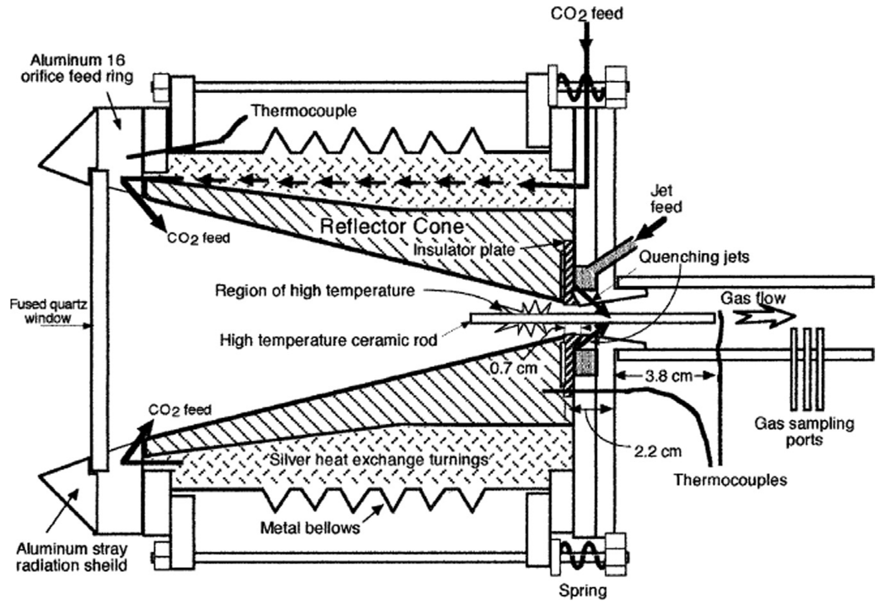


Fig. 21. Converter assembly for direct solar reduction of CO_2 [325].

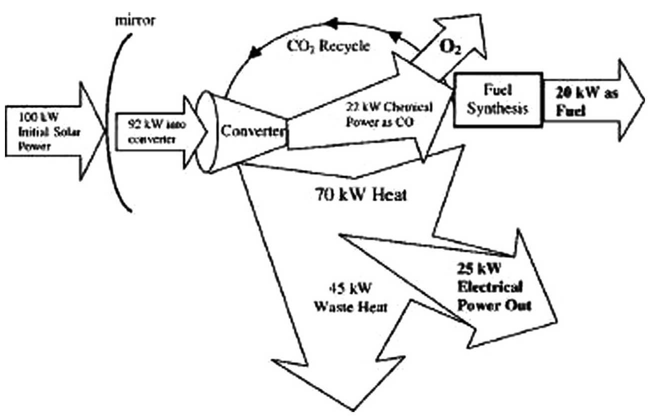


Fig. 22. A schematic diagram showing energy conversion goals for a direct solar reduction system based on 100 kW initial solar input [325].



Fig. 24. Photo of optical-fiber photo reactor [326].

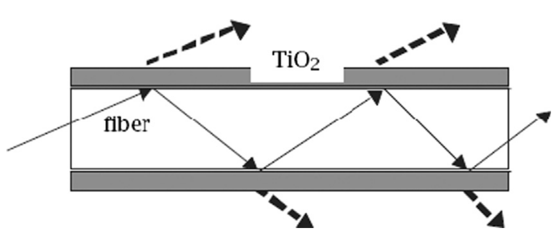


Fig. 23. The schematic of light transmission and spread of TiO_2 coated-optical fiber [326].

A steady-state optical-fiber photo reactor (OFPR) was also employed to reduce CO_2 into methanol over cu-doped TiO_2 [325]. Fig. 23 shows the employed OFPR comprising TiO_2-coated fibers to transmit light from one end of the OFPR module to the fiber-supported TiO_2 film. Nearly 120 fibers with 16 cm long were inserted into this OFPR, which has a diameter of 3.2 cm and length of 16 cm. The both sides of this OFPR were sealed using leak-proof O-rings. TiO_2 film was coated on optical fibers using dip-coating method, and the TiO_2 and Cu-loaded solutions were prepared by a thermal hydrolysis method. The thickness of the formed Cu/TiO_2 film was estimated to be 53 nm, and consisted of very fine spherical particle with a diameter of about 14 nm. The TiO_2 was in an anatase phase in both pure and Cu-doped TiO_2 fibers. This TiO_2 exhibited a wavelength absorption edge of 367 nm (equivalent to nearly 3.3 eV). The Cu was in the form of Cu_2O clusters and played an important role in the methanol formation. Fig. 24 shows transmission of light in an optical fiber reactor [326]. The light spits into two beams when hitting the internal surface fiber due to the difference of refraction index between TiO_2 coating and quartz core. Part of light is reflected and transmitted along the fiber, while the rest penetrates and excites the TiO_2 layer at the interface. Thus the electron–hole pairs are generated, which conduct the photoreactions. Thus, the optical fibers can be used to radiate the light uniformly inside a photoreactor. Fig. 25 schematically illustrates the reactor system employed in this study [326]. The OFPR was illuminated from one side of quartz window by an Hg lamp with a peak light intensity at 365 nm. The light intensity could be adjusted from 1 to 16 W/cm^2. The whole OFPR was wrapped up using an aluminum foil during the reaction to avoid the interference of indoor lamps. Fig. 26 shows the methanol yields vs. light intensity under the partial pressures of CO_2 and H_2O at 1.29 and 0.026 bar, respectively [326]. The methanol yield was found to be increased with the light intensity. Pure TiO_2 produced a very little methanol yield, whereas the Cu/TiO_2 produced significantly high yield. The methanol yields were increased with UV irradiative

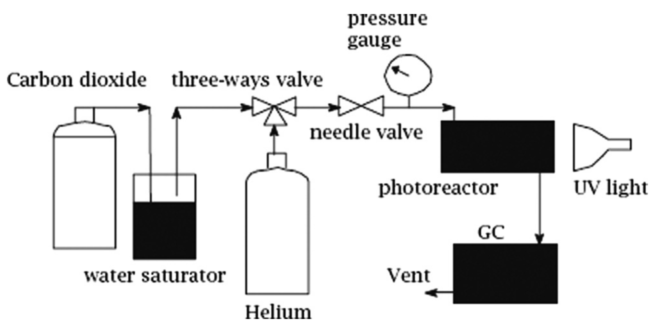


Fig. 25. Schematic of photo reaction system [326].

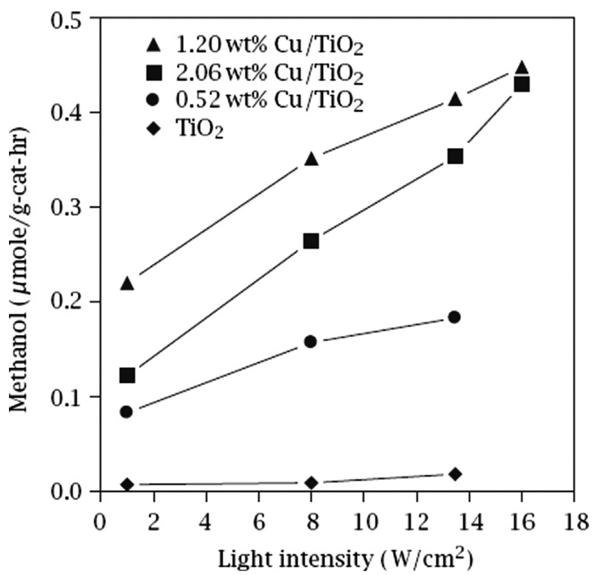


Fig. 26. The methanol yield in optical-fiber photo reactor, reaction temperature 75 °C, CO_2 pressure 1.29 bar, and H_2O pressure 0.026 bar [326].

intensity as well as with Cu loadings. Maximum methanol rate was noted to be 0.45 μmole per gram catalyst per hour over 1.2 wt %-Cu/TiO_2 catalyst under irradiation of a 16 W/cm^2 light when the CO_2 pressure was maintained as 1.3 bar after 5000 s mean residence time of reaction. Furthermore, when the Cu loading was > 1.2 wt%, lower methanol yields were noted because the surface of TiO_2 was found to be masked by Cu_2O clusters [326].

The silver-modified TiO_2 (Ag/TiO_2) nanocomposite catalyst and methanol as a hole scavenger were also employed together for simultaneous formation of H_2, CO and CH_4 in a photocatalytic CO_2 reduction reaction in an aqueous medium [327]. The mesoporous Ag/TiO_2 composite particles were prepared in a simple ultrasonic spray pyrolysis (SP) route using a commercial Degussa P-25 TiO_2 powder and $AgNO_3$ as the starting materials. The material properties and photocatalytic activities of the formed composites in SP method were compared with those formed in a conventional wet-impregnation (WI) method. The composites formed in SP route had a larger specific surface area and a better dispersion of Ag nanoparticles on TiO_2 surface when compared with those of WI TiO_2. As a result, the SP samples provided much higher photocatalytic activities toward H_2 formation as well as to CO_2 reduction products. The H_2 formation rate of the 2 wt% Ag/TiO_2-SP sample was six-times higher when compared with the 2 wt% Ag/TiO_2-WI sample, and 60-times higher when compared with the bare TiO_2. The molar ratio of H_2 and CO in the final products was found to be in the ratio of 2–10. Fig. 27 shows a useful reduction potential for methanol formation in comparison to syngas (H_2 and CO) formation on a NHE scale [327].

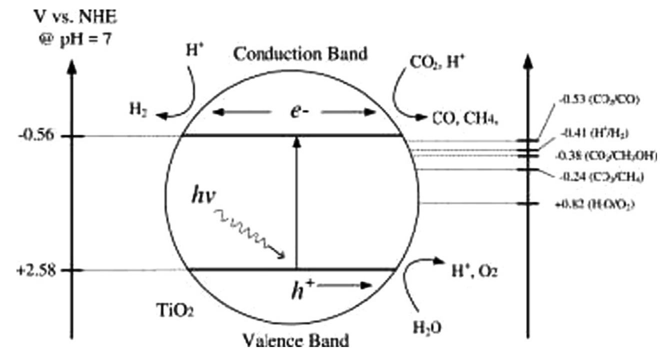


Fig. 27. Mechanism of photocatalytic hydrogen production and CO_2 reduction with water on TiO_2 semiconductor and their reduction potentials at pH 7 vs. NHE [327].

The photochemical CO_2 reduction reaction was also performed over a supramolecular electrode packed with Co(II)tetrabenzoporphyrin [328]. The supramolecular electrode was prepared by stacking Co(II)tetrabenzoporphyrin. The stack was held together by π–π interactions and the first layer of the porphyrin complex was anchored to the glassy carbon surface through the porphyrin's 4-aminopyridine group. A pure electrode formed by Co(II)tetrabenzoporphyrin adsorbed on the glassy carbon surface exhibited no activity towards CO_2 reduction. In contrast to this, the supramolecular electrode exhibited a much improved photoelectrocatalytic activity for the same reaction. The photoelectrocatalytic activity was also found to be enhanced by the illumination of the supramolecular electrode. In the absence of any sensitizer, the illumination of the electrode with visible light induced an appreciable shift of the CO_2 reduction wave towards more positive potentials. The shift of the wave was also observed in experiments with the sensitizer, $[Ru(bpy)_3]^{3+}$, but in this case, the light with a shorter wavelength was needed [328]. The Ru and WO_3 modified TiO_2 catalysts supported on Al_2O_3 were also employed to reduce CO_2 in an aqueous electrolyte circulated in a photocatalytic reactor at room temperature and constant pressure [329]. About 97% of CO_2 was converted into methanol (14 vol%) and into small amount of formic acid, acetic acid and ester. The reactor system employed had a set of bottles having water in which CO_2 was continuously bubbled. The CO_2 dissolved in H_2O was directed into the reactor having catalyst. A membrane system was used to separate the formed methanol product on the surface of the catalyst. This designed bath system allows to transform 370 dm^3 of CO_2 per hour into methanol with a yield of about 97% (when the length of the one reactor is 0.5 m, Φ=4 cm). Fig. 28 shows an ideological scheme for methanol production employed in this study [329].

Single-crystalline Zn_2GeO_4 nanobelts with hundreds of micrometers in length, as small as 7 nm in thicknesses and aspect ratios of up to 10,000 formed in a solvothermal route from a binary ethylenediamine/H_2O solvent were also employed to reduce CO_2 photocatalytically into CH_4 in the presence of H_2O vapor [330]. Fig. 29 shows CH_4 formation over (a) sample formed in a sold-state reaction, (b) nanoribbons, (c) 1 wt% Pt-loaded nanoribbons, (d) 1 wt% RuO_2-loaded nanoribbons, and (e) 1 wt% RuO_2+1 wt% Pt-co-loaded nanoribbons as a function of light irradiation time [330]. It can be seen from this figure that the 1 wt% RuO_2+1 wt% Pt-co-loaded nanoribbons exhibited highest activity towards photoreduction of CO_2 into methane. The CO_2 was also reduced to methane, ethylene, and CO in CO_2-saturated aqueous electrolyte over the surface of illuminated *p*-Si semi-conductor electrode surface modified with small metal particles of Cu, Ag, or Au [331]. These modified *p*-Si semi-conductor electrodes produced products similar to the metal (Cu, Ag, or Au) electrodes, but at ca. 0.5 V (vs. NHE) more positive potentials than their corresponding metal electrodes, contrary to continuous-metal-coated *p*-Si

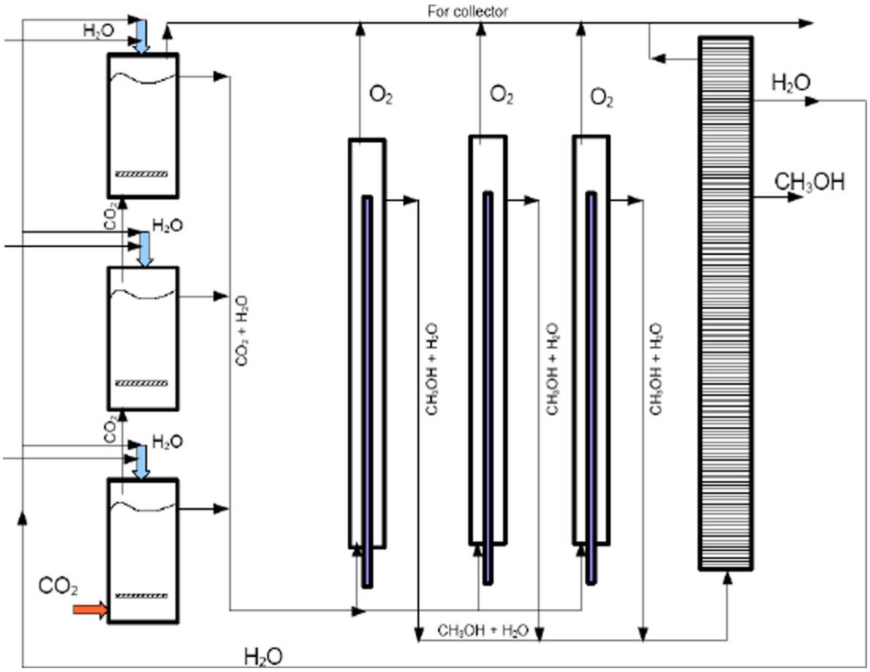


Fig. 28. The system for the photoreduction of CO_2 with H_2O for CH_3OH production [329].

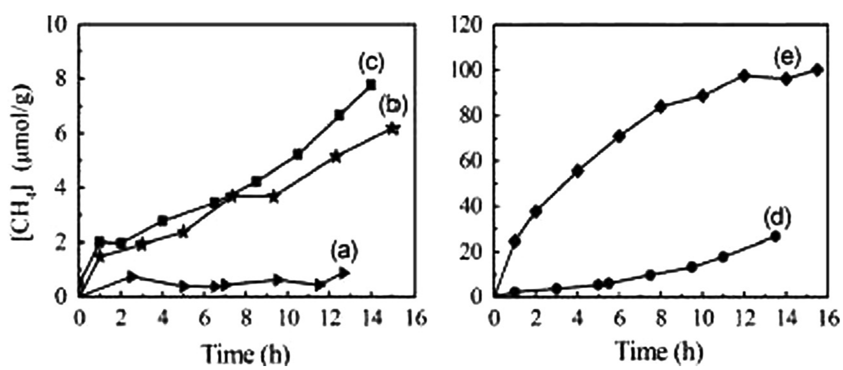
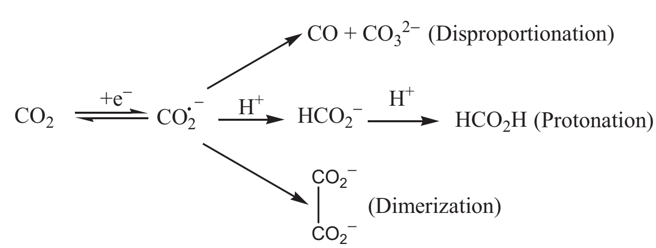


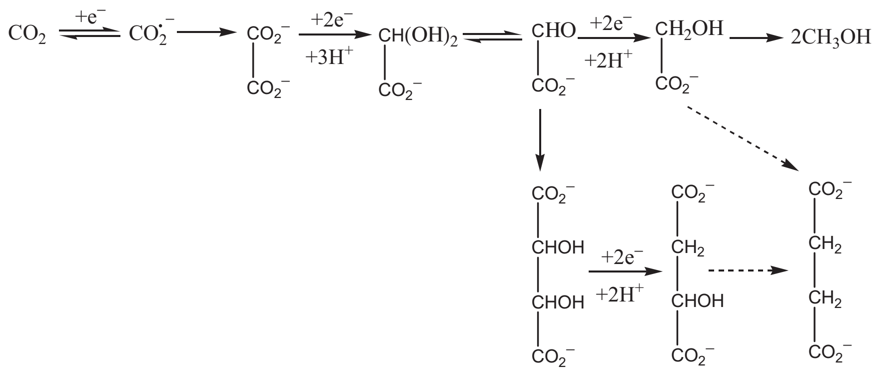
Fig. 29. CH_4 generation over (a) the SSR sample, (b) nanoribbons, (c) 1 wt% Pt-loaded nanoribbons, (d) 1 wt% RuO_2-loaded nanoribbons, and (e) 1 wt% RuO_2 + 1 wt% Pt-co-loaded nanoribbons as a function of light irradiation time [330].

electrodes. These results clearly suggest that the metal-particle-coated *p*-Si electrodes not only possess high catalytic activity for electrode reactions but also generate high photovoltages and thus work as ideal semiconductor electrodes [331]. The formation of the dimeric and tetrameric products namely oxalate, glyoxylate, glycolate and tartrate was also noted in the CO_2 reduction reaction when performed in an aqueous solution of tetramethylammonium chloride suspended with CdS or ZnS colloids [332]. The performance of other semiconducting powders including ZnO, SiC, $BaTiO_3$ and $SrTiO_3$ was also compared with those exhibited by CdS and ZnS colloids. The formation of HCOOH and HCHO was noted in the absence of tetramethylammonium ions. The relative quantum efficiencies of these six semiconductors were found to be influenced by their band-gap energies and conduction band potentials. The role and effectiveness of several hole acceptor (electron donor) compounds in this process were also studied and found that the addition of one electron to a CO_2 molecule produces a $CO_2^{\bullet-}$ radical anion. This radical anion is subsequently protonated to form formate ion that undergoes disproportionation to form CO and carbonate or it dimerizes to form oxalate ion (Scheme 12) [333,334]. Scheme 13 shows the range of products, which can be formed on further reduction of oxalate ion [332]. Electrochemical reduction of CO_2 under these conditions also led to the formation of oxalate [335], glyoxylate [336,337], glycolate



Scheme 12. One electron addition to CO_2 [333,334].

[338,339], tartrate [337] and malate [340]. Table 9 presents the quantum yields recorded for CO_2 reduction reaction over different semiconducting materials [332]. In these experiments no tetraalkylammonium salts or electron donor compounds were added. From this table it can be concluded that the semiconductors, particularly CdS, SiC and ZnS, with the higher negative conduction band potentials provide the best yields [341]. While the effectiveness of different semiconductors in reducing CO_2 is roughly in line with the order of increasing conduction band potentials, the variations, which are fairly small, may also be related to differences in particle size, which in quantum crystallites results in an increase in band-gap and reduction in the rate of recombination of electron–hole pairs. The overall quantum yields exhibited by these



Scheme 13. Overall electrochemical reduction of CO_2 [332].

Table 9
Comparison of different semiconductors' properties and their quantum efficiencies for CO_2 reduction into methanol [332].[a]

Semiconductor	E_{BG} (eV)	V_{CB} (V) vs. SHE	$\phi_{e'}$ (10^{-5})
$SrTiO_3$	3.2	−0.8	0.74
$BaTiO_3$	3.2	−0.4	2.1
CdS	2.5	−0.9	3.8
ZnO	3.2	−0.5	4.3
SiC	3.0	−1.4	6.7
ZnS	3.85	−2.0	[5400][a]

Suspensions of 0.3 g of each semiconductor in water (100 cm^3) at pH 4 saturated with CO_2 irradiated with 2.5 × 10^{-3} Einsteins h^{-1} for 24 h (250 < λ < 580 nm). No TMACl or electron donors added. $\phi_{e'}$ was measured from yields of formic acid and formaldehyde.

[a] From work with ZnS.

six semiconductors followed this trend: ZnS > SiC > ZnO > CdS > $BaTiO_3$ > $SrTiO_3$. Based on the studies on various hole scavenges such as I^-, TSCoPC, $Fe(CN)_6^{3-}$, hydroquinone, sulfite, propan-2-ol, hypophosphite, it was concluded that the log of the quantum yield for most of them is in a linear relationship with their redox potentials [341].

In a solar photocatalytic reactor, the mixture of CO_2 and water vapor was converted into hydrocarbon fuels over the surface of nitrogen-doped titania nanotube arrays loaded with nanodimensional islands of Pt and/or Cu co-catalysts [342]. All experiments were performed in outdoor sunlight at University Park, PA. Intermediate reaction products, H_2 and CO, were also formed with relatively lower concentrations. The hydrocarbon formation rate of 111 ppm cm^{-2} h^{-1} or ≈160 μL/(g h) was noted when the nanotube array samples were loaded with both Cu and Pt nanoparticles and irradiated with outdoor global AM 1.5 sunlight having a power density of about 100 mW/cm^2. This rate of CO_2 to hydrocarbon formation under outdoor sunlight is at least 20 times higher than those reported so far in the literature for similar experiments conducted in the laboratory using UV lamp [342]. Both these Pt and Cu co-catalysts were found to be essential for high rate conversion of CO_2 into hydrocarbon fuels.

From the above presented photocatalytic results, it can be concluded that although encouraging progress has been made toward the photocatalytic conversion of CO_2 using sunlight, further efforts are required for increasing sunlight-to-fuel photoconversion efficiencies [343].

8. Materials and catalysts for H_2O oxidation and splitting reactions

As already mentioned in the previous sections and in the Introduction part, the main objective of this review is to find out the information and methods available in the literature for converting CO_2 into methanol using exclusively solar energy without the need of any external bias voltage or energy that is produced from fossil fuels. It is nothing but realization of an artificial photosynthesis process. Methanol formed in exclusively artificial photosynthesis process can be employed economically with sustainability in place of fossil fuels that are being used at present to meet the energy requirements of the society. Although none of the so far reported processes could convert CO_2 into methanol using exclusively solar energy, in certain studies, CO_2 was converted into methanol under mild reaction conditions using certain molecular catalysts and energy (mainly electricity) that is produced from fossil fuels. For these processes, if the electricity is produced from sunlight using any of the existing methods such as photovoltaics, and utilized in these processes, the artificial photosynthesis process with considerable efficiency could be realized.

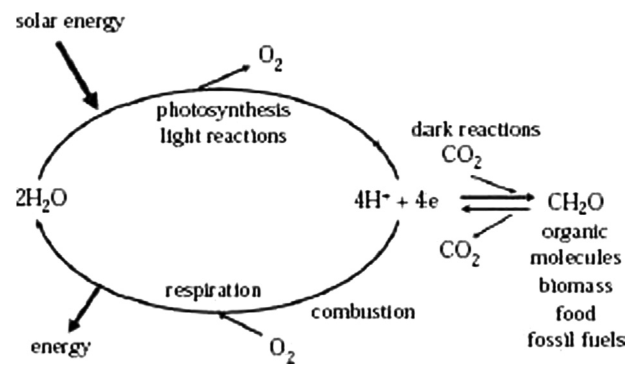


Fig. 30. A schematic of energy flow in biology [344].

As discussed in the previous sections, the reduction of CO_2 into methanol in electrochemical cells is almost similar to the natural photosynthesis (Fig. 30) [344]. As can be seen from Fig. 30, the light reactions of photosynthesis (light absorption, charge separation, water splitting and electron/proton transfer) provide the reducing equivalents or 'hydrogen' electrons (e) and protons (HC) to convert CO_2 to sugars and other organic molecules that make up living organisms (biomass), including those that provide humankind with food. The same photosynthetic reactions gave rise to the fossil fuels formed millions of years ago. The burning of these organic molecules by either respiration (controlled oxidation within our bodies) or combustion of fossil fuels is the reverse to photosynthesis, releasing CO_2 and combining the 'hydrogen' back with oxygen to form water. In doing so, energy is released, which was originated from sunlight.

In electrochemical CO_2 reduction process, the protons and electrons are generated from water (H_2O + energy → $2H^+ + 2e^- + ½ O_2$↑) in an anode compartment by utilizing electricity, and then the reduction of CO_2 with those generated protons and electrons into

Table 10
A list of review articles published on water oxidation/water splitting reactions carried out using various energy sources.

First author	Article title	Published year	Reference
A.J. Nozik	p–n Photoelectrolysis cells	1976	[292]
T. Bak	Photo-electrochemical hydrogen generation from water using solar energy: materials-related aspects	2002	[345]
A. Steinfeld	Solar thermochemical production of hydrogen – a review	2005	[349]
A. Galińska	Photocatalytic water splitting over Pt−TiO2 in the presence of sacrificial reagents	2005	[352]
A.J. Esswein	Hydrogen production by molecular	2007	[294]
T. Kodama	Thermochemical cycles for high-temperature solar hydrogen production	2007	[61,350]
J. Barber	Biological solar energy	2007	[344]
S. Somasundaram	Photocatalytic production of hydrogen from electrodeposited film and sacrificial electron donors	2007	[351]
K. Rajeshwar	Hydrogen generation at irradiated oxide semiconductor–solution interfaces	2007	[347]
J. Nowotny	Titanium dioxide for solar-hydrogen I. Functional properties	2007	[348]
N.A. Kelly	Solar energy concentrating reactors for hydrogen production by photoelectrochemical water splitting	2008	[353]
J.J. Concepcion	Making oxygen with ruthenium complexes	2009	[356]
M.G. Walter	Solar water splitting cells	2010	[354]
X. Chen	Semiconductor-based photocatalytic hydrogen generation	2010	[346]
H. Lv	Polyoxometalate water oxidation catalysts and the production of green fuel	2012	[355]

methanol ($CO_2+6H^++6e^-\rightarrow CH_3OH+H_2O$) takes place in cathode compartment over the surface of a catalyst. These reactions are similar to those light and dark reactions of natural photosynthesis. In natural photosynthesis, CO_2 is reduced to carbohydrates, whereas in this artificial photosynthesis, it is reduced to methanol. When compared the both water oxidation reaction in anode compartment of electrochemical cell or light reaction of the natural photosynthesis, and the CO_2 reduction reaction in cathode compartment of electrochemical cell or dark reaction of the natural photosynthesis, only former reaction needs thermodynamic energy input as it is an endothermic reaction, whereas the latter reaction does not need much of energy inputs but a suitable catalytic system as it is not an endothermic reaction. Hence, in order to realize artificial photosynthesis, it is very important to split water into the protons and electrons using solar energy in order to reduce CO_2 into methanol. In the literature, catalysts and materials that were found to be effective for splitting water into protons and electrons or into H_2 and O_2 as well as for harvesting sunlight in the form of electricity are very well presented and discussed. Various review articles reported so far on water oxidation and water splitting reactions utilizing various catalytic systems and sunlight harvesting systems are listed in Table 10 [61,292,294,344–356]. The catalysts employed in these reported processes for water oxidation reactions consume energy supplied by chemical potentials, sunlight or electricity.

9. Concluding remarks and future perspectives

Development of an efficient process for converting CO_2 into methanol or to any other value added chemical using exclusively solar energy (i.e., the realization of artificial photosynthesis) is of great importance as this process can indeed deal with (i) the CO_2 associated global warming problem, (ii) depletion of fossil fuels, and (iii) the problems associated with storing of energy (electricity as well as solar energy) in the form of high energy density liquid fuels for future applications. At present, the CO_2 sequestration process is being employed to tackle with CO_2 associated global warming problem in many places, which has been found to be expensive. With the same expenditure, instead of disposing off CO_2 following sequestration route, the captured CO_2 at thermal power plants, can be converted into methanol and other useful chemical fuels following any of the existing thermochemical routes being practiced at present in the petrochemical industry as discussed in this review article. Furthermore, the value of the chemical fuels formed from CO_2 could be a bonus. If any of the renewable energy resources such as solar energy or electricity derived from sunlight is employed to meet the energy requirements of these CO_2 reduction reactions, this process can, in fact, considerably solve the problems mentioned above. Since the liquid fuels such as methanol formed from CO_2 could be directly employed in place of fossil fuels in the present energy distribution infrastructure such as internal combustion engines of automobile vehicles without major modifications to the engines, there would not be any severe economical consequences while transforming from fossil fuel energy dependency to non-fossil fuel or renewable energy dependency.

As discussed above in this review article, although by following photoelectrochemical (PEC) routes, the CO_2 could be converted into methanol using certain non-oxide semiconducting photoelectrodes (*p*-GaP) together with homogeneous organic molecular catalysts (pyridine), the recorded quantum efficiencies and the stability and durability of these routes have been rather low and insufficient for practicing on a commercial scale. This is due to the fact that these routes still need certain amount of external bias voltage from grid current, and the associated semiconductors show poor long term stability against photocorrosion being non-oxide materials.

Among the stoichiometric, thermochemical, electrochemical, photoelectrochemical and photocatalytic routes developed so far for reducing CO_2 into value added chemicals, only the electrochemical routes appear to be viable as these latter routes allow mild reaction conditions, most studied and understood systems only next to the thermochemical processes, and can be integrated with electricity that is derived from sunlight using any of the existing technologies such as photovoltaics. Furthermore, CO_2 can be reduced to methanol electrochemically using information that is available at present in the literature. However, the reaction efficiencies and product yields obtained in these electrochemical routes are also low at the moment. Nevertheless, these reaction efficiencies and product yields could be improved suitably (i) by suppressing the hydrogen evolution reaction (HER), which is the main reason for the noted low efficiency of the process, by using certain electrodes having high overpotentials towards HER, (ii) by reducing overpotentials associated with CO_2 reduction reaction into methanol using suitable molecular catalysts, such as room temperature ionic liquids (RTILs), pyridine, and a mixture of nitroso-R salt+Co or Cu sulfate+methanol, which can be employed in conjunction with electrodes, and (iii) by employing electricity that is produced from sunlight using cheaper technologies such as polymer based photovoltaics. Furthermore, the HER could also be suppressed by using certain organic molecular catalysts, such as triethanolamine, in the anode compartment of the electrochemical reaction.

Since CO_2 has been successfully reduced to CO in electrochemical cells using certain RTILs at only few hundred millivolts overpotentials (hence at very low process cost) when compared with the theoretically required ones with desired stability using highly durable, robust and inexpensive metal electrodes, this process can be made available for commercialization by integrating electricity that is derived from sunlight. Furthermore, as H_2 can also be produced by water electrolysis using electricity that is produced from sunlight, by supplying these two CO and H_2 gases produced using electricity derived from sunlight, in the ratio of syngas, methanol can be produced following well-established thermochemical routes, which are being practiced today in the petrochemical industry, and thus obtained methanol can be converted into gasoline (i.e., petrol) again by following thermochemical routes. Thus, electrochemical CO_2 reduction processes discussed and presented in this review have a lot importance from the point of view of solving the above said three problems associated with climate, energy crisis and energy storage.

Acknowledgments

Author wishes to specially acknowledge all the researchers whose work is described in this review for their valuable contributions. Author also wishes to thank Dr. G. Sundararajan, Director, ARCI, Hyderabad, for his kind encouragement and permission to publish this review article. Further, thanks are due to the SERC-DST (Government of India) for the IUSSTF fellowship (IUSSTF Fellowship/2012/Ibram Ganesh/7–2012; dated: 14th March 2012) awarded. Thanks are also due to Prof. Craig L. Hill, Goodrich C. White Professor, Emory University, Atlanta, Georgia, USA, for accepting this author as an IUSSTF Fellow into his research group for one year period.

References

[1] Robinson AB, Robinson NE, Soon A. Environmental effects of increased atmospheric carbon dioxide. J Am Phys Sur 2007;12:79–90.
[2] David J, Herzog H. The cost of carbon capture. In: Fifth international conference on greenhouse gas control technologies 2001, Cairns, Qld., Australia, 13–16th August 2000. Collingwood, Vic., Australia: CSIRO. p. 985.
[3] Mandil C. Prospects for CO_2 capture and storage. In: International energy agency and energy technology analysis; 2004. IEA Publications. ⟨http://www.iea.org/textbase/nppdf/free/2004/prospects.pdf⟩.
[4] Bachu S. Sequestration of CO_2 in geological media: criteria and approach for site selection in response to climate change. Energy Convers Manage 2000;41(9):953.
[5] Bachu S, Adams JJ. Sequestration of CO_2 in geological media in response to climate change: capacity of deep saline aquifers to sequester CO_2 in solution. Energy Convers Manage 2003;44(20):3151.
[6] Bruant RG, Celia MA, Guswa AJ, Peters CA. Safe storage of CO_2 in deep saline aquifers. Environ Sci Technol 2002;36(11):240A.
[7] Gale J. Using coal seams for CO_2 sequestration. Geol Belgica 2004;7:3–4.
[8] Holt T, Jensen JI, Lindeberg E. Underground storage of CO_2 in aquifers and oil reservoirs. Energy Convers Manage 1995;36(6-9):535.
[9] Hustad CW. Infrastructure for CO_2 collection, transport and sequestration. Presented at the third Nordic mini-symposium on carbon dioxide storage, Trondheim, Norway; 3 October 2003.
[10] Bergen FV, Gale J, Damen KJ, Wildenborg AFB. Worldwide selection of early opportunities for CO_2-enhanced oil recovery and CO_2-enhanced coal bed methane production. Energy 2004;29:1611.
[11] Salvador C, Lu D, Anthony EJ, Abanades JC. Enhancement of CaO for CO_2 capture in an FBC environment. Chem Eng J 2003;96(3):187.
[12] Hicks JC, Drese JH, Fauth DJ, Gray ML, Qi G, Jones CW. Designing adsorbents for CO_2 capture from flue gas-hyperbranched aminosilicas capable of capturing CO_2 reversibly. J Am Chem Soc 2008;130(10):2902.
[13] Ritter SK. What can we do with carbon dioxide? Scientists are trying to find ways to convert the plentiful greenhouse gas into fuels and other value-added products Chem Eng News 2007;85(18):11.
[14] Dijkstra JW, Jansen D. Novel concepts for CO_2 capture with SOFC. In: Proceedings of the sixth international conference on greenhouse gas control technologies 2003, Kyoto, Japan; 1–4 October 2002. Oxford, UK: Elsevier Science (Pergamon). p. 161.
[15] Dickson B, Yashayaev I, Meincke J, Turrell B, Dye S, Holfort J. Rapid freshening of the deep North Atlantic Ocean over the past four decades. Nature 2002;416(6883):832.
[16] Priddle R. World energy outlook 2002. In: International energy agency and energy technology analysis 2002, IEA/OECD, 2nd ed., Paris, France. ⟨http://www.iea.org/textbase/nppdf/free/2000/weo2002.pdf⟩.
[17] Gassner K, Popov A, Pushak N. World electric power-plants database. Utility Data Institute; 2003. Washington, DC: McGraw-Hill.
[18] World oil and gas review 2004. ENI 2004, Rome, Italy. ⟨http://www.agip.it/⟩.
[19] World Energy Council. 19th survey of world energy resources. 2001, London, UK. ⟨http://www.worldenergy.org/wec-geis/publications/default/launches/ser/ser.asp⟩.
[20] Moritis G. EOR continues to unlock oil resources. Oil Gas J 2004;12(April):53.
[21] Agency IE. Key world energy statistics 2009. IEA 2009, Paris, France; 2010.
[22] Pehnt M. Fuel cells in the power market: separating the hope from the hype. Presented at CAN Europe meeting, Brussels, Belgium; 27 May 2004. ⟨http://www.climnet.org/CTAP/workshop2004/PresentationsWS2.htm/⟩.
[23] Lewis NS, Crabtree G, Nozik A, Wasielewski M, Alivisatos P. Basic research needs for solar energy utilization. Washington, DC: US Department of Energy; 2005.
[24] Garcia-Martinez J. Nanotechnology for the energy challenge. Weinheim, Germany: Wiley-VCH; 2010.
[25] TBC Group. Batteries for electric cars: challenges, opportunities, and the outlook to 2020. BCG 2010, Boston, MA, USA [September]. ⟨http://www.bcg.com/documents/file36615.pdf⟩.
[26] Exxon Mobil Algae Biofuels Research and Development Program; 2012, vol. 1, no. (1). ⟨http://wwwexxonmobilcom/corporate/files/news_pub_algae_fact sheetpdf/⟩.
[27] Ganesh I, Gupta AK, Kumar PP, Sekhar PSC, Radha K, Padmanabham G, et al. Preparation and characterization of Ni-doped TiO_2 materials for photocurrent and photocatalytic applications. Sci World J 2012.
[28] Budzianowski WM. Value-added carbon management technologies for low CO_2 intensive carbon-based energy vectors. Energy (Oxford, UK) 2012;41:280–97.
[29] Budzianowski WM. Negative carbon intensity of renewable energy technologies involving biomass or carbon dioxide as inputs. Renew Sustain Energy Rev 2012;16(9):6507–21.
[30] Centi G, Perathoner S. CO_2-based energy vectors for the storage of solar energy. Greenhouse Gas Sci Technol 2011;1:21.
[31] Gupta M, Coyle I, Thambimuthu K. CO_2 capture technologies and opportunities in Canada. In: First Canadian CC&S technology roadmap workshop; 18 September 2003.
[32] Khoshtinat M, Amin NAS, Noshadi I. A review of methanol production from methane oxidation via non-thermal plasma reactor. World Acad Sci Eng Technol 2010;62:354.
[33] Tans P. Trends in carbon dioxide. NOAA/ESRL; 29 June 2009. ⟨http://www.esrl.noaa.gov/gmd/ccgg/trends/⟩.
[34] Peters M, Mueller T, Leitner W. CO_2: from waste to value. Tce 2009;813:46.
[35] Aresta M. Carbon dioxide as chemical feedstock. Weinheim: Wiley-VCH; 2010.
[36] Aresta M, Dibenedetto A. Utilisation of CO_2 as a chemical feedstock: opportunities and challenges. Dalton Trans 2007:2975.
[37] Centi G, Perathoner S. Opportunities and prospects in the chemical recycling of carbon dioxide to fuels. Catal Today 2009;148(3 and 4):191.
[38] Hoekman K, Broch A, Robbins C, Purcell R. CO_2 recycling by reaction with renewably-generated hydrogen. Int J Greenhouse Gas Control 2010;4:44.
[39] Ma J, Sun N, Zhang X, Zhao N, Xiao F, Wei W, et al. A short review of catalysis for CO_2 conversion. Catal Today 2009;148(3-4):221.
[40] Patil YP, Tambade PJ, Jagtap SR, Bhanage BM. Carbon dioxide: a renewable feedstock for the synthesis of fine and bulk chemicals. Front Chem Eng China 2010;4(2):213.
[41] Sakakura T, Choi J-C, Yasuda H. Transformation of carbon dioxide. Chem Rev 2007;107(6):2365.
[42] Schaefer M, Behrendt F, Hammer T. Evaluation of strategies for the subsequent use of CO_2. Front Chem Eng China 2010;4(2):172.
[43] Reddy BM, Thrimurthulu G. Carbon dioxide-based technologies: converting greenhouse to value added chemicals. Chem Ind Digest 2009(July):54.
[44] Arakawa H, Aresta M, Armor JN, Barteau MA, Beckman EJ, Bell AT, et al. Catalysis research of relevance to carbon management: progress, challenges, and opportunities. Chem Rev 2001;101(4):953–96.
[45] Aruchamy A, Aravamudan G, Rao GVS. Semiconductor based photoelectrochemical cells for solar energy conversion – an overview. Bull Mater Sci 1982;4(5):483.
[46] Sheppard LR, Nowotny J. Materials for photoelectrochemical energy conversion. Adv Appl Ceram 2007;106(1-2):9.
[47] Thimsen E, Formal FL, Gratzel M, Warren SC. Influence of plasmonic Au nanoparticles on the photoactivity of Fe_2O_3 electrodes for water splitting. Nano Lett 2011;11:35.
[48] Abbott D. Keeping the energy debate clean: how do we supply the world's energy needs? Proc IEEE 2010;98(1): 42–66.
[49] Lewis NS, Nocera DG. Proc Natl Acad Sci USA 2006;103:15729.
[50] Conti JJ, Doman LE, Smith KA, Mayne LD, Yucel EM, Barden JL, et al. International energy outlook 2010. The US Energy Information Administration (EIA), US Department of Energy, DOE/EIA-0484(2010), Washington, DC; 2010, no. (1), p. 338.
[51] Stocker M. Biofuels and biomass-to-liquid fuels in the biorefinery: catalytic conversion of lignocellulosic biomass using porous materials. Angew Chem, Int Ed 2008;47:9200–11.

[52] Gallezot P. Catalytic conversion of biomass: challenges and issues. ChemSusChem 2008;1:734–7.
[53] Huber GW, Iborra S, Corma A. Synthesis of transportation fuels from biomass: chemistry, catalysts, and engineering. Chem Rev 2006;106:4044–98.
[54] Centi G, Perathoner S. Towards solar fuels from water and CO_2. ChemSusChem 2010;3:195–208.
[55] Nozik AJ. Nanoscience and nanostructures for photovoltaics and solar fuels. Nano Lett 2010:2735–2741. 10 [Copyright (C) 2012 American Chemical Society (ACS). All Rights Reserved].
[56] Roy SC, Varghese OK, Paulose M, Grimes CA. Toward solar fuels: photocatalytic conversion of carbon dioxide to hydrocarbons. ACS Nano 2010;4:1259–78.
[57] Tributsch H. Photovoltaic hydrogen generation. Int J Hydrogen Energy 2008;33:5911–30.
[58] Gibson TL, Kelly NA. Optimization of solar powered hydrogen production using photovoltaic electrolysis devices. Int J Hydrogen Energy 2008;33:5931–40.
[59] Manisha S, Banerjee R. Comparison of biohydrogen production processes. Int J Hydrogen Energy 2008;33(1):279–86.
[60] Kotaya SM, Das D. Biohydrogen as a renewable energy resource – prospects and potentials. Int J Hydrogen Energy 2008;33(1):258–63.
[61] Kodama T, Gokon N. Thermochemical cycles for high-temperature solar hydrogen production. Chem Rev 2007;107:4048–77.
[62] Agrafiotis C, Roeb M, Konstandopoulos AG, Nalbandian L, Zaspalis VT, Sattler C, et al. Solar water splitting for hydrogen production with monolithic reactors. Solar Energy 2005;79(4):409–21.
[63] Roeb M, Säck JP, Rietbrock P, Prahl C, Schreiber H, Neises M, et al. Test operation of a 100 kW pilot plant for solar hydrogen production from water on a solar tower. Solar Energy 2011;85(4):634–44.
[64] Kudo A, Miseki Y. Heterogeneous photocatalyst materials for water splitting. Chem Soc Rev 2009;38:253–78.
[65] Navarro YRM, Alvarez GMC, del VF, Villoria dl MJA, Fierro JLG. Water splitting on semiconductor catalysts under visible-light irradiation. ChemSusChem 2009;2:471–85.
[66] Currao A. Photoelectrochemical water splitting. Chimia 2007;61:815819.
[67] Kelly NA, Gibson TL. Design and characterization of a robust photoelectrochemical device to generate hydrogen using solar water splitting. Int J Hydrogen Energy 2006;31:1658–73.
[68] Morris AJ, Meyer GJ, Fujita E. Molecular approaches to the photocatalytic reduction of carbon dioxide for solar fuels. Acc Chem Res 2009;42:1983–94.
[69] Krajacic G, Martins R, Busuttil A, Duic N, da GCM. Hydrogen as an energy vector in the islands' energy supply. Int J Hydrogen Energy 2008;33:1091–103.
[70] Edwards PP, Kuznetsov VL, David WIF. Hydrogen energy. Philos Trans R Soc, A 2007;365:1043–56.
[71] Sartbaeva A, Kuznetsov VL, Wells SA, Edwards PP. Hydrogen nexus in a sustainable energy future. Energy Environ Sci 2008;1:79–85.
[72] Vlachos DG, Caratzoulas S. The roles of catalysis and reaction engineering in overcoming the energy and the environment crisis. Chem Eng Sci 2009;65:18–29.
[73] Farrauto RJ. Building the hydrogen economy. Hydrocarbon Eng 2009;14:25–30.
[74] Muradov NZ, Veziroglu TN. Green path from fossil-based to hydrogen economy: an overview of carbon-neutral technologies. Int J Hydrogen Energy 2008;33:6804–39.
[75] Cooper HW. Fuel cells, the hydrogen economy and you. Chem Eng Prog 2007;103:34–43.
[76] Mueller-Langer F, Tzimas E, Kaltschmitt M, Peteves S. Techno-economic assessment of hydrogen production processes for the hydrogen economy for the short and medium term. Int J Hydrogen Energy 2007;32:3797–810.
[77] Strahan D. Hydrogen's long road to nowhere. New Sci 2008;200:40–3.
[78] Bockris JOM. Hydrogen no longer a high cost solution to global warming: new ideas. Int J Hydrogen Energy 2008;33:2129–31.
[79] Olah GA, Goeppert A, Prakash GKS. Beyond oil and gas: the methanol economy. Weinheim: Wiley-VCH; 2006.
[80] Taniguchi I. Electrochemical and photoelectrochemical reduction of carbon dioxide. In: Bockris JOM, White RE, Conway BE, editors. Modern aspects of electrochemistry, 20. New York: Plenum Press; 1989. p. 327.
[81] Frese Jr KW. In: Sullivan BP, Krist K, Guard HE, editors. Electrochemical and electrocatalytic reactions of carbon dioxide. Amsterdam: Elsevier; 1993. p. 145.
[82] Hori Y. CO_2 reduction catalyzed by metal electrodes. In: Vielstich W, Gasteiger HA, Lamm A, editors. Handbook of fuel cells – fundamentals, technology and applications, 2. West Sussex, England: Wiley; 2003. p. 720–33 (Chapter 48).
[83] Olah GA, Goeppert A, Prakash GKS. Chemical recycling of carbon dioxide to methanol and dimethyl ether: from greenhouse gas to renewable, environmentally carbon neutral fuels and synthetic hydrocarbons. J Org Chem 2009;74:7487–98.
[84] Song C. Global challenges and strategies for control, conversion and utilization of CO_2 for sustainable development involving energy, catalysis, adsorption and chemical processing. Catal Today 2006;115:2–32.
[85] Gattrell M, Gupta N, Co A. A review of the aqueous electrochemical reduction of CO_2 to hydrocarbons at copper. J Electroanal Chem 2006;594:1–19.
[86] Jiang Z, Xiao T, Kuznetsov VL, Edwards PP. Turning carbon dioxide into fuel. Phil Trans R Soc 2010;368(A):3343.
[87] Seki T, Baiker A. Catalytic oxidations in dense carbon dioxide. Chem Rev 2009;109(6):2409–54.
[88] Li W. Electrocatalytic reduction of CO_2 to small organic molecule fuels on metal catalysts. In: Hu Y, editor, Advances in CO_2 conversion and utilization. ACS symposium series. Washington, DC: American Chemical Society; 2010 [Chapter 5].
[89] Oh Y, Hu X. Organic molecules as mediators and catalysts for photocatalytic and electrocatalytic CO_2 reduction. Chem Soc Rev 2013;42:2253–61.
[90] Webster DC. Cyclic carbonate functional polymers and their applications. Prog Org Coatings 2003;47(1):77–86.
[91] Darensbourg DJ. Chemistry of carbon dioxide relevant to its utilization: a personal perspective. Inorg Chem 2010;49(23):10765.
[92] Jitaru M, Lowy DA, Toma M, Toma BC, Oniciu L. Electrochemical reduction of carbon dioxide on flat metallic cathodes. J Appl Electrochem 1997;27(8):875–89.
[93] Collin J-P, Sauvage J-P. Electrochemical reduction of carbon dioxide mediated by molecular catalysts. Coordination Chem Rev 1989;93:245.
[94] Rosen BA. Low temperature electrocatalytic reduction of CO_2 utilizing room temperature ionic liquids. A thesis submitted to Chemical Engineering in the Graduate College, University of Illinois at Urbana-Champaign, Urbana, IL, USA; 2010.
[95] Le MTH. Electrochemical reduction of CO_2 to methanol. A thesis submitted to the Graduate Faculty of the Louisiana State University and Agricultural and Mechanical College, Chemical Engineering, Louisiana State University, Baton Rouge, LA, USA; 2011.
[96] Chaturvedi D, Ray S. Versatile use of carbon dioxide in the synthesis of carbamates. Monatsh Chem 2006;137:127–45.
[97] Ganesh I. Conversion of carbon dioxide to methanol using solar energy – a brief review. Mater Sci Appl 2011;2:1407–15.
[98] Wang W, Wang S, Ma X, Gong J. Recent advances in catalytic hydrogenation of carbon dioxide. Chem Soc Rev 2011;40(7):3703–27.
[99] Omae I. Aspects of carbon dioxide utilization. Catal Today 2006;115(1–4):33–52.
[100] North M, Pasquale R, Young C. Synthesis of cyclic carbonates from epoxides and CO_2. Green Chem 2010;12:1514–39.
[101] Ganesh I. Conversion of carbon dioxide into several potential chemical commodities following different pathways – a review. Mater Sci Forum 2013;764:1–82.
[102] Nowotny J, Sheppard LR. Solar-hydrogen. Int J Hydrogen Energy 2007;32:2607–8.
[103] Olah GA, Geoppert A, Prakash GKS. Chemical recycling of carbon dioxide to methanol and dimethylether: from greenhouse gas to renewable, environmentally carbon neutral fuels and synthetic hydrocarbons. J Org Chem 2009;74:487.
[104] Olah GA. Beyond oil and gas: the methanol economy. Angew Chem, Int Ed, 44; 2005; 2636–9.
[105] Olah GA, Toeroek B, Joschek JP, Bucsi I, Esteves PM, Rasul G, et al. Efficient chemoselective carboxylation of aromatics to arylcarboxylic acids with a superelectrophilically activated carbon dioxide–Al_2C_{l6}/Al system. J Am Chem Soc 2002;124:11379–91.
[106] Joo F, Laurenczy G, Karady P, Elek J, Nadasdi L, Roulet R. Homogeneous hydrogenation of aqueous hydrogen carbonate to formate under mild conditions with water soluble rhodium(I)– and ruthenium(II)–phosphine catalysts. Appl Organomet Chem 2000;14:857–9.
[107] Leitner W. Carbon dioxide as a raw material: the synthesis of formic acid and its derivatives from CO_2. Angew Chem, Int Ed Engl 1995;34:2207–21.
[108] Courtemanche M-A, Légaré M-A, Maron L, Fontaine F-G. A highly active phosphine–borane organocatalyst for the reduction of CO_2 to methanol using hydroboranes. J Am Chem Soc 2013;135(25):9326–9.
[109] Menard G, Stephan DW. Room temperature reduction of CO_2 to methanol by Al-based frustrated Lewis pairs and ammonia borane. J Am Chem Soc 2010;132(6):1796–7.
[110] Geier SJ, Stephan DW. Lutidine/$B(C_6F_5)_3$: at the boundary of classical and frustrated Lewis pair reactivity. J Am Chem Soc 2009;131:3476–7.
[111] Ashley AE, Thompson AL, O'Hare D. Non-metal-mediated homogeneous hydrogenation of CO_2 to CH_3OH. Angew Chem, Int Ed 2009;48:9839–43.
[112] Matsuo T, Kawaguchi H. From carbon dioxide to methane: homogeneous reduction of carbon dioxide with hydrosilanes catalyzed by zirconium–borane complexes. J Am Chem Soc 2006;128:12362–3.
[113] Riduan SN, Zhang Y, Ying JY. Conversion of carbon dioxide into methanol with silanes over N-heterocyclic carbene catalysts. Angew Chem, Int Ed 2009;48:3322–5.
[114] Enders D, Niemeier O, Henseler A. Organocatalysis by N-heterocyclic carbenes. Chem Rev 2007;107:5606–55.
[115] Marion N, Diez-Gonzalez S, Nolan SP. N-heterocyclic carbenes as organocatalysts. Angew Chem, Int Ed 2007;46:2988–3000.
[116] Zeitler K. Extending mechanistic routes in heterazolium catalysis – promising concepts for versatile synthetic methods. Angew Chem, Int Ed 2005;44:7506–10.
[117] Seayad J, Patra PK, Zhang Y, Ying JY. Organocatalytic synthesis of N-phenylisoxazolidin-5-ones and a one-pot synthesis of β-amino acid esters. Org Lett 2008;10:953–6.
[118] Wong FT, Patra PK, Seayad J, Zhang Y, Ying JY. N-heterocyclic carbene (NHC)-catalyzed direct amidation of aldehydes with nitroso compounds. Org Lett 2008;10:2333–6.

[119] Zhang Y, Riduan SN, Ying JY. Microporous polyisocyanurate and its application in heterogeneous catalysis. Chem-Eur J 2009;15:1077–81.
[120] Yong G, Zhang Y, Ying J. Efficient catalytic system for the selective production of 5-hydroxymethylfurfural from glucose and fructose. Angew Chem, Int Ed 2008;47:9345–8.
[121] Duong HA, Tekavec TN, Arif AM, Louie J. Reversible carboxylation of N-heterocyclic carbenes. Chem Commun 2004:112–3.
[122] Voutchkova AM, Feliz M, Clot E, Eisenstein O, Crabtree RH. Imidazolium carboxylates as versatile and selective N-heterocyclic carbene transfer agents: synthesis, mechanism, and applications. J Am Chem Soc 2007;129:12834–46.
[123] Tommasi I, Sorrentino F. Utilization of 1,3-dialkylimidazolium-2-carboxylates as CO_2-carriers in the presence of Na^+ and K^+: application in the synthesis of carboxylates, monomethyl carbonate anions and halogen-free ionic liquids. Tetrahedron Lett 2005;46:2141–5.
[124] Zimmerman PM, Zhang Z, Musgrave CB. Simultaneous two-hydrogen transfer as a mechanism for efficient CO_2 reduction. Inorg Chem 2010;49(19):8724–8.
[125] Jeoung J-H, Dobbek H. Carbon dioxide activation at the Ni, Fe-cluster of anaerobic carbon monoxide dehydrogenase. Science 2007;318:1461–4.
[126] Parkin A, Seravalli J, Vincent KA, Ragsdale SW, Armstrong FA. Rapid and efficient electrocatalytic CO_2/CO interconversions by carboxydothermus hydrogenoformans CO dehydrogenase I on an electrode. J Am Chem Soc 2007;129:10328–9.
[127] Zimmerman PM, Paul A, Zhang Z, Musgrave CB. The role of free N-heterocyclic carbene (NHC) in the catalytic dehydrogenation of ammonia borane in the nickel NHC system. Angew Chem, Int Ed 2009;48:2201–5.
[128] Zimmerman PM, Paul A, Musgrave CB. Catalytic dehydrogenation of ammonia borane at Ni monocarbene and dicarbene catalysts. Inorg Chem 2009;48:5418–33.
[129] Obert R, Dave BC. Enzymatic conversion of carbon dioxide to methanol: enhanced methanol production in silica sol–gel matrices. J AM Chem Soc 2009;121(51):12192–3.
[130] Ellerby LM, Nishida CR, Nishida F, Yamanaka SA, Dunn B, Valentine JS, et al. Encapsulation of proteins in transparent porous silicate glasses prepared by the sol–gel method. Science 1992;255:1113–5.
[131] Xu S-W, Lu Y, Li J, Jiang Z-Y, Wu H. Efficient conversion of CO_2 to methanol catalyzed by three dehydrogenases co-encapsulated in an alginate–silica (ALG–SiO_2) hybrid gel. Ind Eng Chem Res 2006;45:4567–73.
[132] Freund HJ, Roberts MW. Surface chemistry of carbon dioxide. Surf Sci Reports 1996;25(8):225–73.
[133] Centi G, Perathoner S. The role of nanostructure in improving the performance of electrodes for energy storage and conversion. Eur J Inorg Chem 2009;2009(26):3851–78.
[134] Pan X, Fan Z, Chen W, Ding Y, Luo H, Bao X. Enhanced ethanol production inside carbon-nanotube reactors containing catalytic particles. Nat Mater 2007;6(7):507–11.
[135] Song C, Pan W. Tri-reforming of methane: a novel concept for catalytic production of industrially useful synthesis gas with desired H_2/CO ratios. Catal Today 2004;98(4):463–84.
[136] Bell AT. Basic research needs: catalysis for energy. Report from the US Department of Energy, basic energy sciences workshop; 2007. p. 69.
[137] Frese Jr KW. In: Sullivan BP, Krist K, Guard HE, editors. Electrochemical and electrocatalytic reactions of carbon dioxide. Amsterdam: Elsevier; 1993. p. 145.
[138] Hori Y. Electrochemical CO_2 reduction on metal electrodes. Modern aspects of electrochemistry. New York: Springer; 2008; 89–189.
[139] Benson EE, Kubiak CP, Sathrum AJ, Smieja JM. Electrocatalytic and homogeneous approaches to conversion of CO_2 to liquid fuels. Chem Soc Rev 2009;38:89–99.
[140] Latimer WM. Oxidation potentials. Englewood Cliffs, NJ: Prentice-Hall; 1952.
[141] Keene FR, Creutz C, Sutin N. Reduction of carbon dioxide by tris(2,2'-bipyridine)cobalt(I). Coord Chem Rev 1985;64:247–60.
[142] Lilie J, Beck G, Henglein A. Pulse radiolysis and polarography. Halfwave potentials for the oxidation and reduction of short-lived organic radicals at the mercury electrode. Ber Bunsenges Phys Chem 1971;75:458–65.
[143] Gambarotta S, Arena F, Floriani C, Zanazzi PF. Carbon dioxide fixation: bifunctional complexes containing acidic and basic sites working as reversible carriers. J Am Chem Soc 1982;104:5082–92.
[144] Yamamoto A, Kitazume S, Pu LS, Ikeda S. Synthesis and properties of hydridodinitrogentris(triphenylphosphine)cobalt(I) and the related phosphine–cobalt complexes. J Am Chem Soc 1971;93:371–80.
[145] Palmer DA, Van ER. The chemistry of metal carbonato and carbon dioxide complexes. Chem Rev 1983;83:651–731.
[146] Toyir J, De lPPR, Fierro JLG, Homs N. Highly effective conversion of CO_2 to methanol over supported and promoted copper-based catalysts: influence of support and promoter. Appl Catal B 2001;29:207–15.
[147] Toyir J, Ramirez dlPP, Fierro JLG, Homs N. Catalytic performance for CO_2 conversion to methanol of gallium-promoted copper-based catalysts: influence of metallic precursors. Appl Catal B 2001;34:255–66.
[148] Liu J, Shi J, He D, Zhang Q, Wu X, Liang Y, et al. Surface active structure of ultra-fine Cu/ZrO_2 catalysts used for the CO_2+H_2 to methanol reaction. Appl Catal A 2001;218:113–9.
[149] Liu X-M, Lu GQ, Yan Z-F. Nanocrystalline zirconia as catalyst support in methanol synthesis. Appl Catal A 2005;279:241–5.
[150] Sloczynski J, Grabowski R, Olszewski P, Kozlowska A, Stoch J, Lachowska M, et al. Effect of metal oxide additives on the activity and stability of Cu/ZnO/ZrO_2 catalysts in the synthesis of methanol from CO_2 and H_2. Appl Catal A 2006;310:127–37.
[151] Raudaskoski R, Niemelae MV, Keiski RL. The effect of ageing time on co-precipitated Cu/ZnO/ZrO_2 catalysts used in methanol synthesis from CO_2 and H_2. Top Catal 2007;45:57–60.
[152] Guo X, Mao D, Wang S, Wu G, Lu G. Combustion synthesis of CuO–ZnO–ZrO_2 catalysts for the hydrogenation of carbon dioxide to methanol. Catal Commun 2009;10:1661–4.
[153] Sloczynski J, Grabowski R, Kozlowska A, Olszewski P, Stoch J, Skrzypek J, et al. Catalytic activity of the M/(3ZnO·ZrO_2) system (M=Cu, Ag, Au) in the hydrogenation of CO_2 to methanol. Appl Catal A 2004;278:11–23.
[154] Guo X, Mao D, Lu G, Wang S, Wu G. Glycine–nitrate combustion synthesis of CuO–ZnO–ZrO_2 catalysts for methanol synthesis from CO_2 hydrogenation. J Catal 2010;271:178–85.
[155] An X, Li J, Zuo Y, Zhang Q, Wang D, Wang JA. Cu/Zn/Al/Zr fibrous catalyst that is an improved CO_2 hydrogenation to methanol catalyst. Catal Lett 2007;118:264–9.
[156] Liang X-L, Dong X, Lin G-D, Zhang H-B. Carbon nanotube-supported Pd–ZnO catalyst for hydrogenation of CO_2 to methanol. Appl Catal B 2009;88:315–22.
[157] Collins SE, Chiavassa DL, Bonivardi AL, Baltanas MA. Hydrogen spillover in Ga_2O_3–Pd/SiO_2 catalysts for methanol synthesis from CO_2/H_2. Catal Lett 2005;103:83–8.
[158] Jia L, Gao J, Fang W, Li Q. Carbon dioxide hydrogenation to methanol over the pre-reduced $LaCr_{0.5}Cu_{0.5}O_3$ catalyst. Catal Commun 2009;10:2000–3.
[159] Chinchen GC, Waugh KC, Whan DA. The activity and state of the copper surface in methanol synthesis catalysts. Appl Catal 1986;25(1 and 2):101–7.
[160] Chinchen GC, Spencer MS, Waugh KC, Whan DA. Promotion of methanol synthesis and the water–gas shift reactions by adsorbed oxygen on supported copper catalysts. J Chem Soc Faraday Trans 1: Phys Chem Condens Phases 1987;83(7):2193–212.
[161] Joo O-S, Jung K-D, Moon I, Rozovskii AY, Lin GI, Han S-H, et al. Carbon dioxide hydrogenation to form methanol via a reverse-water–gas-shift reaction (the CAMERE Process). Ind Eng Chem Res 1999;38(5):1808–12.
[162] Wu J, Saito M, Takeuchi M, Watanabe T. The stability of Cu/ZnO-based catalysts in methanol synthesis from a CO_2-rich feed and from a CO-rich feed. Appl Catal A: Gen 2001;218(1–2):235–40.
[163] Saito M, Murata K. Development of high performance Cu/ZnO-based catalysts for methanol synthesis and the water–gas shift reaction. Catal Surv Asia 2004;8(4):285–94.
[164] Bart JCJ, Sneeden RPA. Copper–zinc oxide–alumina methanol catalysts revisited. Catal Today 1987;2:1–124.
[165] Chinchen GC, Denny PJ, Jennings JR, Spencer MS, Waugh KC. Synthesis of methanol. Part 1. Catalysts and kinetics. Appl Catal 1988;36:1–65.
[166] Millar GJ, Rochester CH, Waugh KC. An in situ high pressure FT-IR study of carbon dioxide/hydrogen interactions with model zinc oxide/silica, copper/silica and copper/zinc oxide/silica methanol synthesis catalysts. Catal Lett 1992;14:289–95.
[167] Liu X-M, Lu GQ, Yan Z-F, Beltramini J. Recent advances in catalysts for methanol synthesis via hydrogenation of CO and CO_2. Ind Eng Chem Res 2003;42(25):6518–30.
[168] Pan WX, Cao R, Roberts DL, Griffin GL. Methanol synthesis activity of copper/zinc oxide catalysts. J Catal 1988;114:440–6.
[169] Rasmussen PB, Holmblad PM, Askgaard T, Ovesen CV, Stoltze P, Nørskov JK, et al. Methanol synthesis on Cu(100) from a binary gas mixture of CO_2 and H_2. Catal Lett 1994;26(3):373–81.
[170] Rasmussen PB, Kazuta M, Chorkendorff I. Synthesis of methanol from a mixture of H_2 and CO_2 on Cu(100). Surf Sci 1994;318(3):267–80.
[171] Askgaard TS, Norskov JK, Ovesen CV, Stoltze P. A kinetic model of methanol synthesis. J Catal 1995;156(2):229–42.
[172] Jingfa D, Qi S, Yulong Z, Songying C, Dong W. A novel process for preparation of a Cu/ZnO/Al_2O_3 ultrafine catalyst for methanol synthesis from CO_2+H_2. Comparison of various preparation methods. Appl Catal A: Gen 1996;139(1):75–85.
[173] Herman RG, Klier K, Simmons GW, Finn BP, Bulko JB, Kobylinski TP. Catalytic synthesis of methanol from CO–H_2. I. Phase composition, electronic properties, and activities of the Cu/ZnO/M_2O_3 catalysts. J Catal 1979;56(3):407–29.
[174] Szanyi J, Goodman DW. Methanol synthesis on a copper(100) catalyst. Catal Lett 1991:383–90.
[175] Bailey S, Froment GF, Snoeck JW, Waugh KC. A DRIFTS study of the morphology and surface adsorbate composition of an operating methanol synthesis catalyst. Catal Lett 1994;30(1):99–111.
[176] Klier K, Chatikavanij V, Herman RG, Simmons GW. Catalytic synthesis of methanol from CO–H_2: IV. The effects of carbon dioxide. J Catal 1982;74(2):343–60.
[177] Nakamura J, Choi Y, Fujitani T. On the issue of the active site and the role of ZnO in Cu/ZnO methanol synthesis catalysts. Top Catal 2003;22(3):277–85.
[178] Choi Y, Futagami K, Fujitani T, Nakamura J. The role of ZnO in Cu/ZnO methanol synthesis catalysts – morphology effect or active site model? Appl Catal A: Gen 2001;208(1and 2):163–7.
[179] Twigg MV, Spencer MS. Deactivation of supported copper metal catalysts for hydrogenation reactions. Appl Catal A: Gen 2001;212(1 and 2):161–74.
[180] Alperowicz N. Mitsui seeks partners for CO_2-based methanol plant. Chem Week; March 2010.

[181] Braunstein P, Matt D, Nobel D. Reactions of carbon dioxide with carbon–carbon bond formation catalyzed by transition-metal complexes. Chem Rev 1988;88:747–64.
[182] Damodar J, Krishna MSR, Jayarama RSR. Synthesis of 2-arylpropionic acids by electrocarboxylation of benzyl chlorides catalysed by $PdCl_2(PPh_3)_2$. Electrochem Commun 2001;3:762–6.
[183] Otero MD, Batanero B, Barba F. CO_2 anion-radical in organic carboxylations. Tetrahedron Lett 2006;47:2171–3.
[184] Tokuda M, Kabuki T, Katoh Y, Suginome H. Regioselective synthesis of β,γ-unsaturated acids by the electrochemical carboxylation of allylic bromides using a reactive-metal anode. Tetrahedron Lett 1995;36:3345–8.
[185] Kamekawa H, Senboku H, Tokuda M. Facile synthesis of aryl-substituted 2-alkenoic acids by electroreductive carboxylation of vinylic bromides using a magnesium anode. Electrochim Acta 1997;42:2117–23.
[186] Senboku H, Fujimura Y, Kamekawa H, Tokuda M. Divergent electrochemical carboxylation of vinyl triflates: new electrochemical synthesis of phenyl-substituted α,β-unsaturated carboxylic acids and aliphatic β-keto carboxylic acids. Electrochim Acta 2000;45:2995–3003.
[187] Silvestri G, Gambino S, Filardo G. Use of sacrificial anodes in synthetic electrochemistry. Processes involving carbon dioxide. Acta Chem Scand 1991;45:987–92.
[188] Koshechko VG, Titov VE, Lopushanskaya VA. Electrochemical carboxylation of benzoyl bromide as effective phenylglyoxylic acid synthesis route. Electrochem Commun 2002;4:655–8.
[189] Ramesh RR, Krishna MS, Jayarama RS. Electroorganic synthesis of 6-aminonicotinic acid from 2-amino-5-chloropyridine. Tetrahedron Lett 2003;44:4133–5.
[190] Bringmann J, Dinjus E. Electrochemical synthesis of carboxylic acids from alkenes using various nickel–organic mediators: CO_2 as C_1-synthon. Appl Organomet Chem 2001;15:135–40.
[191] Koster F, Dinjus E, Dunach E. Electrochemical selective incorporation of CO_2 into terminal alkynes and diynes. Eur J Org Chem 2001:2507–11.
[192] Yang H, Gu Y, Deng Y, Shi F. Electrochemical activation of carbon dioxide in ionic liquids: synthesis of cyclic carbonates under mild reaction conditions. Chem Commun 2002:274–5.
[193] Lee S. Methanol-to-gasoline vs. DME-to-gasoline. II. Process comparison and analysis. Fuel Energy Abst 1995;36(6):414.
[194] Jayamurthy M, Vasudevan S. Methanol-to-gasoline(MTG)conversion over ZSM-5. A temperature programmed surface reaction study. Catal Lett 1996;36(1 and 2):111–4.
[195] Dean AJ. Lange's handbook of chemistry. 13th ed.. . New York: McGraw-Hill; 1985; 9–4 – 9-107.
[196] Hori Y. Electrochemical CO_2 reduction on metal electrodes. Modern aspects of electrochemistry. New York: Springer; 2008; 89–189.
[197] Murata A, Hori Y. Electrochemical reduction of carbon dioxide to carbon monoxide at nickel electrodes modified with cadmium. Chem Lett 1991:181–4.
[198] Hori Y, Murata A, Ito S. Enhanced evolution of carbon monoxide and suppressed formation of hydrocarbons in electroreduction of carbon dioxide at a copper electrode modified with cadmium. Chem Lett 1990:1231–4.
[199] Hori Y, Murata A, Ito SY, Yoshinami Y, Koga O. Nickel and iron modified copper electrode for electroreduction of carbon dioxide by in-situ electrodeposition. Chem Lett 1989:1567–70.
[200] Hori Y, Kikuchi K, Murata A, Suzuki S. Production of methane and ethylene in electrochemical reduction of carbon dioxide at copper electrode in aqueous hydrogen carbonate solution. Chem Lett 1986:897–8.
[201] Hori Y, Kikuchi K, Suzuki S. Production of carbon monoxide and methane in electrochemical reduction of carbon dioxide at metal electrodes in aqueous hydrogen carbonate solution. Chem Lett 1985:1695–8.
[202] Watanabe M, Shibata M, Kato A, Azuma M, Sakata T. Design of alloy electrocatalysts for CO_2 reduction. J Electrochem Soc 1991;138(11):3382–9.
[203] Katoh A, Uchida H, Shibata M, Watanabe M. Design of electrocatalyst for CO_2 reduction. J Electrochem Soc 1994;141(8):2054–8.
[204] Cook RL, MacDuff RC, Sammells AF. On the electrochemical reduction of carbon dioxide at in situ electrodeposited copper. J Electrochem Soc 1988;135(6):1320–6.
[205] Lynch FE, Marmaro RW. Special purpose blends of hydrogen and natural gas; 1992. USA: Hydrogen Consultants, Inc. 30 pp.
[206] Lynch FE. Metal hydrides: the missing link in automotive hydrogen technology. In: 1975 NTIS; 1975. p. 408–421.
[207] Mahmood MN, Masheder D, Harty CJ. Use of gas-diffusion electrodes for high-rate electrochemical reduction of carbon dioxide. I. Reduction at lead, indium- and tin-impregnated electrodes. J Appl Electrochem 1987;17: 1159–70.
[208] Kapusta S, Hackerman N. The electroreduction of carbon dioxide and formic acid on tin and indium electrodes. J Electrochem Soc 1983;130(3):607–13.
[209] Hara K, Kudo A, Sakata T. Electrochemical reduction of carbon dioxide under high pressure on various electrodes in an aqueous electrolyte. J Electroanal Chem 1995;391(1 and 2):141–7.
[210] Furuya N, Yamazaki T, Shibata M. High performance Ru–Pd catalysts for CO_2 reduction at gas-diffusion electrodes. J Electroanal Chem 1997;431(1):39–41.
[211] Frese KW Jr, Leach SC, Summers DP. Electrochemical reduction of aqueous carbon dioxide to methanol. US patent no. 4,609,441; 2 September 1986.
[212] Hussain ST, Muhammad MM, Rehman HU. Novel process and catalyst for carbon dioxide conversion to energy generating products. US patent 2007. Application number: 11/751,026 (May 20): Publication number: US 2008/ 0287555 A0287551.
[213] Coehn A, Jahn S. Electrolytic reduction of carbon dioxide. Ber Dtsch Chem Ges 1904:37.
[214] Fischer F, Prziza O. Electrolytic reduction of carbon oxides dissolved under pressure. Ber Dtsch Chem Ges 1914:47.
[215] Teeter TE, Rysselberghe PV. Reduction of carbon dioxide on mercury cathodes. J Chem Phys 1954:22.
[216] Paik W, Andersen TN, Eyring H. Kinetic studies of electrolytic reduction of carbon dioxide on mercury electrode. Electrochim Acta 1969;14(12):1217–32.
[217] Udupa KS, Subramanian GS, Udupa HVK. Electrolytic reduction of carbon dioxide to formic acid. Electrochim Acta 1971;16(9):1593.
[218] Russell PG, Kovac N, Srinivasan S, Steinberg M. Electrochemical reduction of carbon dioxide, formic acid, and formaldehyde. J Electrochem Soc 1977;124 (9):1329–38.
[219] Canfield D, Frese Jr KW. Reduction of carbon dioxide to methanol on n-GaAs and p-GaAs and p-InP. Effect of crystal face, electrolyte and current density. J Electrochem Soc 1983;130(8):1772–3.
[220] Frese KW, Leach Jr S. Electrochemical reduction of carbon dioxide to methane, methanol, and CO on Ru electrodes. J Electrochem Soc 1985;132 (1):259–60.
[221] Summers DP, Leach S, Frese Jr KW. The electrochemical reduction of aqueous carbon dioxide to methanol at molybdenum electrodes with low overpotentials. J Electroanal Chem 1986;205(1 and 2):219–32.
[222] Hori Y, Suzuki S. Electrolytic reduction of carbon dioxide at mercury electrode in aqueous solution. Bull Chem Soc Jpn 1982;55:660–5.
[223] Hori Y, Murata A. Electrochemical evidence of intermediate formation of adsorbed carbon monoxide in cathodic reduction of carbon dioxide at a nickel electrode. Electrochim Acta 1990;35:1777–80.
[224] Taguchi S, Aramata A. Surface-structure sensitive reduced CO_2 formation on Pt single crystal electrodes in sulfuric acid solution. Electrochim Acta 1994;39(17):2533–7.
[225] Hori Y, Wakebe H, Tsukamoto T, Koga O. Electrocatalytic process of CO selectivity in electrochemical reduction of CO_2 at metal electrodes in aqueous media. Electrochim Acta 1994;39(11 and 12):1833–39.
[226] Azuma M, Hashimoto K, Hiramoto M, Watanabe M, Sakata T. Electrochemical reduction of carbon dioxide on various metal electrodes in low-temperature aqueous $KHCO_3$ media. J Electrochem Soc 1990;137(6):1772–8.
[227] Kita H, Kurisu T. Electrocatalysis by d- and sp-metals. J Res Inst Catal, Hokkaido Univ 1973;21(3):200–46.
[228] Yamamoto T, Tryk DA, Fujishima A, Ohata H. Production of syngas plus oxygen from CO_2 in a gas-diffusion electrode-based electrolytic cell. Electrochim Acta 2002;47:3327–34.
[229] Rakowski Dubois M, Dubois DL. Development of molecular electrocatalysts for CO_2 reduction and H_2 production/oxidation. Acc Chem Res 2009;42 (12):1974–82.
[230] Jensen R, Lyman J. Solar conversion of CO_2 to fuel. In: Proceedings of the fourth international conference on greenhouse gas control technology, Interlaken, Switzerland; 30 August–2 September 1998.
[231] Halmann M. Photoelectrochemical reduction of aqueous carbon-dioxide on p-type gallium–phosphide in liquid junction solar-cells. Nature 1978;275: 115.
[232] Eggins BR, Brown EM, McNeill EA, Grimshaw J. Carbon dioxide fixation by electrochemical reduction in water to oxalate and glyoxylate. Tetrahedron Lett 1988;29(8):945–8.
[233] Bell AT. Basic research needs: catalysis for energy. Report from the US Department of Energy. Basic energy sciences workshop; 2007. p. 69.
[234] Delacourt C, Ridgway PL, Kerr JB, Newman J. Design of an electrochemical cell making syngas ($CO+H_2$) from CO_2 and H_2O reduction at room temperature. J Electrochem Soc 2007;155:B42–9.
[235] Bandi A. Electrochemical reduction of carbon dioxide on conductive metallic oxides. J Electrochem Soc 1990;137(7):2157–60.
[236] Popic JP, Avramov-Ivic ML, Vukovic NB. Reduction of carbon dioxide on ruthenium oxide and modified ruthenium oxide electrodes in 0.5 M $NaHCO_3$. J Electroanal Chem 1997;421:105–10.
[237] Spataru N, Tokuhiro K, Terashima C, Rao TN, Fujishima A. Electrochemical reduction of carbon dioxide at ruthenium dioxide deposited on boron-doped diamond. J Appl Electrochem 2003;33:1205–10.
[238] Qu J, Zhang X, Wang Y, Xie C. Electrochemical reduction of CO_2 on RuO_2/TiO_2 nanotubes composite modified Pt electrode. Electrochim Acta 2005;50: 3576–80.
[239] Frese Jr KW. Electrochemical reduction of CO_2 at intentionally oxidized copper electrodes. J Electrochem Soc 1991;138(11):3338–44.
[240] Kim JJ, Summers DP, Frese Jr KW. Reduction of carbon dioxide and carbon monoxide to methane on copper foil electrodes. J Electroanal Chem Interfacial Electrochem 1988;245:223–44.
[241] Koga O, Nakama K, Murata A, Hori Y. Effects of surface state of copper electrode on the selectivity of electrochemical reduction of carbon dioxide. Denki Kagaku Oyobi Kogyo Butsuri Kagaku 1989;57:1137–40.
[242] Kyriacou G, Anagnostopoulos A. Electroreduction of carbon dioxide on differently prepared copper electrodes. The influence of electrode treatment on the current efficiencies. J Electroanal Chem Interfacial Electrochem 1992;322:233–46.
[243] Hara K, Tsuneto A, Kudo A, Sakata T. Change in the product selectivity for the electrochemical CO_2 reduction by adsorption of sulfide ion on metal electrodes. J Electroanal Chem 1997;434:239–43.
[244] Hara K, Kudo A, Sakata T. Electrochemical CO_2 reduction on a glassy carbon electrode under high pressure. J Electroanal Chem 1997;421:1–4.

[245] Pinsent BRW, Pearson L, Roughton FJW. The kinetics of combination of carbon dioxide with hydroxide ions. Trans Faraday Soc 1956;52:1512–20.
[246] Ogura K, Fujita M. Electrocatalytic reduction of carbon dioxide to methanol. Part 7. With quinone derivatives immobilized on platinum and stainless steel. J Mol Catal 1987;41:303–11.
[247] Ogura K, Takamagari K. Electrocatalytic reduction of carbon dioxide to methanol. Part 2. Effects of metal complex and primary alcohol. J Chem Soc, Dalton Trans 1986;8:1519–23.
[248] Ogura K, Yamasaki S. Conversion of carbon monoxide into methanol at room temperature and atmospheric pressure. J Chem Soc, Faraday Trans 1 1985;81:267–71.
[249] Neff VD. Electrochemical oxidation and reduction of thin films of Prussian blue. J Electrochem Soc 1978;125:886–7.
[250] Ogura K, Takamagari K. Electrocatalytic reduction of carbon dioxide to methanol. Part 2. Effects of metal complex and primary alcohol. J Chem Soc, Dalton Trans 1986:1519–23.
[251] Ogura K, Salazar-Villalpando MD. CO_2 electrochemical reduction via adsorbed halide anions. JOM 2011;63:35–8.
[252] Ogura K. Carbon dioxide fixation and catalysts. Hyomen 1991;29:945–54.
[253] Ogura K. Fixation of carbon dioxide by electrolytic reduction. Kagaku (Kyoto) 1991;46:307–9.
[254] Ogura K, Yoshida I. Electrocatalytic reduction of carbon dioxide to methanol. Part 9. Mediation with metal porphyrins. J Mol Catal 1988;47:51–7.
[255] Ogura K, Yoshida I. Electrocatalytic reduction of carbon dioxide to methanol – VI. Use of a solar cell and comparison with that of carbon monoxide. Electrochim Acta 1987;32:1191–5.
[256] Ogura K, Yamasaki S. Selective conversion of carbon monoxide into methanol at ordinary temperature. Part 4. Activation by iron (II), iron (III), and chromium (III) complexes. J Chem Soc, Dalton Trans 1985: 2499–504.
[257] Ogura K, Uchida H. Electrocatalytic reduction of carbon dioxide to methanol. Part VIII. Photoassisted electrolysis and electrochemical photocell with n-titanium dioxide anode. J Electroanal Chem Interfacial Electrochem 1987;220:333–7.
[258] Ogura K, Uchida H. Electrocatalytic reduction of carbon dioxide to methanol. Part 5. Relationship between the ability of metal complexes to engage in homogeneous catalysis and their coordination chemistry. . J Chem Soc, Dalton Trans 1987:1377–80.
[259] Ogura K, Takagi M. Electrocatalytic reduction of carbon monoxide with a photocell. J Electroanal Chem Interfacial Electrochem 1985;195(2):357–62.
[260] Ogura K. Catalytic conversion of carbon monoxide and carbon dioxide into methanol with an electrochemical photocell and a solar cell. Proc – Electrochem Soc 1986;86 and 87:591–605.
[261] Ogura K, Takagi M. Electrocatalytic reduction of carbon dioxide to methanol. Part IV. Assessment of the current–potential curves leading to reduction. J Electroanal Chem Interfacial Electrochem 1986;206:209–16.
[262] Ogura K, Takagi M. Electrocatalytic reduction of carbon dioxide to methanol. Part III. Use of an electrochemical photocell. J Electroanal Chem Interfacial Electrochem 1986;201:359–65.
[263] Ogura K, Yoshida I. Electrocatalytic reduction of carbon dioxide to methanol in the presence of (1,2-dihydroxybenzene-3,5-disulfonato)ferrate(III) and ethanol. J Mol Catal 1986;34:67–72.
[264] Seshadri G, Lin C, Bocarsly AB. A new homogeneous electrocatalyst for the reduction of carbon dioxide to methanol at low overpotential. J Electroanal Chem 1994;372(1 and 2):145–50.
[265] Raghavan R, Iwamoto RT. Characterization of the dimeric one-electron electrolytic reduction products of 1-alkylpyridinium ions in acetonitrile. J Electroanal Chem Interfacial Electrochem 1978;92:101–14.
[266] Baumgartel H, Retzlav KJ. Encyclopedia of electrochemistry of the elements. In: Bard AJ, Lund H, editors. Derivatives of ammonia, heteroaromatic compounds, 12. New York: Dekker; 1984. p. 168.
[267] Yasukouchi K, Taniguchi I, Yamaguchi H, Shiraishi M. Cathodic reduction of pyridinium ion in acetonitrile. J Electroanal Chem Interfacial Electrochem 1979;105:403–8.
[268] Bandi A, Kühne HM. Electrochemical reduction of carbon dioxide in water: analysis of reaction mechanism on ruthenium–titanium–oxide. J Electrochem Soc 1992;139(6):1605–10.
[269] Schwartz M, Cook RL, Kehoe VM, MacDuff RC, Patel J, Sammells AF. Carbon dioxide reduction to alcohols using perovskite-type electrocatalysts. J Electrochem Soc 1993;140:614–8.
[270] Parkinson BA, Weaver PF. Photoelectrochemical pumping of enzymic carbon dioxide reduction. Nature 1984;309:148–9.
[271] Klibanov AM, Alberti BN, Zale SE. Enzymic synthesis of formic acid from hydrogen and carbon dioxide and production of hydrogen from formic acid. Biotechnol Bioeng 1982;24:25–36.
[272] Stalder CJ, Chao S, Wrighton MS. Electrochemical reduction of aqueous bicarbonate to formate with high current efficiency near the thermodynamic potential at chemically derivatized electrodes. J Am Chem Soc 1984;106:3673–5.
[273] O'Toole TR, Sullivan BP, Bruce MRM, Margerum LD, Murray RW, Meyer TJ. Electrocatalytic reduction of carbon dioxide by a complex of rhenium in thin polymeric films. J Electroanal Chem Interfacial Electrochem 1989;259: 217–39.
[274] Sullivan BP. Reduction of carbon dioxide with platinum metals electrocatalysts. A potentially important route for the future production of fuels and chemicals. Platinum Met Rev 1989;33:2–9.
[275] Sullivan BP, Bolinger CM, Conrad D, Vining WJ, Meyer TJ. One- and two-electron pathways in the electrocatalytic reduction of carbon dioxide by fac-(2,2'-bipyridine)tricarbonylchlororhenium. J Chem Soc, Chem Commun 1985:1414–6.
[276] Bolinger CM, Sullivan BP, Conrad D, Gilbert JA, Story N, Meyer TJ. Electrocatalytic reduction of carbon dioxide based on polypyridyl complexes of rhodium and ruthenium. J Chem Soc, Chem Commun 1985:796–7.
[277] Beden B, Bewick A, Razaq M, Weber J. On the nature of reduced carbon dioxide an IR spectroscopic investigation. J Electroanal Chem Interfacial Electrochem 1982;139:203–6.
[278] Schiffrin DJ. Application of the photoelectrochemical effect to the study of the electrochemical properties of radicals. CO_2 radical anion and methyl radical. Faraday Discuss Chem Soc 1973;56:75–95.
[279] Frank AJ. Organic conductive films for semiconductor electrodes; 1984. USA: United States Department of Energy. 31 pp. Avail. NTIS order no. PAT-APPL-36-465 418.
[280] Williams RM, Rembaum A. Photoelectrochemical electrodes. USA: United States National Aeronautics and Space Administration; 1983. 29 pp. Avail. NTIS order no. PAT-APPL-26-376 306.
[281] Jensen RJ, Lyman JL, King JD, Guettler RD. Solar reduction of carbon dioxide, USA; 2000. 11 pp.
[282] Ohashi K, McCann J, Bockris JO. Stable photoelectrochemical cells for the splitting of water. Nature 1977;266:610–1.
[283] Bhardwaj R, Pan RL, Gross EL. Solar energy conversion by chloroplast photoelectrochemical cells. Nature 1981;289:396–8.
[284] Nozik AJ. Energetics of photoelectrolysis. Proc – Electrochem Soc 1977;77-3:272–89.
[285] Nozik AJ. Photoelectrolysis cell for manufacturing hydrogen using solar energy; 1978. USA: Allied Chemical Corp.; 34 pp. Addn. to Ger. Offen. 32,650,267.
[286] Williams F, Nozik AJ. Irreversibilities in the mechanism of photoelectrolysis. Nature 1978;271:137–9.
[287] Nozik AJ. Electrode materials for photoelectrochemical devices. J Cryst Growth 1977;39:200–9.
[288] Nozik AJ. Photochemical diodes. Appl Phys Lett 1977;30:567–9.
[289] Nozik AJ. Hydrogen generation by the photoelectrolysis of water, vol. 5B. University of Miami; 1976. p. 31–54.
[290] Nozik AJ. Energy conversion via photoelectrolysis. In: Proceedings of the Intersociety Energy Conversion Engineering Conference, vol. 11, no. (1); 1976. p. 43–50.
[291] Nozik AJ. Photoelectrolysis of water by solar radiation. USA: Allied Chemical Corp.; 1977. 10 pp.
[292] Nozik AJ. p–n Photoelectrolysis cells. Appl Phys Lett 1976;29:150–3.
[293] Nozik AJ. Photoelectrolysis of water using semiconducting titanium dioxide crystals. Nature 1975;257:383–6.
[294] Esswein AJ, Nocera DG. Hydrogen production by molecular photocatalysis. Chem Rev 2007;107(10):4022–47.
[295] Tan SS, Zou L, Hu E. Photocatalytic reduction of carbon dioxide into gaseous hydrocarbon using TiO_2 pellets. Catal Today 2006;115(1–4):269–73.
[296] Tomkiewicz M, Woodall JM. Photoassisted electrolysis of water by visible irradiation of a p-type gallium phosphide electrode. Science 1977;196:990–1.
[297] Gerischer H. Electrochemical photo and solar cells principles and some experiments. J Electroanal Chem Interfacial Electrochem 1975;58(1):263–74.
[298] Frese Jr KW, Canfield D. Reduction of carbon dioxide on n-gallium arsenide electrodes and selective methanol synthesis. J Electrochem Soc 1984;131: 2518–22.
[299] Bard AJ, Wrighton MS. Thermodynamic potential for the anodic dissolution of n-type semiconductors. A crucial factor controlling durability and efficiency in photoelectrochemical cells and an important criterion in the selection of new electrode/electrolyte systems. J Electrochem Soc 1977;124:1706–10.
[300] Inoue T, Fujishima A, Konishi S, Honda K. Photoelectrocatalytic reduction of carbon dioxide in aqueous suspensions of semiconductor powders. Nature 1979;277(5698):637–8.
[301] Eggins BR, Irvine JTS, Murphy EP, Grimshaw J. Formation of two-carbon acids from CO_2 by photoreduction on cadmium sulphide. J Chem Soc Chem Commun 1988:1123–4.
[302] Hirota K, Tryk DA, Yamamoto T, Hashimoto K, Okawa M, Fujishima A. Photoelectrochemical reduction of CO_2 in a high-pressure CO_2+CH_3OH medium at p-type semiconductor electrodes. J Phys Chem B 1998;102: 9834–43.
[303] Aurian-Blajeni B, Halmann M, Manassen J. Electrochemical measurements on the photoelectrochemical reduction of aqueous carbon dioxide on p-gallium phosphide and p-gallium arsenide semiconductor electrodes. Sol Energy Mater 1983;8:425–40.
[304] Willner I, Maidan R, Mandler D, Durr H, Dorr G, Zengerle K. Photosensitized reduction of CO_2 to CH_4 and H_2 evolution in the presence of ruthenium and osmium colloids: strategies to design selectivity of products distribution. J Am Chem Soc 1987;109:6080–6.
[305] Maidan R, Willner I. Photoreduction of CO_2 to CH_4 in aqueous solutions using visible light. J Am Chem Soc 1986;108:8100–1.
[306] Lehn JM, Ziessel R. Photochemical generation of carbon monoxide and hydrogen by reduction of carbon dioxide and water under visible light irradiation. Proc Natl Acad Sci USA 1982;79(2):701–4.

[307] Barton EE, Rampulla DM, Bocarsly AB. Selective solar-driven reduction of CO_2 to methanol using a catalyzed *p*-GaP based photoelectrochemical cell. J Am Chem Soc 2008;130:6342–4.
[308] Barton Cole E, Lakkaraju PS, Rampulla DM, Morris AJ, Abelev E, Bocarsly AB. Using a one-electron shuttle for the multielectron reduction of CO_2 to methanol: kinetic, mechanistic, and structural insights. J Am Chem Soc 2010;132(33):11539–51.
[309] Grant WM. Colorimetric microdetermination of formic acid based on reduction to formaldehyde. Anal Chem 1948;20:267–9.
[310] Ganesh I, Gupta AK, Kumar PP, Chandra Sekhar PS, Radha K, Padmanabham G, et al. Preparation and characterization of Co-doped TiO_2 materials for solar light induced current and photocatalytic applications. Mater Chem Phys 2012;135(1):220–34.
[311] Ganesh I. Conversion of carbon dioxide to methanol using solar energy. Curr Sci 2011;101(6):731–3.
[312] Ganesh I, Kumar PP, Gupta AK, Sekhar PSC, Radha K, Padmanabham G, et al. Preparation and characterization of Fe-doped TiO_2 powders for solar light response and photocatalytic applications. Process Appl Ceram 2012;6:21–36.
[313] Ganesh I, Sekhar PSC, Padmanabham G, Sundararajan G. Influence of Li-doping on structural characteristics and photocatalytic activity of ZnO nano-powder formed in a novel solution pyro-hydrolysis route. Appl Surf Sci 2012;259:524–37.
[314] Hirano K, Inoue K, Yatsu T. Photocatalyzed reduction of CO_2 in aqueous TiO_2 suspension mixed with copper powder. J Photochem Photobiol A: Chem 1992;64(2):255–8.
[315] Hemminger JC, Carr R, Somorjai GA. Photoassisted reaction of gaseous water and carbon dioxide adsorbed on $SrTiO_2$ (111) crystal face to form methane. Cheml Phys Lett 1978;57(1):100–4.
[316] Tseng IH, Chang WC, Wu JCS. Photoreduction of CO_2 using sol–gel derived titania and titania-supported copper catalysts. Appl Catal B: Environ 2002;37 (1):37–48.
[317] Wu JCS, Lin HM, Lai CL. Photo reduction of CO_2 to methanol using optical-fiber photoreactor. Appl Catal A: Gen 2005;296(2):194–200.
[318] Nakatsuji H, Hu ZM. Mechanism of methanol synthesis on Cu(100) and Zn/Cu (100) surfaces: Comparative dipped adcluster model study. Int J Quant Chem 2010;77(1):341–9.
[319] Slamet Nasution HW, Purnama E, Riyani K, Gunlazuardi J. Effect of copper species in a photocatalytic synthesis of methanol from carbon dioxide over copper-doped titania catalysts. World Appl Sci J 2009;6:1.
[320] Fujitani T, Nakamura J. The chemical modification seen in the Cu/ZnO methanol synthesis catalysts. Appl Catal A: Gen 2000;191(1 and 2):111–29.
[321] Yang YX, Evans J, Rodriguez JA, White MG, Liu P. Fundamental studies of methanol synthesis from CO_2 hydrogenation on Cu(111), Cu clusters, and Cu/ZnO(000(1)over-bar). Phys Chem Chem Phys 2010;12(33):9909–17.
[322] Ichikawa S, Doi R. Hydrogen production from H_2O and conversion of CO_2 to useful chemicals by room temperature photoelectrocatalysis. Catal Today 1996;27:271–7.
[323] Sakka S, Kamiya K, Makita K, Yamamoto Y. Formation of sheets and coating films from alkoxide solutions. J Non-Crystal Solids 1984;63(1 and 2):223–35.
[324] Shiratsuchi R, Aikoh Y, Nogami G. Pulsed electroreduction of CO_2 on copper electrodes. J Electrochem Soc 1993;140:3479–82.
[325] Traynor AJ, Jensen RJ. Direct solar reduction of CO_2 to fuel: first prototype results. Ind Eng Chem Res 2002;41(8):1935–9.
[326] Wu JCS, Lin H-M. Photoreduction of CO_2 to CH_3OH via TiO_2 photocatalyst. Int J Photoenergy 2005;7:115–9.
[327] Zhao C, Krall A, Zhao H, Zhang Q, Li Y. Ultrasonic spray pyrolysis synthesis of Ag/TiO_2 nanocomposite photocatalysts for simultaneous H2 production and CO_2 reduction. Int J Hydrogen Energy 2012;37(13):9967–76.
[328] Ramırez G, Ferraudi G, Chen Y-Y, Trollund E, Villagra D. Enhanced photoelectrochemical catalysis of CO_2 reduction mediated by a supra-molecular electrode of packed Co II (tetrabenzoporphyrin). Inorg Chim Acta 2009;362:5–10.
[329] Nazimek D, Czech B. Artificial photosynthesis – CO_2 towards methanol. In: IOP conference series: materials science and engineering; 2011. p. 19: 012010/012011-012010/012017.
[330] Liu Q, Zhou Y, Kou J, Chen X, Tian Z, Gao J, et al. High-yield synthesis of ultralong and ultrathin Zn_2GeO_4 nanoribbons toward improved photocatalytic reduction of CO_2 into renewable hydrocarbon fuel. J Am Chem Soc 2010;132:14385–7.
[331] Hinogami R, Nakamura Y, Yae S, Nakato Y. An approach to ideal semiconductor electrodes for efficient photoelectrochemical reduction of CO_2 by modification with small metal particles. J Phys Chem B 1998;102:974–80.
[332] Eggins BR, Robertson PKJ, Murphy EP, Woods E, Irvine JTS. Factors affecting the photoelectrochemical fixation of CO_2 with semiconductor colloids. J Photochem Photobiol A: Chem 1998;118:31–40.
[333] Aylmer-Kelly AWB, Bewick A, Cantrill PR, Tuxford AM. Studies of electrochemically generated reaction intermediates using modulated specular reflectance spectroscopy. Faraday Discuss Chem Soc 1973;56:96–107.
[334] Lamy E, Nadjo L, Saveant JM. Standard potential and kinetic parameters of the electrochemical reduction of carbon dioxide in dimethylformamide. J Electroanal Chem Interfacial Electrochem 1977;78:403–7.
[335] Tyssee DA, Wagenknecht JH, Baizer MM, Chruma JL. Cathodic organic syntheses involving carbon dioxide. Tetrahedron Lett 1972:4809–12.
[336] Bennett EM, Eggins BR, McNeill J, McMullan EA. Recycling carbon dioxide from fossil fuel combustion. Anal Proc (Lond) 1980;17:356–8.
[337] Eggins BR, Brown EM, McNeill EA, Grimshaw J. Carbon dioxide fixation by electrochemical reduction in water to oxalate and glyoxylate. Tetrahedron Lett 1988;29:945–8.
[338] Bewick A, Greener GP. Electroreduction of carbon dioxide to malate on a mercury cathode. Tetrahedron Lett 1969:4623–6.
[339] Eggins BR, Ennis C, McConnell R, Spence M. Improved yields of oxalate, glyoxylate and glycolate from the electrochemical reduction of carbon dioxide in methanol. J Appl Electrochem 1997;27:706–12.
[340] Bewick A, Greener GP. Electroreduction of carbon dioxide to glycollate on a lead cathode. Tetrahedron Lett 1970:391–4.
[341] Eggins BR, Bennett EM, McMullan EA. Voltammetry of carbon dioxide. Part 2. Voltammetry in aqueous solutions on glassy carbon. J Electroanal Chem 1996:165–71.
[342] Varghese OK, Paulose M, LaTempa TJ, Grimes CA. High-rate solar photocatalytic conversion of CO_2 and H_2O vapor to hydrocarbon fuels. Nano Lett 2009;9(2):731–7.
[343] Paulose M, Shankar K, Yoriya S, Prakasam HE, Varghese OK, Mor GK, et al. Anodic growth of highly ordered TiO_2 nanotube arrays to 134 μm in length. J Phys Chem B 2006;110(33):16179–84.
[344] Barber J. Biological solar energy. Philos Trans A Math Phys Eng Sci 2007;365 (1853):1007–23.
[345] Bak T, Nowotny J, Rekas M, Sorrell CC. Photo-electrochemical hydrogen generation from water using solar energy. Materials-related aspects. Int J Hydrogen Energy 2002;27:991–1022.
[346] Chen X, Shen S, Guo L, Mao SS. Semiconductor-based photocatalytic hydrogen generation. Chem Rev 2010;110(11):6503–70.
[347] Rajeshwar K. Hydrogen generation at irradiated oxide semiconductor–solution interfaces. J Appl Electrochem 2007;37(7):765–87.
[348] Nowotny J, Bak T, Nowotny MK, Sheppard LR. Titanium dioxide for solar-hydrogen I. Functional properties. Int J Hydrogen Energy 2007;32 (14):2609–29.
[349] Steinfeld A. Solar thermochemical production of hydrogen – a review. Solar Energy 2005;78(5):603–15.
[350] Kodama T, Gokon N. Thermochemical cycles for high-temperature solar hydrogen production. ChemInform 2007;38:51.
[351] Somasundaram S, Raman Nair Chenthamarakshan C, de Tacconi NR, Rajeshwar K. Photocatalytic production of hydrogen from electrodeposited film and sacrificial electron donors. Int J Hydrogen Energy 2007;32 (18):4661–9.
[352] Galińska A, Walendziewski J. Photocatalytic water splitting over $Pt-TiO_2$ in the presence of sacrificial reagents. Energy Fuels 2005;19(3):1143–7.
[353] Kelly NA, Gibson TL. Solar energy concentrating reactors for hydrogen production by photoelectrochemical water splitting. Int J Hydrogen Energy 2008;33(22):6420–31.
[354] Walter MG, Warren EL, McKone JR, Boettcher SW, Mi Q, Santori EA, et al. Solar water splitting cells. Chem Rev 2010;110(11):6446–73.
[355] Lv H, Geletii YV, Zhao C, Vickers JW, Zhu G, Luo Z, et al. Polyoxometalate water oxidation catalysts and the production of green fuel. Chem Soc Rev 2012;41:7572–89.
[356] Concepcion JJ, Jurss JW, Brennaman MK, Hoertz PG, AOvT Patrocinio, Murakami Iha NY, et al. Making oxygen with ruthenium complexes. Acc Chem Res 2009;42(12):1954–65.
[357] Pinsent BRW, Pearson L, Roughton FJW. The kinetics of combination of carbon dioxide with hydroxide ions. Trans Faraday Soc 1956;52:1512–20.